

OSMOLALITY TOLERANCE AND ION CHANNELS IN
PROTOPLASTS OF ENTOMOPHTHOREAN FUNGI

CENTRE FOR NEWFOUNDLAND STUDIES

**TOTAL OF 10 PAGES ONLY
MAY BE XEROXED**

(Without Author's Permission)

MARY PATRICIA LAMB

INFORMATION TO USERS

This manuscript has been reproduced from the microfilm master. UMI films the text directly from the original or copy submitted. Thus, some thesis and dissertation copies are in typewriter face, while others may be from any type of computer printer.

The quality of this reproduction is dependent upon the quality of the copy submitted. Broken or indistinct print, colored or poor quality illustrations and photographs, print bleedthrough, substandard margins, and improper alignment can adversely affect reproduction.

In the unlikely event that the author did not send UMI a complete manuscript and there are missing pages, these will be noted. Also, if unauthorized copyright material had to be removed, a note will indicate the deletion.

Oversize materials (e.g., maps, drawings, charts) are reproduced by sectioning the original, beginning at the upper left-hand corner and continuing from left to right in equal sections with small overlaps. Each original is also photographed in one exposure and is included in reduced form at the back of the book.

Photographs included in the original manuscript have been reproduced xerographically in this copy. Higher quality 6" x 9" black and white photographic prints are available for any photographs or illustrations appearing in this copy for an additional charge. Contact UMI directly to order.

UMI

A Bell & Howell Information Company
300 North Zeeb Road, Ann Arbor MI 48106-1346 USA
313/761-4700 800/521-0600



National Library
of Canada

Acquisitions and
Bibliographic Services

395 Wellington Street
Ottawa ON K1A 0N4
Canada

Bibliothèque nationale
du Canada

Acquisitions et
services bibliographiques

395, rue Wellington
Ottawa ON K1A 0N4
Canada

Your file Votre référence

Our file Notre référence

The author has granted a non-exclusive licence allowing the National Library of Canada to reproduce, loan, distribute or sell copies of this thesis in microform, paper or electronic formats.

The author retains ownership of the copyright in this thesis. Neither the thesis nor substantial extracts from it may be printed or otherwise reproduced without the author's permission.

L'auteur a accordé une licence non exclusive permettant à la Bibliothèque nationale du Canada de reproduire, prêter, distribuer ou vendre des copies de cette thèse sous la forme de microfiche/film, de reproduction sur papier ou sur format électronique.

L'auteur conserve la propriété du droit d'auteur qui protège cette thèse. Ni la thèse ni des extraits substantiels de celle-ci ne doivent être imprimés ou autrement reproduits sans son autorisation.

0-612-34198-4

OSMOLALITY TOLERANCE AND ION CHANNELS IN
PROTOPLASTS OF
ENTOMOPHTHORALEAN
FUNGI

by

Mary Patricia Lamb

A thesis submitted to the
School of Graduate Studies
in partial fulfillment of the
requirements for the degree of
Master of Science



Department of Biology
Memorial University of Newfoundland

1997

St. John's

Newfoundland

ABSTRACT

This thesis documents the tolerance of *E. maimaiga* protoplasts to media with a broad range of pH levels and osmolalities. Growth curve data were statistically analyzed using a general linear model approach which utilizes the data from the entire growth curve. Although *E. maimaiga* grew in media ranging from pH 5.5 to 7.1, sensitivity to pH 5.5 was evident. Growth of *E. maimaiga* in media with osmolality levels of 250 to 400 mOsm did not show any significant differences. Further investigation of osmotic tolerance showed that this organism was capable of surviving osmolality treatments in solutions of 0 to 550 mOsm. However, a 350 to 550 mOsm range appeared optimal. The osmotolerance of *E. aulicae* was also determined and found to be similar to that exhibited by *E. maimaiga*. Further investigation is required to determine the mechanism used by these protoplasts for osmoregulation. Such a mechanism may include the activity of ion channels in the cell membrane.

A protocol developed for patch clamping *E. aulicae* protoplasts is presented in this paper. An appropriate pipette solution (140 mM NaCl, 5mM KCl, 2 mM CaCl₂, 2.4 mM MgCl₂•6H₂O, 10 mM MES, 3.8 mM glucose, 2.2 mM fructose, 29.8 mM sucrose, pH 6.2) and bath solution (140 mM NaCl, 5 mM KCl, 1 mM CaCl₂, 1.2 mM MgCl₂•6H₂O, 10 mM MES, 3.8 mM glucose, 2.2 mM fructose, 36 mM sucrose, pH 6.2) were developed. Recording from cells 30 to 90 minutes after suspension in the bath solution using the cell-attached recording configuration and a pipette size of 20 Mega Ω resulted in low noise gigaseal recordings.

Use of the developed patch clamping methodology resulted in the identification of outward rectifying, voltage-gated multichannel activity sensitive to membrane

depolarization. Using the mean channel amplitude, the current-voltage relationship was identified as having a conductance value of 31 pS. Use of K⁺ channel blockers, TEA⁺ and Ba²⁺, caused reduced channel activity suggesting that the channels are involved in K⁺ transport. Further evidence of this classification is based on the reduced membrane conductance values obtained when elevated levels of K⁺ were present in the pipette solution. The conductance values were reduced to 10.6 pS and -20.1 pS with K⁺ concentrations of 60 and 140 mM respectively. This serves as further evidence that the voltage-gated channels in the protoplast membrane of *E. auilcae* are K⁺ channels.

Acknowledgments

I would like to thank my supervisor, Dr. Faye Murrin, for her patience and guidance during my sojourn as her graduate student. The encouragement given, especially during the darkest hours of patch clamping, was greatly appreciated.

I would like to acknowledge the information gained and moral support obtained from a number of individuals associated with Faye's lab. They are Norbert Lake, Kelley Hicks, Damian Power and Jim Houston. The introduction to the wonderful world of *E. aulicae* would not have been the same without Jim's clarification on the differences between early and "airly" fusion spheres.

A major portion of this thesis would not have been possible without the support of Dr. Penny Moody-Corbett and her graduate students Scott Hancock and Mark Fry. Their time given and patience shown to me while patch clamping is greatly appreciated.

Dr. Roger Lew of York University is also acknowledged for his help in deciphering my early patch clamp recordings and questions. Dr. Natalia Levina also helped with my fungal patch clamp queries.

The final acknowledgment of academic help rests with Dr. David Day of the Australian National University. Without the computer access furnished by him this thesis would not have been completed as soon as it was.

Financial support for my work came from two sources. They are the provincially sponsored Special Scholarship for Students to Pursue Graduate Studies Related to Resource Development and Faye Murrin's NSERC award.

Last, but not least, I want to acknowledge the huge amount of support received from my husband, Kevin, and my children, Graeme and Sean. Without their

accommodation of another student in the house this would not have been possible.

TABLE OF CONTENTS

	<u>Page</u>
Abstract	ii
Acknowledgments	iv
Table of Contents	vi
List of Figures	xii
List of Tables	xiv
List of Abbreviations	xv
Chapter 1 - General Introduction	
1.1 The Organism	1
1.2 Osmolality	3
1.3 Ion Channels	
1.3.1 Introduction	4
1.3.2 Patch Clamping	5
1.3.3 Fungal Ion Channels	7
1.4 Aims Of This Study	9
Chapter 2 - pH and Osmotolerance of <i>Entomophaga</i> Protoplasts	
2.1 Introduction	13
2.2 Materials & Methods	
2.2.1 Stock Cultures	14
2.2.2 Growth Curves Comparing Different Media, pH Levels and	

Osmolalities	14
2.2.3 Osmotic Tolerance Test	15
2.3 Results	
2.3.1 Growth Curves Comparing Different Media, pH Levels and Osmolalities	16
2.3.2 Osmotic Tolerance Test	19
2.4 Discussion	
2.4.1 Growth Curves Comparing Different Media, pH levels and Osmolalities	21
2.4.2 Osmotic Tolerance Test	23
2.5 Summary	25
Chapter 3 - Development of Patch-clamp Methodology for Studying <i>Entomophaga</i> Protoplasts	
3.1 Introduction	33
3.2 Materials & Methods	
3.2.1 Culture Preparation	34
3.2.2 Recording Equipment & Methods	
3.2.2.1 Agar Bridges	35
3.2.2.2 Microelectrodes (Pipettes)	35
3.2.2.3 Recording Hardware	36
3.2.2.4 Measurement of Pipette Resistance	36
3.2.2.5 Pipette-cell Contact	38

3.2.2.6 Whole-cell Studies	38
3.2.2.7 On-cell Configuration - Single Channel Activity	40
3.2.2.7.1 140 mM Na ⁺ & 5 mM K ⁺ Recording Solutions	41
3.2.2.7.2 Sucrose & 11.5 mM NaCl Recording Solutions	42
3.2.2.7.3 Improving Chances of Gigaseal Formation	43
3.2.2.7.4 Formulation Changes to Reduce Channel Rundown	44
3.2.3 Setting Recording Period Guidelines	45
3.3 Results	
3.3.1 Pipette Size - Resistance Measurements	46
3.3.2 Pipette-cell Contact	46
3.3.3 Whole-cell Recordings	46
3.3.4 On-cell Single Channel Studies	
3.3.4.1 140 mM NaCl & 5 mM KCl Recording Solutions	47
3.3.4.2 Sucrose & 11.5 mM NaCl Recording Solutions	47
3.3.4.3 Improving Chances of Gigaseal Formation	47
3.3.4.4 Formulation Changes to Reduce Channel Rundown	49
3.3.5 Setting Recording Period Guidelines.....	49
3.4 Discussion	
3.4.1 Pipette Preparation & Size - Resistance Measurements	50
3.4.2 Pipette-cell Contact	51
3.4.3 Whole-cell Recordings	52
3.4.4 On-cell Single Channel Studies	56
3.4.4.1 140 mM NaCl & 5 mM KCl Solutions	58

3.4.4.2 Sucrose & 11.5 mM KCl Recording Solutions	59
3.4.4.3 Improving Chance of Gigaseals	60
3.4.4.4 Formulation Changes to Reduce Channel Rundown	62
3.4.5 Setting Recording Period Guidelines	63
3.5 Summary	64

Chapter 4 - Potassium Ion Channels in Protoplasts of *Entomophaga aulicae*

4.1 Introduction	86
4.2 Materials & Methods	
4.2.1 Culture Preparation	88
4.2.2 Recording Methods	89
4.2.3 Ramp Voltage Studies	90
4.2.4 Hyperpolarization Studies	91
4.2.5 Depolarization Studies	
4.2.5.1 Channel Recordings	92
4.2.5.2 Analysis of Multiple Current Level Recordings	92
4.2.5.3 Current-voltage Relationship	94
4.2.5.4 Channel Blockers	94
4.2.5.5 Effect of Elevated K ⁺ Levels on Conductance	95
4.3 Results	
4.3.1 Ramp Voltage Studies	97
4.3.2 Hyperpolarization Studies	97

4.3.3 Depolarization Studies	
4.3.3.1 Channel Recordings	98
4.3.3.2 Analysis of Multiple Current Level Recordings.....	98
4.3.3.3 Current-voltage Relationship	102
4.3.3.4 Channel Blockers	102
4.3.3.5 Effect of Elevated K^+ Levels on Conductance	102
4.4 Discussion	103
4.4.1 Ramp Voltage Studies	103
4.4.2 Hyperpolarization Studies	104
4.4.3 Depolarization Studies	
4.4.3.1 Channel Recordings	105
4.4.3.2 Analysis of multilevel channel recordings.....	105
4.4.3.3 Current-voltage Relationship	107
4.4.3.4 Channel Blockers	108
4.4.3.5 Effect of Elevated K^+ Levels on Conductance	109
4.4.4 Suggested Roles of Identified Channels	110
4.5 Summary	111
 Chapter 5 - Conclusions and Future Research	
5.1 Summary and Discussion of Findings	148
5.2 Future Research	151
 References	154

Appendix 1 - Data Acquisition Parameters

Ramp5S	168
Singles	171
Set-Up	174
K100MSD	177
K100MSH	180

Appendix 2 - Data Analysis Parameters

Demohist	184
-----------------------	------------

LIST OF FIGURES

Fig. 1.1	Patch clamp recording configurations	12
Fig. 2.1	<i>E. maimaiga</i> growth in two different media	26
Fig. 2.2	Effect of pH on <i>E. maimaiga</i> growth	27
Fig. 2.3	Effect of osmolality on <i>E. maimaiga</i> growth	28
Fig. 2.4	Osmotic tolerance of <i>E. maimaiga</i>	30
Fig. 2.5	Osmotic tolerance of <i>E. aulicae</i>	32
Fig. 3.1	Patch clamp recording equipment	65
Fig. 3.2	Patch clamp recording equipment -close up view	67
Fig. 3.3	<i>E. aulicae</i> protoplast with attached pipette	69
Fig. 3.4	Whole cell oscilloscope pattern.....	71
Fig. 3.5	Method for monitoring seal formation	73
Fig. 3.6	Whole-cell recordings	74
Fig. 3.7	Noise associated with 5X divalent cation bath solution	76
Fig. 3.8	Rundown of channel activity - cell 1	78
Fig. 3.9	Rundown of channel activity - cell 2	80
Fig. 3.10	No evidence of channel rundown	82
Fig. 3.11	Changes on protoplast morphology	84
Fig. 4.1	Ramp voltages - hyperpolarization activated channels	112
Fig. 4.2	Limited activity in response to Ramp voltages	114
Fig. 4.3	Depolarization sensitive channels using Ramp voltages	116
Fig. 4.4	Hyperpolarization activated channels - cell 1	118
Fig. 4.5	Hyperpolarization activated channels - cell 2	120

Fig. 4.6 Depolarization activated channels	122
Fig. 4.7 a Multiple current activity	124
Fig. 4.7b Current amplitude histogram	126
Fig. 4.8 Gaussian fit to current amplitude histogram	128
Fig. 4.9 Residuals plot of Gaussian fit in Fig. 4.8	130
Fig. 4.10 Current amplitude histogram	132
Fig. 4.11 Channel activity at 60, 80 and 100 mV	134
Fig. 4.12 Amplitude histogram of activity in Fig. 4.11	136
Fig. 4.13 Current-voltage relationship	138
Fig. 4.14 Channel activity at 80 mV	140
Fig. 4.15 Channel activity at 80 mV with 5 mM Ba ²⁺	142
Fig. 4.16 Channel activity at 80 mV with 10 mM TEA ⁺	144
Fig. 4.17 Effect of elevated K ⁺ levels on current-voltage relationship.....	146

LIST OF TABLES

Table 2.1	Effect of pH on generation times of <i>E. maimaiga</i>	18
Table 2.2	Effect of osmolality on generation times of <i>E. maimaiga</i>	20
Table 3.1	Whole cell recording solutions	40
Table 3.2	140 mM Na ⁺ & 5 mM K ⁺ recording solutions	42
Table 3.3	11.5 mM Na ⁺ & sucrose recording solutions	43
Table 3.4	Solutions with different level of divalent cations	44
Table 3.5	Solutions used to eliminate rundown	45
Table 3.6	Occurrence of gigaseals with changes to voltage and divalent cations	48
Table 4.1	Recording solutions for Ramp voltage studies	91
Table 4.2	Solutions for channel blocker experiments	95
Table 4.3	Solutions using elevated K ⁺ levels	96
Table 4.4	pSTAT generated data from current amplitude data	101

Chapter 1

General Introduction

1.1 The Organism

Entomopathogenic fungi belonging to the genus *Entomophaga* are potential biocontrol agents for use against forest defoliators and agricultural pests (Lacey and Goettel, 1995). Two species pathogenic to forest pests are currently being investigated in our laboratory. The host range of *E. aulicae* includes the eastern hemlock looper, *Lambdina fiscellaria* (Otvos et al., 1973), and eastern spruce budworm, *Choristoneura fumiferana* (Vandenberg and Soper, 1975). *E. maimaiga* is a pathogen of the gypsy moth, *Lymantria dispar* (Soper et al., 1988). Both *E. aulicae* and *E. maimaiga* are responsible for epizootics in the field (Otvos et al., 1973; Hajek et al., 1990).

The infection process and subsequent propagation of *E. aulicae* in spruce budworm larvae has been documented (Murrin and Nolan, 1987). Pathogenesis begins with the adhesion of fungal conidia to the cuticle. After conidia attach, they germinate and develop appressoria. At the site of appressorial development, electron-dense material is present in association with the fungal wall. Suggested roles of this material are to secure fungal/host attachment and for enzymatic digestion of the insect cuticle (Murrin and Nolan, 1987). Infection hyphae develop from the appressoria and penetrate the cuticle, underlying tissues and hemocoel. The cell wall of the infection hypha is not continuous at its tip. Protoplasts are released directly from the hyphal tip into the hemocoel. The wall-free protoplast phase of the fungal life cycle allows for easy nutrient uptake and rapid cell division in the hemocoel. This wall-free state also allows for avoidance of the host

immune system (Beauvais and Latgé, 1991).

Following protoplast proliferation, cell wall formation is initiated, resulting in the presence of hyphal bodies in the hemocoel. The fourth or fifth day of the infection process results in hyphal bodies in most of the insect tissue. Those located directly beneath the host cuticle produce conidiophores. These structures protrude through the cuticle. Conidia produced and ejected from the conidiophores may contact host larvae directly, or, they may germinate and produce secondary conidia. This completes the asexual life cycle of the fungus. Conidial discharge is dictated by environmental factors, with moisture being very influential. *E. maimaiga* infected gypsy moth have been shown to initiate and terminate sporulation when favorable and adverse relative humidity levels exist (Hajek and Soper, 1992).

The approach of using environmentally acceptable biocontrol agents for insect pests has led to the investigation of fungi as control agents (Lacey and Goettel, 1995). *E. maimaiga* has been shown to naturally control gypsy moth populations with 60-88% mortality (Hajek et al., 1990). The naturally occurring *E. aulicae* is pathogenic to major forest defoliators (Otvos et al., 1973). Based on the economic importance of controlling their host insects and the effectiveness of their pathogenesis, these two fungal species are candidates for biocontrol development. An artificial fermentation medium, supporting *E. aulicae* hyphal body production, has been developed using protoplast inoculum (Nolan, 1993). *E. aulicae* hyphal bodies have been shown to be viable for up to one year when produced *in vivo* and air dried (Tyrrell, 1988). These documented methodologies in production, drying and storage suggest that the development of inoculum for field application is attainable.

Entomophaga species also serve as model organisms for studies in fungal cell biology. They readily grow in artificial medium in their naturally-occurring protoplast state. This distinguishes them from most fungi that grow only as walled hyphae. Since protoplasts eventually form walled hyphal bodies, research on these cells are expected to contribute to the understanding of fungal morphogenesis (Farkas, 1985). Investigations involving *E. aulicae* protoplasts include those on genome composition, nuclear cycle, cytoskeletal distribution and adhesion properties (Murrin et al., 1986; Murrin et al., 1988; Taylor, 1992; Lake, 1994).

1.2 Osmolality

The identity of favourable growth conditions is required in the development of artificial media capable of supporting *E. aulicae* and *E. maimaiga* protoplast growth and proliferation. *E. aulicae* protoplasts lack cell wall material (Murrin and Nolan, 1987; Beauvais et al., 1989) that could otherwise serve as a protective barrier. An important factor in determining suitable artificial growth media is osmolality. Cell shrinkage, i.e., crenation or plasmolysis, can occur when the osmolality of a bath solution is high (Arnold, 1981). At low osmolalities, protoplast lysis can occur (Boulton, 1965).

Cells are generally capable of surviving some fluctuations in medium osmolality. Maintenance of cell volume is due to a balanced movement of solutes across the cell membrane (Sarkadi and Parker, 1991). Ion movement is performed by channels, or by coupling to cotransport or countertransport. Channel opening and closing as well as transport mechanisms respond to a number of stimuli including changes in cell volume (Hoffmann and Simonsen, 1989). When cells are subjected to solutions of low osmolality

they swell up due to the influx of water into the cell. The cells then decrease their volume by extruding solutes and water from their cytoplasm. Cells subjected to high osmolality solutions tend to shrink. This activates the intake of water and solutes, which causes a volume increase.

Microfilaments are believed to play a role in cell volume regulation since the use of microfilament-specific disruptive agents have been shown to affect volume regulation of cells. However, the mechanism by which the cytoskeleton is involved is not clear (Pierce and Politis, 1990).

In order to propagate protoplasts in artificial medium the identity of compatible osmolality levels is required. Commercially available osmometers have been used to measure solution osmolalities in *E. aulicae* studies (Dunphy and Nolan, 1979; Dunphy and Chadwick, 1985). The values generated by osmometers are in close agreement with theoretical calculations of a solution. The discrepancies are believed to be due to errors encountered in weighing the contents of the solutions. In theory, the osmolality of a solution can be determined by calculating the millimolar concentration of the ions present in a solution. Millimolar levels of components having a completely covalent nature are also determined. A solution's osmolality is the sum of the millimolar values of the ions and covalent compounds and has the units of milliosmoles (mOsm). Using this method one milliosmole is equivalent to one millimolar unit.

1.3 Ion Channels

1.3.1 Introduction

Ion movement across cell membranes is involved in a number of vital cell processes including osmoregulation (Hoffmann, 1992), cell growth (Kropf, 1994) and signaling (Neher, 1992). One way in which ions move across membranes is through ion channels. Ion channels are pore-forming proteins that traverse the cell membrane (Neher and Sakmann, 1992).

The opening and closing, i.e., gating, of channels can be triggered a number of ways (Garrill and Davies, 1994). Channels that open or close with changes in membrane potential are referred to as voltage-gated. Ligand-gated channels respond to the addition of a chemical. Channels that respond to mechanical stretching of the membrane are referred to as stretch-activated or mechanosensitive.

1.3.2 Patch Clamping

The patch clamp technique, first reported in 1976 (Neher and Sakmann, 1976), records current flowing across cell membranes through ion channels. The methodology is based on having a glass microelectrode tightly sealed onto a cell membrane. Current flowing through ion channels in the membrane is detected and recorded.

For recording, the cells are suspended in a bath solution. The microelectrode, a glass pipette filled with the pipette solution, is mounted over a silver wire coated with silver chloride. The terms pipette and electrode are used interchangeably for microelectrode. A gigaseal refers to a gigaohm level of seal resistance between the pipette and the membrane. A level greater than $1 \times 10^9 \Omega$, which equals 1 gigaohm, reduces background noise and allows for the detection of current levels in the picoampere (pA) range.

A number of recording configurations can be used for studying channel activity: each configuration has advantages and disadvantages (Sakmann and Neher, 1995a). The major configurations include cell-attached, whole cell, outside-out and inside-out. 'Cell-attached' mode (Fig. 1.1) consists of having an electrode on the cell membrane with a gigaseal level of resistance. This arrangement is non-invasive to the cell and allows the investigator to study the channel properties in a near-physiological environment. However, information on the cell's resting membrane potential cannot be determined. Also, since no access to the cytoplasm is made, changing the composition of the solutions on both sides of the membrane is not possible. This limits the amount of information one can obtain about the properties of a channel.

The 'whole cell' recording configuration is achieved by first forming a gigaseal with the pipette and membrane followed by disruption of the membrane in the patch by using a voltage pulse or suction (Fig. 1.1). This allows investigation of the ion channel population of the whole cell and a means of introducing agents to the cytoplasm through the pipette solution. Information on resting membrane potentials can be collected. A major limitation with this set-up, is the inability to easily change pipette solutions while working with the same cell.

'Outside-out' and 'inside-out' patch recordings again require a gigaseal at 'cell-attached' mode. The 'outside-out' name refers to a patch of membrane which has the non-cytoplasmic side, i.e., the outside, exposed to the bath solution. This is achieved by first achieving a 'whole-cell' configuration and then pulling the pipette away from the cell (Fig. 1.1). The membrane bilayer which then forms at the pipette tip is then oriented in the 'outside-out' fashion. An 'inside-out' patch has a portion of membrane on the pipette tip.

with the cytoplasm side of the membrane, i.e, the inside, exposed to the bath solution. It requires a gigaseal at 'cell-attached' mode. Then the pipette is pulled away from the cell pinching off a small portion of the membrane (Fig.1.1). After exposure to air, a patch of membrane remains on the pipette tip in the 'inside-out' orientation. With these two patch recording modes, one can easily change bath solutions which facilitates data collection on channel properties. However, some cytoplasmic factors controlling channel behaviour may be lost in these configurations (Sakmann and Neher, 1995a). These procedures are possible only with cells that adhere to the recording dish while pipette manipulation is performed. This drawback may limit applications of these techniques.

Transmembrane potential (V_m) is the potential at the cytoplasmic side of the membrane relative to the potential at the extracellular side of the membrane. In 'whole cell' recordings the pipette forms a continuum with the inside of the cell. Therefore the V_m equals that which is applied by the pipette (V_c). The resting membrane potential (RMP) does not affect the V_m in 'whole cell' recordings.

In 'cell-attached' recordings any voltage applied by the pipette (V_c) will not be the actual membrane potential (V_m). In fact $V_m = RMP - V_c$ (Axonnet, 1996). For example, an applied voltage, V_c , of -60 mV, the V_m is changed from its RMP to 60 mV more positive. Since one cannot determine the RMP of a cell during 'cell-attached' mode, the actual V_m is unknown. In this thesis, the relative change in the V_m , +60 mV in the above case, is the voltage referred to in discussions involving single channel studies.

1.3.3 Fungal Ion Channels

Ion channels have been found in the plasma membrane of a number of fungi.

Stretch-activated channels permeable to Ca^{2+} have been found in growing tips of *Saprolegnia ferax* (Garrill et al., 1992b; Levina et al., 1994). The channels are located in a tip-high gradient and are believed to be involved in hyphal tip growth (Garrill et al., 1992b). Another tip growing fungus, *Neurospora crassa*, also has stretch-activated channels involved in Ca^{2+} movement (Levina et al., 1995). However, they are not present in a tip-high gradient. A tip-high gradient of cytoplasmic Ca^{2+} is present in these cells and is associated with tip growth. Ca^{2+} transporting mechanosensitive channels have been incorporated in a proposed model of calcium regulation in fungal tips (Jackson and Heath, 1993).

Other mechanosensitive channels have been found in yeast (Gustin et al., 1986; Zhou and Kung, 1992). They may be involved in osmoregulation. Since they are Ca^{2+} permeable, they may also be involved in areas of new growth in the cell, i.e., yeast budding (Garrill and Davies, 1994).

Depolarizing voltage-activated channels involved in K^{+} efflux have been identified in the plasma membranes of *Saccharomyces cerevisiae* (Gustin et al., 1986; Bertl and Slayman, 1992). They may be involved in osmotic regulation. The large amounts of K^{+} may be accumulated in a cell during nutrient uptake. With a co-ordinated anion intake and opening of outward rectifying K^{+} channels, excess K^{+} could be eliminated (Bertl and Slayman, 1992). These channels may also be involved in charge balancing during proton-coupled transport. A K^{+} efflux has been noted in *Saccharomyces* during H^{+} -coupled maltose uptake (Serrano, 1977).

Ion channels have also been identified in fungal vacuolar membranes (Garrill and Davies, 1994). Voltage-activated and mechanosensitive K^{+} channels have been found in

this membrane as well as stretch-activated cation and cation/anion channels. Two recent review articles use schematic diagrams to summarize the types of channels present in fungi (Garrill and Davies, 1994; Garrill, 1994). The latter article focuses on transport processes used by fungi and includes carrier-mediated and pump mechanisms in addition to ion channels.

Investigations of the structure and function of ion channels is facilitated by their incorporation into foreign membranes (Elinder et al., 1996; Yu et al., 1996) or lipid bilayers (Chen and Miller, 1996). Recent applications of patch clamping in a fungal system involves the expression of transport proteins in yeast. Inward rectifying K⁺ channels from a plant, Kat 1, and guinea pig cells, gpIRK1, have been incorporated into the membrane of *Saccharomyces cerevisiae* (Bertl et al., 1995 and Tang et al., 1995, respectively). Expression in the yeast system resulted in functional ion channel behaviour. Oocytes from *Xenopus laevis* are often used for heterologous expression since they are large and easy to manipulate (Bertl et al., 1995). However, expression is not always successful using this system (Gaymard et al., 1996). The two 1995 studies (Bertl et al., 1995; Tang et al., 1995) show that *S. cerevisiae* can be used for heterologous protein expression. Therefore, the yeast system can be used as an alternative to expression in *Xenopus*.

1.4 Aims of this study

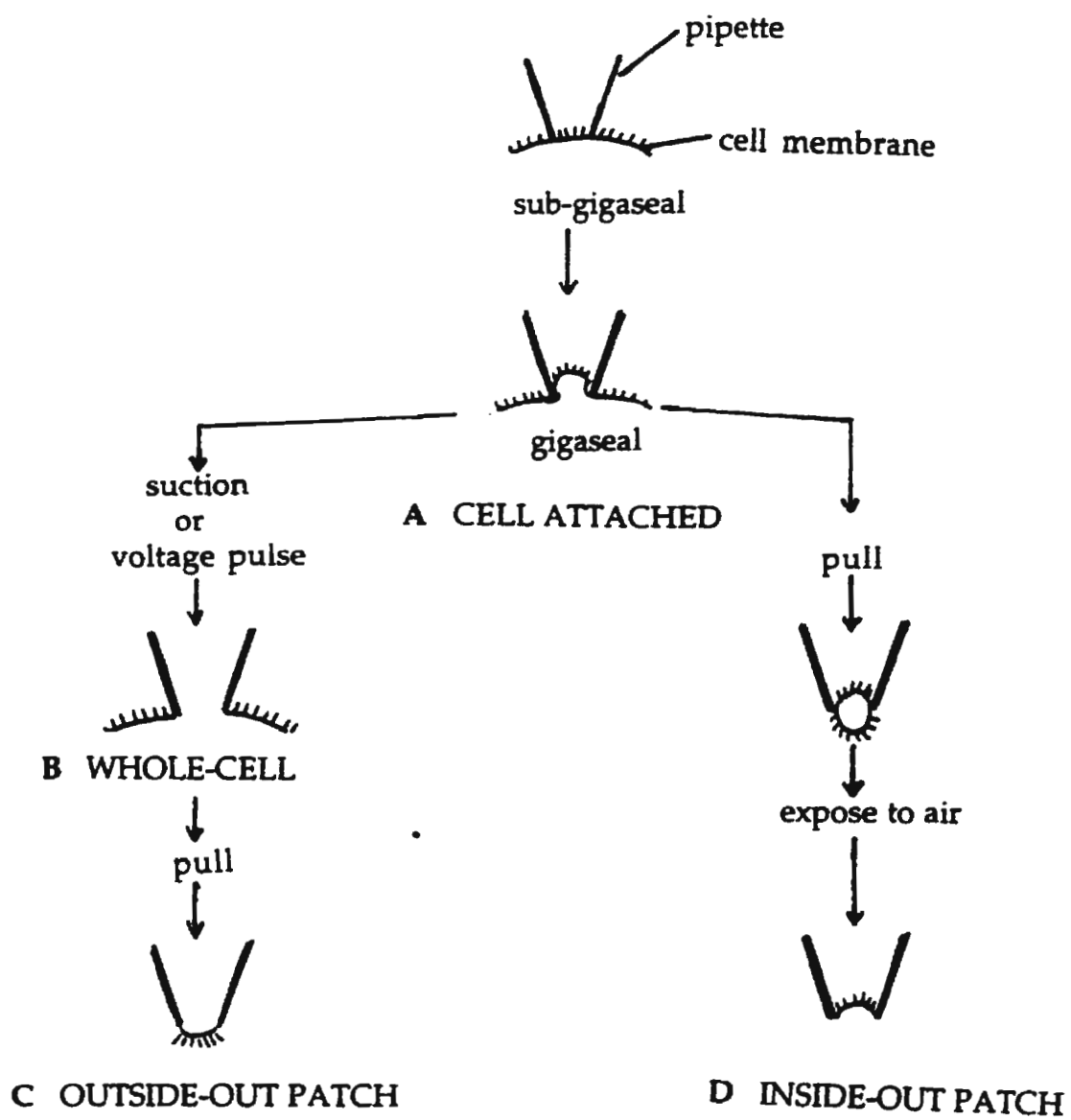
In order for *E. maimaiga* and *E. aulicae* to be used in field applications, mass production of infective propagules is required. Protoplast inoculum is used in mass

fermentation production of *E. aulicae* hyphal bodies (Nolan, 1993). The medium developed by Nolan has physical parameters that are compatible for *E. aulicae* protoplast growth. In order to identify a suitable medium for *in vitro* growth of *E. maimaiga*, appropriate growth conditions must be identified. Temperature effects on *E. maimaiga* have been investigated (Butt et al., 1994). However, the effects of osmolality and pH have not been studied. This study investigates the effects of these parameters on *E. maimaiga* protoplasts.

The second area of research undertaken here involves the area of membrane transport which may shed some light on the mechanisms of osmoregulation in protoplasts of entomophthoralean fungi. Since the introduction of patch clamp technology ion channel activity has been studied in a number of systems including fungi (Caldwell et al., 1986; Garrill et al., 1992a and 1992b; Levina et al., 1994; Levina et al., 1995). A major challenge in adapting the patch clamp technique to these organisms is the establishment of a gigaseal. The inability to form high resistance seals has been stated by investigators in a number of fields (Elzenga et al., 1991; Lew et al., 1992; Saimi et al., 1992). The main obstacle for high level pipette/membrane seals with plant and fungal cells is the existence of a cell wall. Since *E. aulicae* forms wall-free protoplasts spontaneously in artificial medium (Nolan, 1985), it is an attractive candidate for fungal patch clamp studies.

No patch clamp protocol exists for *E. aulicae* protoplasts. A major goal of my research was to develop a reproducible methodology from which ion channel activity could be assessed. Use of the developed protocols to identify *E. aulicae* protoplast ion channels constituted the final aspect of research undertaken.

Fig. 1.1: Patch clamp recording configurations. A, cell-attached; B, whole- cell; C, outside-out patch; D, inside-out patch. || | indicates the exterior of the cell.
(adapted from Sakmann and Neher, 1995a)



Chapter 2

pH and Osmotolerance of *Entomophaga* protoplasts.

2.1 Introduction

Entomophthoralean fungi have potential for use as biological control agents against a number of insects including major forest defoliators and agricultural pests (Lacey and Goettel, 1995). *Entomophaga maimaiga* a naturally occurring pathogen of gypsy moth, *Lymantria dispar* (Soper et al., 1988), has established epizootics in gypsy moth populations (Hajek et al., 1990). The closely related species, *E. aulicae*, is a pathogen of eastern hemlock looper (Otvos et al., 1973) and eastern spruce budworm (Vandenberg and Soper, 1975). It has been successfully grown under mass fermentation conditions, a major advance in the technology for development of entomophthoralean fungi as biocontrol agents (Nolan, 1993).

Protoplast formation is a naturally occurring phase in the life cycle of these fungi (Tyrrell, 1977; Soper et al., 1988). Protoplasts are released from the infection hypha as it enters the hemocoel where these spindle-shaped cells multiply in the nutrient-rich hemolymph prior to wall formation (Murrin and Nolan, 1987). Protoplast inoculum is important for mass fermentation production of infective cells and requires a medium with physical parameters compatible with protoplast growth (Nolan, 1993). Thus, identifying appropriate growth conditions for protoplasts is crucial for development of these fungi for biocontrol purposes.

Previous studies of *E. aulicae* concentrated on identifying an optimal value for pH and osmolality (Dunphy and Nolan, 1979; Dunphy and Chadwick, 1985) in which the criterion used to assess these parameters was cell yield at mid-log phase growth. Although

the effect of temperature on *E. maimaiga* has been investigated (Butt et al., 1994) pH and osmolality effects have not. The focus of this study was to identify ranges of pH and osmolality tolerated by *E. maimaiga* protoplasts. Growth of the organism through both log and stationary phases was monitored in different test solutions. In addition, an assessment of osmotic tolerance based on the effects of solution osmolality on protoplast morphology was performed with both *E. maimaiga* and *E. aulicae*.

2.2 Materials & Methods

2.2.1 Stock Cultures.

Protoplasts of *Entomophaga maimaiga* (isolate FPMI 990-4 s12B) and *E. aulicae* (isolate FPMI 646) were maintained at 20⁰ C in modified Grace's insect tissue culture medium (GM, Canadian Life Technologies, Inc., Burlington) supplemented with 2.7% fetal calf serum (FCS, as above). In this paper this medium will be referred to as GM+FCS.

2.2.2 Growth Curves Comparing Different Media, pH Levels and Osmolalities.

Growth of protoplasts of *E. maimaiga* was initially compared in GM+FCS and a modification of the basal medium described previously (Nolan, 1993). The modified basal medium was used for all subsequent experiments and consisted of the following changes: glucose and sucrose levels of 0.3g/10L and 338g/10L respectively as well as the addition of 2.7% FCS. This medium will be referred to as BM+FCS. The pH was adjusted to 6.2 using 3N NaOH and the medium filter sterilized through a 0.45 μ pore size Nalgene disposable filter unit prior to the addition of the FCS.

Media with different pH values were prepared from BM+FCS using 3N NaOH and 3N HCl for pH adjustments. pH manipulation was performed prior to the addition of FCS.

Media of different osmolalities were prepared by altering sucrose levels of BM+FCS. Theoretical milliosmolar (mOsm) calculations were confirmed by osmolality readings from an Osmette A Automatic Osmeter (Precision Systems, Inc.) Thirty millilitres of medium were added to duplicate, oven sterilized, 125ml Bellco flasks. They were inoculated with 1×10^4 cells delivered in a 0.1 ml volume of a 24-48 hour old culture. Flasks were incubated at 20°C in a New Brunswick Scientific Controlled Environment Incubator at 100 rpm.

All counts were made using an Almedic haemocytometer. Individual uninucleate protoplasts and each nucleate swelling on a multinucleate protoplast chain were recorded as one cell. The average count from four haemocytometer chambers was recorded. Cell counts were performed until clumps of hyphal bodies were noted.

Generation time calculations were determined by the following mathematical expression for exponential cellular growth: $2 = e^{rt}$ where t is the generation time and r is the rate of increase in the natural log of cell numbers (Rhodes and Fletcher, 1966). All statistical analysis was determined using Minitab Statistical Software (Release 9.1, Minitab, Inc. University Park, PA). The approach was General Linear Model (GLM)-based. Type I error (α) was set at 0.05 for numerical analysis.

2.2.3 Osmotic Tolerance Test.

Test solutions from zero to 550 mOsm, at pH 6.2, were prepared as follows. The 0

mOsm test solution consisted of distilled water. The 10 mOsm solution was 10 mM 2-(*N*-morpholino) ethanesulfonic acid (MES). The 150-550 mOsm solutions consisted of 10 mOsm MES with additions of sucrose to attain their respective osmolality values. The Osmette A Automatic Osmometer was used to validate mOsm levels.

Equal aliquots from a 24–48 hour protoplast culture in GM+FCS were centrifuged at 150xG for 5 minutes in 15ml Falcon conical centrifuge tubes. Duplicate pellets were resuspended in test solutions for 1 hour at room temperature without shaking, and then examined by light microscopy for cell numbers and shape. Control pellets were resuspended in GM to determine the number of cells subjected to each treatment.

Cell viability was determined using duplicate 30 ml volumes of GM+FCS inoculated with 0.3 ml volumes from the different test solutions. Growth conditions were as stated above. Cell concentration levels were monitored using a haemocytometer as described above.

2.3 Results

2.3.1 Growth Curves Comparing Different Media, pH Levels and Osmolalities.

The growth pattern of *E. maimaiga* in BM+FCS was similar to that of growth in GM+FCS (Fig. 2.1). Growth in the two media did not significantly differ ($F_{[1,24]}=2.93$ $p=0.100$). This is based on a GLM with log transformed cell concentration values. Generation times (GTs) for the two media were 9.0 hours for BM+FCS and 10.1 hours for

GM+FCS

E. maimaiga grew at all pH levels tested, but at the lowest pH levels reduced growth was noted (Fig. 2.2). There is a significant difference in growth of *E. maimaiga* in media of different pH ($F_{[6,54]}=11.85$ $p<0.001$). This is based on a GLM incorporating log transformations of both cell concentration and time values as well as a time-based level at 80 hours. Based on further analysis of the data using Gabriel's Approximate Method (Sokal and Rohlf, 1995), growth in media with pH values ranging from 5.8 to 7.1 do not significantly differ (lower and upper limits for regression coefficients were as follows: 2.951 to 4.009 for pH 5.8, 3.298 to 7.760 for pH 6.0, 3.001 to 5.559 for pH 6.2, 3.442 to 5.058 for pH 6.5, 2.940 to 6.020 for pH 6.8 and 3.088 to 5.272 for pH 7.1). However, growth at pH 5.5 does differ significantly from the others (lower and upper range: 0.986 to 2.894). This is evident from the generation times obtained from the growth curves (Table 2.1). The GT for growth in pH 5.5 medium was 20.75 hours whereas the GT for growth in the pH 5.8 to 7.1 media ranged from 10.0 to 12.01 hours. The correlation coefficient, r , for pH ranging from 5.8-7.1 and generation time was - 0.103.

Table 2.1: Effect of pH on generation time of *Entomophaga maimaiga*.

pH ^a	Generation Time ^b (hours)
5.5	20.75
5.8	12.01
6.0	10.28
6.2	10.98
6.5	10.88
6.8	10.00
7.1	11.75

^a medium is BM+FCS

^b derived from exponential cellular growth equation

$2 = e^{rt}$ (Rhodes & Fletcher, 1966).

Growth patterns in medium with osmolality values of 250 to 400 mOsm were very similar (Fig. 2.3). Statistical analysis resulted in the decision that no significant difference in growth exists between the media of different osmolalities tested ($F_{[6,54]} = 0.88$

$p=0.518$). This is based on a model with a log transformation of the cell concentration values with the addition of a time-based level at 80 hours. The shortest GT, 8.76 hours, was found with 350 mOsm medium (Table 2.2). However, the GTs across the osmolality spectrum tested exhibited little deviation with a mean value of 9.36 ± 0.54 hours. The correlation value, r , for osmolality and GT is 0.533 suggesting little association between the two.

2.3.2 Osmotic Tolerance Tests.

The osmotic tolerance tests resulted in the loss of some cells through lysis, the adoption of a round shape by a number of cells and the retention, by other cells, of the characteristic spindle shape. The percent distributions of these three cell types in the solutions of different osmolality are given for *E. maimaiga* (Fig. 2.4) and *E. aulicae* (Fig. 2.5). The general pattern of cell types was the same for both species. The highest level of cell loss was in the 0 mOsm solution. At this osmolality only round cells were noted representing 30 to 45% of control cells. For both species, the highest numbers of round cells were associated with the 10 mOsm treatment. Spindle shaped cells were found in solutions of osmolality equal to or greater than 150 mOsm with the highest levels of these cells at 550 mOsm. Growth was noted in all GM+FCS inoculated flasks with the initiation of logarithmic phase growth occurring 55-70 hours after inoculation. Therefore, cells survived all osmolality treatments.

Table 2.2: Effect of osmolality on generation time of *Entomophaga maimaiga*.

Osmolality ^a (mOsm)	Generation Time ^b (hours)
250	9.05
275	9.11
300	9.72
325	8.87
350	8.76
375	10.03
400	10.00

^a medium is BM+FCS

^b derived from exponential cellular growth equation

$2 = e^{rt}$ (Rhodes & Fletcher, 1966).

2.4 Discussion

The major focus of this paper was to determine the tolerance of *E. maimaiga* to different osmolality and pH levels. Whereas earlier studies identifying optimal growth conditions for *Entomophaga aulicae* protoplasts were based on cell concentration values at mid-log phase growth (Dunphy and Nolan, 1979; 1982), we used a statistical modelling approach for data evaluation. By using a General Linear Model method, the complete growth curve was used in the analysis. This advantage of having all growth information incorporated in the analysis makes it an attractive approach for assessing physical

parameter tolerance.

2.4.1 Growth curves comparing different media, pH levels and osmolalities.

In order to determine optimal pH and osmolality levels for *E. maimaiga*, a medium that would accommodate pH and osmolality adjustments was required. Commercially available Grace's medium cannot accommodate reductions in osmolality. Due to the complexity of Grace's medium identification of a more simplified preparation was desirable. A highly modified Grace's medium, BM+FCS (Nolan, 1993), was investigated for its ability to support *E. maimaiga* growth. Using GM+FCS as the benchmark medium, the growth of *E. maimaiga* in BM+FCS was assessed. The resultant growth curves (Fig. 2.1) clearly showed the ability of *E. maimaiga* growth in BM+FCS to mimic that of growth in GM+FCS. The close agreement of the GTs, 9.0 and 10.1 hours for BM+FCS and GM+FCS respectively, suggested that these media are comparable in supporting growth of *E. maimaiga*. In fact, statistical analysis of the growth curve data resulted in the decision that there was no significant difference in the growth between these media ($F_{[1,24]}=2.93$ $p=0.100$). Based on this information and the relative ease of preparation, BM+FCS was deemed appropriate for use in pH and osmolality studies.

E. maimaiga growth was supported in BM+FCS with pH levels ranging from 5.5 to 7.1 (Fig. 2.2). This is in agreement with earlier reports on *E. aulicae* protoplasts and walled cells (Dunphy and Chadwick, 1985; Vandenberg and Soper, 1975). The GT was 20.75 hours for the pH 5.5 medium (Table 2.1). This parameter was reduced to 12.01 hours when the media's pH was 5.8. This suggests protoplast sensitivity at pH values in the acidic range below 5.8. GLM-based statistical analysis of pH growth curve data identified pH as having a significant effect on cell growth ($F_{[6,54]}=11.85$ $p<.001$). For

further analysis, Gabriel's Approximate Method was chosen. The results from this computation indicate that there is no difference in *E. maimaiga* growth in media ranging from pH 5.8 to 7.1. However growth in media with a pH value of 5.5 significantly differs from that in media of higher pH. This is based on the fact that the upper and lower limits of the regression coefficients overlap for pH 5.8-7.1 but do not for pH 5.5. This documented sensitivity to acidic pH may be due to a number of factors. pH indirectly affects cell growth through changes in the extracellular medium or on the cell surface (Griffin, 1994). Medium constituents may become unavailable due to precipitation at low pH levels. Acidic pH levels may also be detrimental to components on the outer membrane surface involved in metabolic processes.

The shortest GTs were found in the 5.8 to 7.1 range with the lowest value of 10.00 hours at pH 6.8 (Table 2.1). However, the second shortest GT was found in the pH 6.0 medium. A pattern of pH/GT association is evident when the data is grouped in GTs less than or greater than 11 hours. This results in a pH 6.0-6.8 group with a mean GT value of 10.54 ± 0.47 hours and a pH 5.8/7.1 group having a mean GT value of 11.88 ± 0.18 hours. GT calculations are based on only logarithmic phase growth. Therefore protoplasts of *E. maimaiga* do not have one optimal pH level but rather a favourable pH range of 6.0 to 6.8 for log phase growth. Based on mid-log phase cell concentration levels, *Entomophaga* species have been documented as having optimal pH values of 6.2 for *E. aulicae* and 6.7 for *E. grylli* (Nolan, 1985). These values are in agreement with the acceptable range found for *E. maimaiga*.

In order to investigate the effect of osmolality on protoplasts, sucrose levels were adjusted to achieve the desired osmolality levels. This compound was chosen since it is

not metabolized by a number of entomophthoralean species (Latgé, 1975). The *E. maimaiga* growth pattern did not vary in 250 to 400 mOsm media (Fig. 2.3). No significant effect by osmolality on growth was derived by statistical analysis ($F_{[6,54]}=0.88$ $p=.518$). The GTs of the cells grown in different media (Table 2.2) show little deviation (mean = 9.36 ± 0.54). No clear pattern of osmolality/GT association is evident as reflected by the value of the correlation coefficient ($r=0.503$). Based on this information, it is proposed that the protoplast has an osmoregulation system capable of sustaining comparable growth in media with osmolality levels from 250 to 400 mOsm.

2.4.2 Osmotic tolerance tests

Earlier studies (Dunphy and Nolan, 1979; Dunphy and Chadwick, 1985) based optimal osmolality on the ability of the medium to retain spindle protoplast morphology. This approach was adopted for *E. maimaiga* to further investigate the osmotolerance of this organism. Our results (Fig. 2.4) showed that cell responses fit into three categories. These included cells that maintained their spindle shape, those that became round due to depolymerization of shape-maintaining microtubules (Taylor, 1992) and those that were lost through lysis in the most extreme hypo-osmotic media. The percent of cells lost due to a treatment was also recorded. In some cases, the total number of cells enumerated exceeded the average number of control cells. The percent difference is displayed as a negative value of lysed cells. Observations of increased cell numbers may be due to the occurrence of cytokinesis during processing or an error in counting individual nucleate swellings in protoplast chains that have coalesced with one another, i.e., formed fusion spheres (Nolan, 1985). Fusion spheres are inherent to *in vitro* growth of *Entomophaga*

species and therefore cannot be avoided. This source of error would be present in lower osmolality solutions too. Assuming a uniform degree of counting error with fusion spheres and a uniform level of cytokinesis, the effects would be evenly distributed over all of the treatments and the trends resulting from the osmotic tolerance tests remain valid.

Protoplasts maintained spindle morphology at osmolality levels equal to or greater than 150 mOsm. The highest level, 98.8%, was found at 550 mOsm. The second highest level was 91.4% at 450 mOsm. Growth of these treated cells in GM+FCS is evidence that they were viable. These data suggest that *E. maimaiga* protoplasts are osmotolerant at high osmolality levels. At the other end of the spectrum, 0 mOsm, the majority of the cells were lost but 45.7% of the cells maintained intact membranes and adopted a round cell shape. Some of these cells were viable since when transferred to GM+FCS, growth was noted. Based on these data, *E. maimaiga* is an osmotolerant organism. It is not known whether or not this is due to an osmoregulation mechanism, a tough cell membrane or a combination of the two.

The range of osmotolerance of *E. maimaiga* led us to question whether this trend was common with other *Entomophaga* species. *E. aulicae* showed a similar trend of cell survival at low osmolality levels and a high level of spindle shape retention in the 350 to 550 mOsm range (Fig. 2.5). Again, survival across the osmolality range tested was noted. All of the GM+FCS flasks inoculated with treated cells supported growth. Dunphy and Chadwick (1985) showed a peak percent spindle protoplast level at 350 to 375 mOsm for *E. aulicae* with a significant drop at 400 mOsm. The isolate used in this study approached maximal percent spindle protoplasts in solutions of 450-550 mOsm. This suggests that broad range osmotolerance may be isolate specific.

Both transmission electron microscopy and fluorescence microscopy show that protoplasts of *E. aulicae* are devoid of cell wall material (Murrin and Nolan, 1987; Beauvais et al., 1989) and indeed possess a glucan synthetase inhibitor (Beauvais, 1989). Based on light microscopy, their tendency to round up quickly in hyposmotic media, and on fluorescence microscopy using wheat germ agglutinin-FITC labelling, protoplasts of *E. maimaiga* are also devoid of wall material which might otherwise contribute to osmotic tolerance (unpublished results). Thus the mechanism by which some of these cells survived the osmolality extremes used in this study warrants further investigation.

2.5 *Summary*

E. maimaiga protoplasts are capable of broad range pH and osmotic tolerance. No significant difference in growth was found in 350 mOsm medium ranging in pH from 5.8 to 7.1. At a pH level of 5.5 growth was adversely affected. Also no difference in growth was found in pH 6.2 media ranging from 250 to 400 mOsm. Further investigation of osmotic tolerance showed that *E. maimaiga* and *E. aulicae* protoplasts are capable of surviving one hour treatments in solutions ranging in osmolality from 0 to 550 mOsm. The mechanism involved in osmoregulation by these organisms is not clear and warrants further investigation.

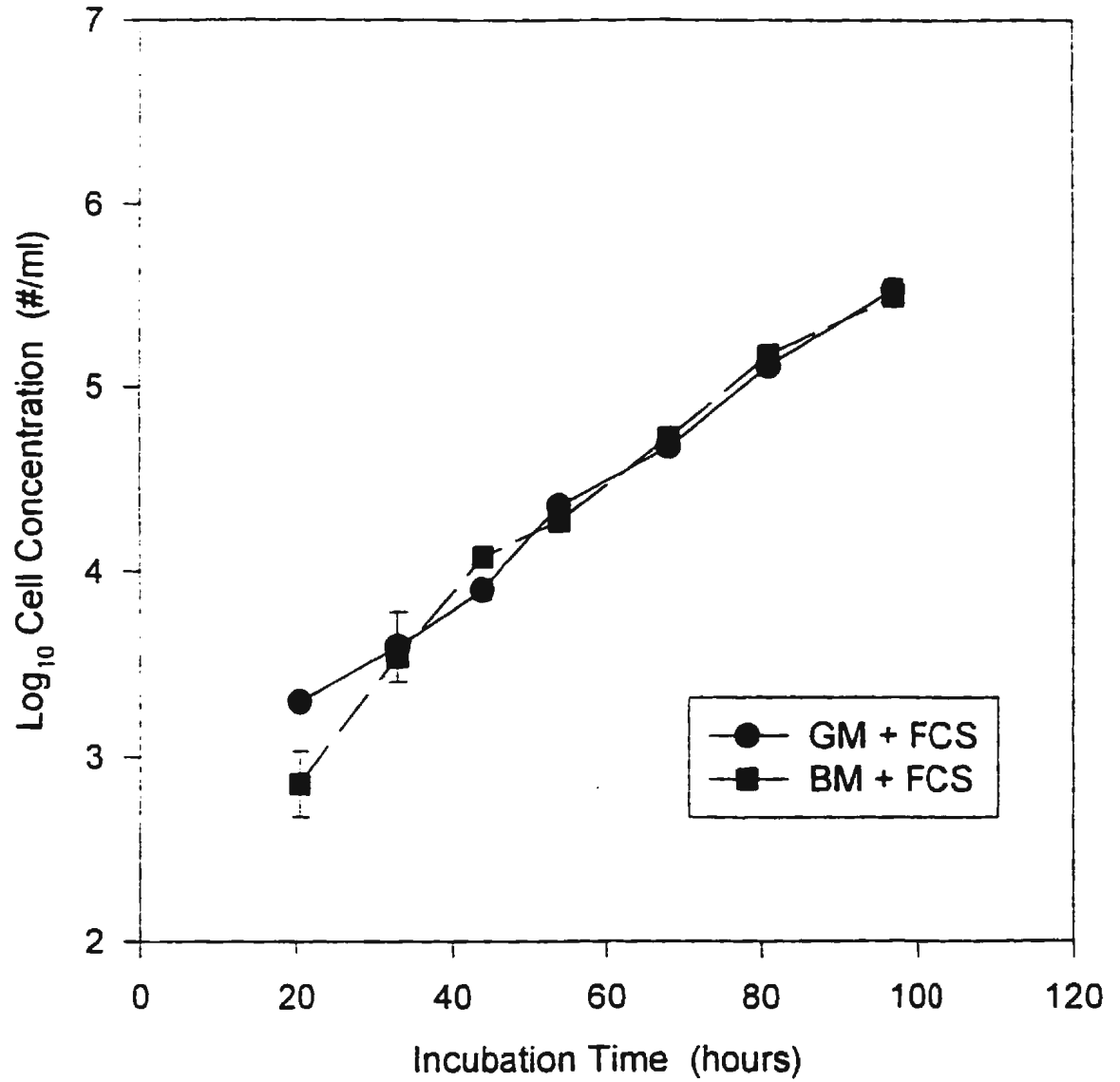


Fig. 2.1: Comparison of growth of *Entomophaga maimaiga* in GM+FCS and BM+FCS. Data points represent mean \pm standard error (SE) of duplicates. SE values in most cases less than symbol size.

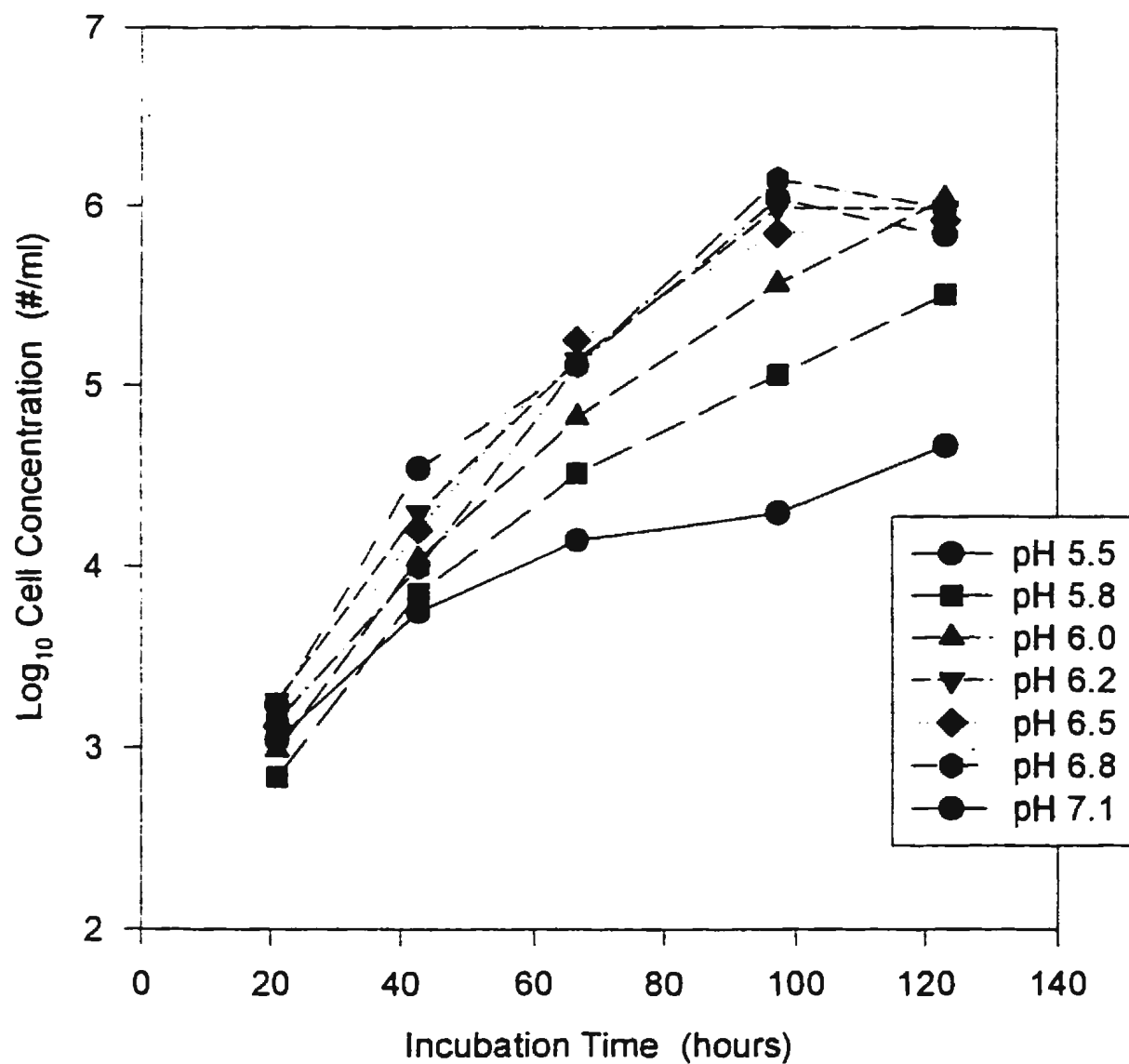


Fig. 2.2: Effect of media pH on growth of *Entomophaga maimaiga*.
Media is BM+FCS. Data points represent mean of duplicates.

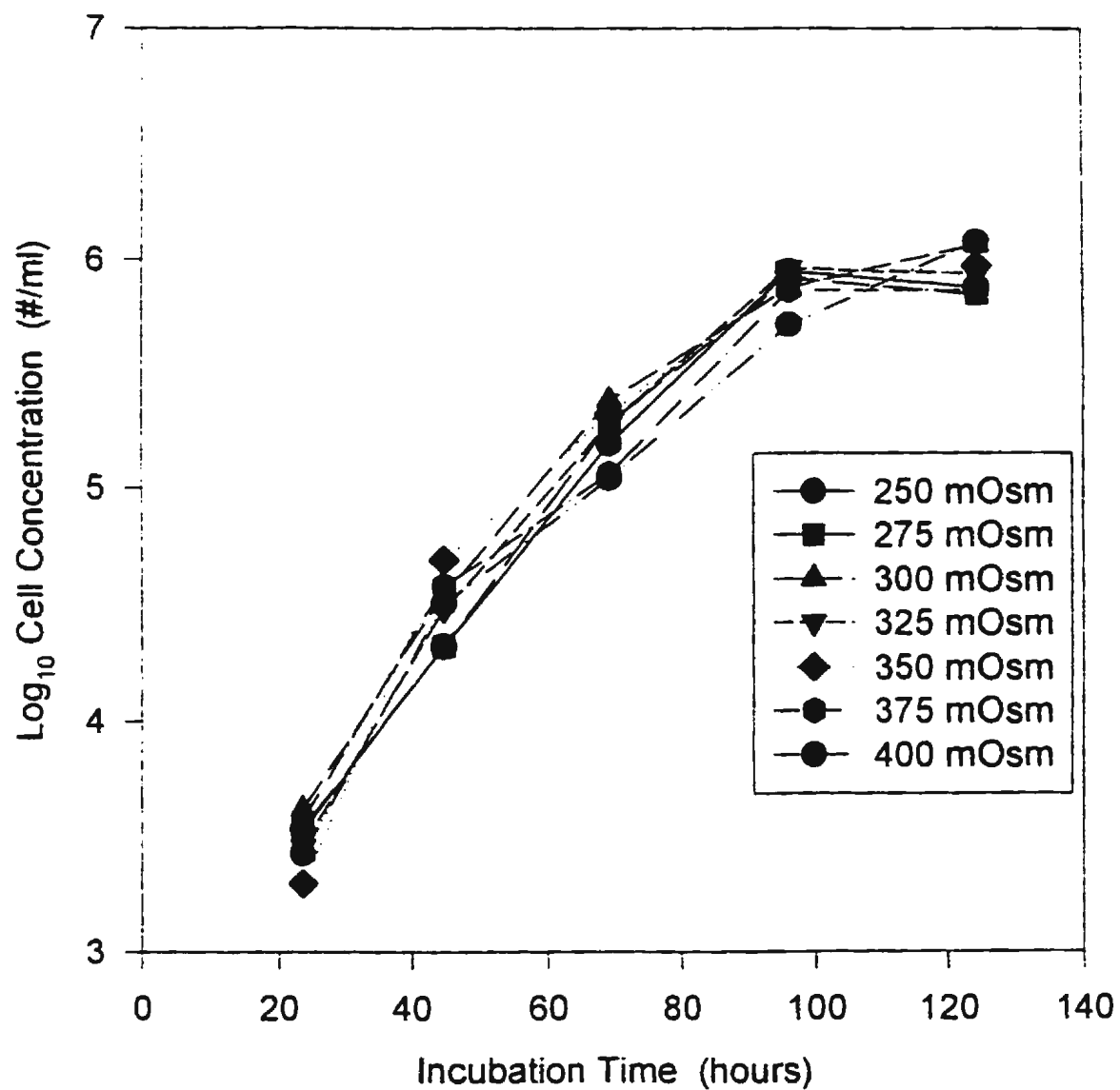


Fig. 2.3: Effect of medium osmolality on growth of *Entomophaga maimaigu*. Media is BM+FCS. Data points represent mean of duplicates.

Fig. 2.4: Osmotic tolerance of *Entomophaga maimaiga*. Values are mean of duplicates. Data shown is from one trial. Two earlier trials ranging in medium osmolality from 10 to 600 mOsm had similar patterns. In some cases, the total number of cells enumerated exceeded the average number of control cells. The percent difference is displayed as a negative value of lysed cells.

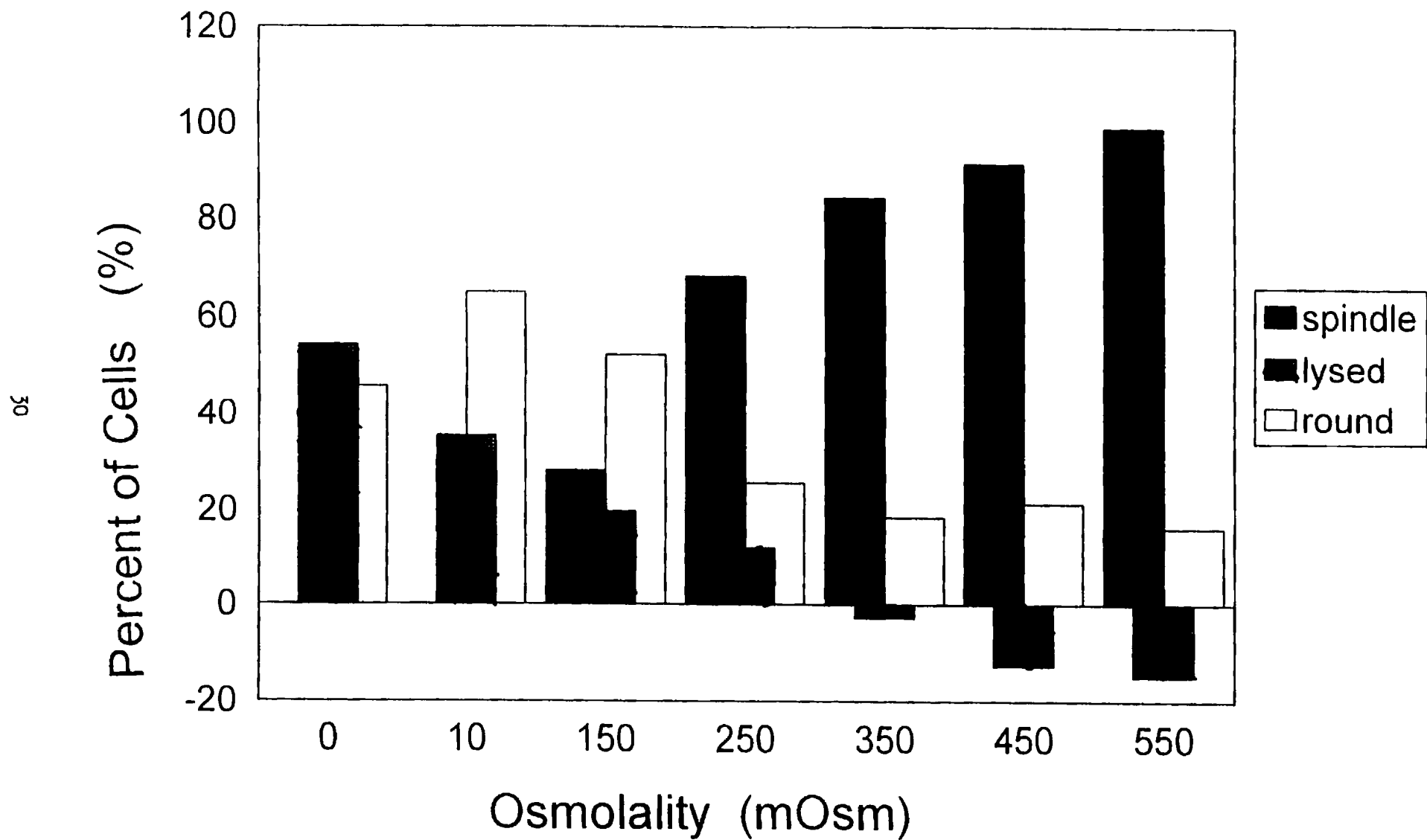
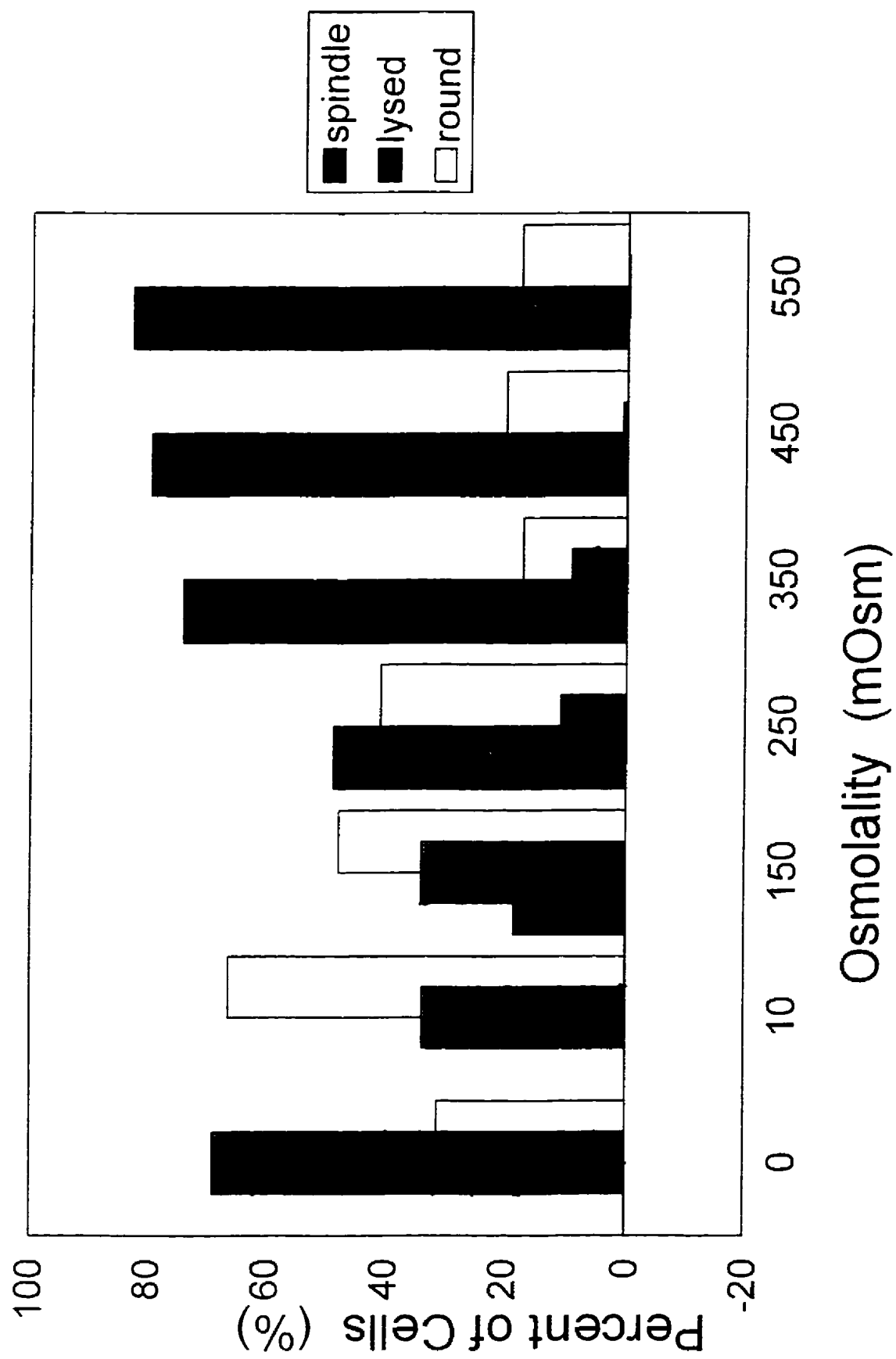


Fig. 2.5: Osmotic tolerance of *Entomophaga aulicae*. Values are mean of duplicates.
Data shown is from one trial. An earlier trial had a similar pattern.



Chapter 3

Development of patch-clamp methodology for studying *Entomophaga aulicae* protoplasts.

3.1 Introduction

The study of the movement of ions across cell membranes is of interest since their transport is involved in cell signalling (Neher, 1992), growth (Kropf, 1994) and osmoregulation (Hoffmann, 1992). With the introduction of the patch clamp technique (Neher and Sakmann, 1976) came the ability to study current flow across cell membranes through ion channels. The methodology is based on having a glass microelectrode tightly sealed onto a cell membrane. The ion-generated current, flowing through channels in the membrane, is detected and recorded. In order to detect small current fluctuations, in the picoAmpere range, the level of seal resistance between the pipette and membrane should be in the gigaOhm range, i.e. a gigaseal.

Investigators studying plant, bacterial and fungal systems have reported an inability to form high resistance seals (Elzenga et al., 1991; Saimi et al., 1992; Lew et al., 1992). The cell wall of plants and fungi interfere with the formation of a high level pipette/membrane seal. Protocols incorporating the enzymatic digestion of wall material have been developed for some systems (Barbara et al., 1994; Garrill et al., 1992b). However, even with the removal of the cell wall, gigaseal recordings are rare in some fungal systems (Lew et al., 1992; Levina et al., 1994; Levina et al., 1995).

The entomopathogenic fungus, *Entomophaga aulicae*, spontaneously forms protoplasts *in vivo* (Tyrrell, 1977) and *in vitro* (Nolan, 1985) and these cells show a broad

range of osmotolerance (Chapter 1). The mechanism by which this osmotolerance is maintained is unknown but may include the activity of ion channels in the protoplast membrane. The easy propagation of *E. aulicae* in artificial medium as a protoplast is a desirable feature for patch clamping studies, since no wall digestion protocol is required. However, a protocol generating reproducible, high quality patch clamp recordings for this fungal system does not exist.

This chapter documents the parameters investigated during the development of a patch clamping methodology suitable for *E. aulicae* protoplasts. The appropriate recording configuration, pipette size, recording solutions and optimal recording times for attaining gigaseal-generated data are identified.

3.2 Materials and Methods

3.2.1 Culture Preparation

Entomophaga aulicae (isolate FPMI 893) protoplasts were maintained at 20°C in Grace's insect tissue culture medium (Canadian Life Technologies, Inc.) supplemented with 2.7% fetal calf serum (Canadian Life Technologies, Inc.).

Culture dishes for cell recording were prepared from 35x10 mm petri dishes (Becton Dickson Labware). A 15mm diameter circular disk was excised from the bottom of each dish and discarded. Glass coverslips, 22x22 mm, were ethanol cleaned. Prior to assembly, the culture dishes, coverslips and a syringe filled with valve lubricant/sealant (Dow Corning 111 Compound) were UV sterilized. Using a thin layer of the sealant, the coverslip was mounted on the exterior of the dish bottom covering the excised area. The

assembled dishes were UV sterilized prior to use.

A 24-hour culture was transferred to a 15 ml conical centrifuge tube, centrifuged at 150xG for 5 min and the pellet resuspended in the appropriate recording bath solution. Approximately 30 minutes after introduction of the bath solution, an aliquot of the cell suspension was transferred to the coverslip section of a prepared culture dish.

3.2.2 Recording Equipment & Methods

All preparation and experimentation was performed at room temperature.

3.2.2.1 Agar Bridges

Agar bridges were prepared from glass capillary tubes (Drummond Scientific Co.) bent at a 90° angle. They were filled with a solution consisting of 2%(w/w) agar (Difco Laboratories) prepared in the appropriate recording bath solution. Bridge holders were filled with the same bath solution passed through a 0.22 µm syringe filter.

3.2.2.2 Microelectrodes (Pipettes)

Patch pipettes were made from fiber-filled borosilicate glass capillary tubes (World Precision Instruments, Inc., Narco Scientific). They were cut on a two stage vertical puller (Narishige Model PP-83, Japan). For single channel recording studies, the pipettes were heat polished to assist in forming pipette/membrane seals. They were heated for 3 seconds at approximately 800µm from a wire passing a 1.7 ampere current at 0.5 volts. Heat polishing was viewed at 100x magnification with a Micromaster microscope. Pipette solutions were passed through a 0.22µm syringe filter and then loaded in a finely

tapered, heat-pulled, 1 ml syringe. The pipettes were filled by placing the tapered end of the syringe in the patch pipette and moving it to the tip. Application of pressure to the syringe while pulling it away from the tip of the pipette resulted in a backfilled pipette. Pipettes were inspected for evidence of bubbles and, if present, were dislodged by tapping the pipette. The tips were then dipped in Sigmacote (Sigma Chemical Co.) and mounted on the pipette holder with care being taken to minimize glass contact with the electrode wire.

3.2.2.3 Recording Hardware

The hardware used for all recordings consisted of the following components: Zeiss IM-35 inverted microscope, Zeiss micromanipulator, List patch clamp probe and controller L/M-EPC7 (Medical Systems Corp) with a 10 kHz filter setting, TL-1 Interface (Axon Instruments, Inc.), and a Nicolet Model 310 digital oscilloscope. An IBM compatible Impulse computer with a Samsung monitor was used to control and monitor data acquisition. For equipment orientation refer to Fig. 3.1. A close-up view of the equipment located in the area of the microscope stage is found in Fig. 3.2.

3.2.2.4 Measurement of Pipette Resistance

The protocol used for measuring pipette and seal resistance was as follows. The amplifier was set on Search mode. Using PCLAMP version 5.5.1 (Axon Instruments, Inc.) the Clampex Set-Up data acquisition program (see Appendix 1) was initiated. This ran a +10mV pulse. The oscilloscope grid size was set at 250mV per square and the amplifier had a gain of 1 pA/mV. The pipette was lowered to the bath solution while

applying a slight positive pressure in the pipette. The oscilloscope trace was viewed and the transient spikes reduced resulting in a plateau-like oscilloscope pattern. The height of the plateau, measured in both grid squares (*gsq*) and grid voltage (*gv*) of one square, was recorded. The calculation of pipette resistance was based on the following equation:

$$R = \frac{V}{I} \quad (\text{Eq'n. 3.1})$$

where

R = resistance (Ohms),

V = voltage (volts)

I = current (pico amps (pA))

and where

$$I = (\text{gain}) \cdot (\text{gsq } \#) \cdot (\text{gv } \#) \quad (\text{Eq'n. 3.2})$$

Since the applied voltage in Set-Up was 10mV and the gain setting was 1 pA/mV the above equation was simplified in the following manner:

$$\begin{aligned} R &= \frac{10 \times 10 \text{ volts}}{1 \frac{\text{pA}}{\text{mV}} \cdot \text{gsq } \# \cdot \text{gv } \# (\text{mV})} & (\text{Eq'n. 3.3}) \\ &= \frac{1 \times 10 \text{ volts}}{1 \times 10^{-12} \text{ A} \cdot \text{gsq } \# \cdot \text{gv } \#} \\ &= \# \text{ ohms } (\Omega). \end{aligned}$$

The calculated resistance values of the pipette were recorded.

3.2.2.5 Pipette-cell contact

Before proceeding to cell attachment, offset potentials were reduced by adjusting the pipette offset control until the corresponding voltage LED reading approached zero.

In general, initiation of gigaseal formation consisted of running the same SET UP data acquisition software as stated earlier. While viewing the cells at 400x magnification, the pipette was brought into close proximity of a cell. The pipette was positioned near a cell, by use of a micromanipulator, and then pushed up against it. During this procedure, care was taken to choose only the cytoplasmic-rich areas of the nucleate region of the cell while avoiding terminal extensions, internuclear restrictions and vacuolated areas. Fig. 3.3 shows a typical uninucleate cell with an attached pipette. Suction was applied to the pipette, held for approximately 30 seconds and gently released. During the 30 second suction period, the rapid transients were reduced using the fast capacitance controls.

3.2.2.6 Whole-cell Studies

After achieving pipette-cell contact, as described in section 3.2.2.5, preparation for whole-cell recording could be made. Attainment of whole cell mode was based solely on the transient pattern viewed on the oscilloscope. An acceptable pattern consisted of a sharp vertical rise in the current at the beginning of the SET UP 10 mV pulse, followed by an exponential decay to the baseline (Fig. 3.4). When this pattern was obtained, the amplifier was switched to current clamp (CC) mode and the resting membrane potential

was recorded. With the amplifier mode at voltage clamp (VC), data acquisition programs were initiated.

The data acquisition programs used in whole cell recordings were a hyperpolarization program, K100MSH, and a depolarization program, K100MSD. Their parameters are stated in Appendix 1. The K100MSH protocol consists of holding the cell at a potential of -60 mV and applying 10 voltage steps which changed by -10 mV every 10 msec. The first hyperpolarizing voltage step was -70 mV and the maximum hyperpolarizing voltage step was -160 mV. The K100MSD protocol consisted of applying 13 voltage steps which increased by 10 mV every 10 msec. The first depolarizing step was -80 mV and the maximum depolarizing voltage step was +50 mV. The voltage steps were 10 msec in duration. The acquisition protocols were set up to record current for 5 msec before the voltage step, 10 msec during the voltage step and 5 msec after the voltage step.

The recording solutions used in whole-cell recordings are stated below in Table 3.1.

Table 3.1: Pipette and bath solutions used for whole-cell recordings.

Chemical	¹ HEPES-based Solns.		² MES-based Solutions	
	Bath Soln.	Pipette Soln.	Bath Soln.	Pipette Soln.
NaCl	140 mM	5 mM	140 mM	-
KCl	5 mM	140 mM	5 mM	140 mM
CaCl ₂	1 mM	1 mM	1 mM	-
MgCl ₂ ·6H ₂ O	1.2 mM	1.2 mM	1.2 mM	5 mM
HEPES	10 mM	10 mM	-	-
MES	-	-	10 mM	10 mM
³ BAPTA	-	1 mM	-	1 mM
final pH	7.4	7.4	6.2	7.0

¹ n-2-hydroxyethylpiperazine-N'-2-ethanesulphonic acid

² N-morpholino ethanesulfonic acid

³ 1,2-bis (o-aminophenoxy)-ethane- N,N,N',N-tetraacetic acid

3.2.2.7 On-cell Configuration - Single Channel Activity

Quality of on-cell single channel seals was determined by calculating the resistance of the seal in a manner similar to that described for pipette resistance (Eq'ns.

3.1& 3.2). Since a gigaseal requires a current value, I , of 10 pA, the amplifier gain and oscilloscope grid voltage were changed to enlarge the pattern on the oscilloscope. This allowed for a more accurate reading of the gsq #, which would result in a more precise value for the current, I , in Eq'n. 3.2.

The methodology used after the pipette was on the cell, including seal quality monitoring and initiation of data collection was as follows. After suction was applied (see previous section) and with the pulse to the membrane turned off, the membrane was allowed to rest. If a gigaseal formed, recordings were made; if not, a new electrode was used. The specific process followed for this is summarized in Fig. 3.5. This figure is in flow-chart format and represents the reproducible approach used in attempts to attain gigaseals. If seal levels did not reach gigaohm values after 3 runs of the Singles data acquisition program, the patch pipette was replaced with a new one and the process of seal formation with another cell was initiated.

The Singles data acquisition program was used for single channel recordings (for parameters see Appendix 1). Each episode involves subjecting the membrane to a specified voltage for a period of 5 seconds followed by 10 seconds with no applied voltage, i.e., the resting membrane potential (RMP). Ten episodes were run in the Singles program with the same applied voltage for each episode. Patches with gigaseal levels of resistance were obtained with approximately 40 cells in total, and cells exhibiting activity suitable for data analysis, i.e. flat baseline and uniform activity within each episode, were analyzed.

3.2.2.7.1 140 mM Na⁺ & 5 mM K⁺ Recording Solutions

The bath and pipette solutions used in early single-channel studies are listed below in Table 3.2.

Table 3.2: Single channel recording solutions using 140 mM Na⁺ and 5 mM K⁺.

Chemical	Bath & Pipette Solutions
NaCl	140 mM
KCl	5 mM
CaCl ₂	1 mM
MgCl ₂ •6H ₂ O	1.2 mM
MES	10 mM
sucrose	42.4 mM
final pH	6.2

3.2.2.7.2 Sucrose & 11.5 mM NaCl Recording Solutions

The recording solutions investigating a lower sodium chloride composition and the use of sucrose as the osmotic stabilizer are shown in Table 3.3.

Table 3.3: Recording solution formulations incorporating a low level of NaCl and the use of sucrose as an osmotic stabilizer.

<u>Chemical</u>	<u>Pipette and Bath Solutions</u>
NaCl	11.5 mM
KCl	5 mM
CaCl ₂	1 mM
MgCl ₂ •6H ₂ O	1.2 mM
MES	10 mM
sucrose	299 mM
final pH	6.2

3.2.2.7.3 Improving Chances of Gigaseal Formation

In general, the approaches taken in attaining pipette-cell contact and gigaseals were as stated in section 3.2.2.5 and 3.2.2.7. A modification of this procedure was investigated for its potential in improving pipette-membrane seals. It involved setting the data acquisition program to SINGLES with an Epoch A amplitude initial setting of +40 mV prior to approaching the cell. Shortly after cell contact was made the data acquisition program was changed to SET UP to determine the level of seal resistance.

Another approach investigated for improvements in gigaseal formation was formulation changes in the recording solutions. In particular, the divalent cation levels were altered (see Table 3.4 below). Data were collected on different combinations of pipette and bath formulations and different pipette voltages when approaching a cell.

Table 3.4: Single channel recording solutions with different levels of divalent cations.

Chemical	¹ 1X Divalent Cations		² 2X Divalent Cations		³ 5X Divalent Cations	
	Bath Soln.	Pipette Soln.	Bath Soln.	Pipette Soln.	Bath Soln.	Pipette Soln.
NaCl	140 mM	140 mM	140 mM	140 mM	140 mM	140 mM
KCl	5 mM	5 mM	5 mM	5 mM	5 mM	5 mM
CaCl ₂	1 mM	1 mM	2 mM	2 mM	5 mM	5 mM
MgCl ₂ 6H ₂ O	1.2 mM	1.2 mM	2.4 mM	2.4 mM	6 mM	6 mM
MES	10 mM	10 mM	10 mM	10 mM	10 mM	10 mM
sucrose	42.4 mM	42.4 mM	42.4 mM	35.8 mM	42.4 mM	16 mM
final pH	6.2	6.2	6.2	6.2	6.2	6.2

¹ level of divalent cations in Table 3.2 multiplied by 1.

² level of divalent cations in Table 3.2 multiplied by 2.

³ level of divalent cations in Table 3.2 multiplied by 5.

3.2.2.7.4 Formulation Changes to Reduce Channel Rundown

In order to eliminate channel rundown, the addition of an energy source was required. Glucose and fructose were added to the recording solution formulations (see below, Table 3.5).

Table 3.5: Recording solutions used to eliminate channel rundown in single-channel recordings.

Chemical	Bath Solution	Pipette Solution
NaCl	140 mM	140 mM
KCl	5 mM	5 mM
CaCl ₂	1 mM	2 mM
MgCl ₂ •6H ₂ O	1.2 mM	2.4 mM
MES	10 mM	10 mM
glucose	3.8 mM	3.8 mM
fructose	2.2 mM	2.2 mM
sucrose	36 mM	14.8 mM
final pH	6.2	6.2

3.2.3 Setting Recording Period Guidelines

Changes in protoplast morphology were noted during patch clamp experiments. Also, the probability of attaining a gigaseal was higher during the early part of a patch clamping session. In order to determine whether or not a correlation existed between patch clamping time and morphological changes, protoplasts, suspended in the bath solution listed in Table 3.5, were photographed in a time series. At different time periods, aliquots were removed and wet mounts were prepared. Cells were viewed using a Zeiss Axioscope microscope at 100X. Photographs were taken using a Zeiss camera.

3.3 Results

3.3.1 Pipette Size - Resistance Measurements

The average pipette size, measured using Eq'n. 3.3, was 20 Mega Ω .

3.3.2 Pipette-Cell Contact

In most cases the cells did not adhere to the glass coverslip in the recording dish. They often moved when approached by a pipette. Their microtubule-rich extensions were prone to movement and/or depolymerization during recordings. When an attached pipette was removed from solution, the cell usually remained attached to the pipette.

3.3.3 Whole-cell Recordings

The n-2-hydroxyethylpiperazine-N'-2-ethanesulphonic acid (HEPES)-based recording solutions (Table 3.1) were used for experimentation for a number of weeks. Whole-cell configuration was never obtained when using the HEPES-containing solutions.

Using the N-morpholino ethanesulfonic acid (MES)-based solutions (Table 3.1) few positive results were obtained. The majority of the cells showed no activity during depolarization (Fig. 3.6a). No increase in the slope of the episodes was evident. Only one cell out of 15 showed activity in the last four episodes corresponding to voltages of +20, +30, +40 and +50 mV (Fig. 3.6b). In the 15 cells tested, there was no evidence of sensitivity to hyperpolarization (Fig. 3.6c). The RMPs were recorded for 5 cells in which 'whole cell' configuration was achieved. The RMPs were -1.4, -1.9, -3.0, -20 and -23.4 mV.

3.3.4 On Cell Single Channel Studies

3.3.4.1 140 mM NaCl & 5 mM KCl Recording Solutions

Use of the recording solutions listed in Table 3.2 resulted in none of the cells forming a gigaseal with the pipette (n ~ 8 cells).

3.3.4.2 Sucrose & 11.5 mM NaCl Recording Solutions

Use of sucrose as an osmotic stabilizer and 11.5 mM NaCl in the recording solutions did not prove to be compatible with *E. aulicae* patch clamping. The current patterns shown on the oscilloscope during pipette and seal resistance measurements were not the rectangular traces expected. The signal pattern did not respond to transient cancellation controls. Also, adjustments in the pipette offset control did not affect the corresponding LED reading. Due to the atypical signal pattern, no pipette or seal resistance readings could be made. The solutions using 11.5 mM NaCl (Table 3.3) were deemed inappropriate for use in patch clamp studies of *E. aulicae* (n~5 cells).

3.3.4.3 Improving Chances of Gigaseal Formation

Table 3.6 documents the frequency of gigaseals when different pipette voltages, +10 and -40 mV, were used in combination with different recording solutions. The solutions differed in their levels of Ca^{2+} and Mg^{2+} , i.e. their divalent cations. The sample sizes are low and, while not statistically significant, they may suggest trends and are reproduced here for their potential usefulness in future work.

Table 3.6: Effect of pipette voltage and divalent cations on the occurrence of gigaseals between pipettes and *E. aulicae* protoplasts

Pipette Solution	Pipette Voltage (mV)	Bath Solutions		
		1 X ¹	2 X ²	5 X ³
1 X ¹	+10	0/1 ⁴	0/1	1/1*
	-40	0/1	-	-
2 X ²	+10	3/15	1/3	-
	-40	0/1	-	-
3 X ³	+10	0/1	0/2	-
	-40	0/1	-	-

¹ 1 X divalent cations solutions as listed in Table 3.4.

² 2 X divalent cations solutions as listed in Table 3.4.

³ 5 X divalent cations solutions as listed in Table 3.4.

⁴ numerator = # of cells that formed a gigaseal

denominator = total # of cells attempted.

* high level of noise in current recording.

Three combinations did result in gigaseals. With a 2X divalent cation pipette solution combined with a 1X divalent cation bath solution and the pipette at +10 mV had gigaseals in 3 out of 15 cells. One out of 3 cells had gigaseals using 2X divalent cation pipette and bath solutions and a pipette voltage of +10 mV. A third combination, using

5X divalent cation bath solution, 1X divalent cation pipette solution and the pipette at +10 mV, did give a gigaseal; however, the data collected had more background noise associated with it compared to other gigaseal data (Fig. 3.7). Although the highest success rate, 1/3 (bath solution: 2X , pipette solution: 1X, pipette voltage: +10 mV) is considerably higher than 3/15 (bath solution: 2X, pipette solution: 2X, pipette voltage: +10 mV), early in the data collection process the latter parameter settings gave a success rate of 2/3 cells.

3.3.4.4 Formulation Changes to Reduce Channel Rundown

Data collected from gigaseal patches showed some evidence of reduced channel activity over the 10 episodes of the Singles data acquisition program. Figs. 3.8 and 3.9 show high levels of activity in episodes 1 and 2 with a noticeable decrease in the last episode; although the majority of the cells showed no evidence of channel rundown with uniform activity present in all episodes (Fig. 3.10). Channel rundown is undesirable since it would interfere with the interpretation of recordings from channel blocker characterization studies. Blockers, in the presence of their specific ion channel targets, cause reduced activity. If a decrease in activity is noted, one would not know whether it is due to rundown or the blocker.

The addition of 3.8 mM glucose and 2.2 mM fructose to the recording solutions resulted in the absence of rundown from all recordings. Their addition did not affect the noise level of the data collected.

3.3.5 Setting Recording Period Guidelines

While collecting patch clamping data, the chance of obtaining a gigaseal appeared

to be highest when the cells were in the recording bath solution for approximately 30 to 90 minutes. Within that time frame the cells were rich in cytoplasm and had tapered internuclear restrictions (Fig. 3.11a). At times greater than 90 minutes the cells became highly vacuolated (Fig. 3.11b & c). A number of vacuoles were also present in cells exposed to bath solutions for less than 30 minutes (Fig. 3.11d). Thus, cells in solution for from 30 to 90 minutes were used routinely for patch clamping.

3.4 Discussion

3.4.1 Pipette Preparation & Size - Resistance Measurements

Pipette fabrication plays an important role in recording noise and the formation of a gigaseal. Borosilicate glass used in these experiments are associated with low noise (Cavalie et al., 1992; Penner, 1995; Rae and Levis, 1996). The pipettes were heat polished to smooth their edges in order to assist in the formation of high level seals. A source of noise associated with the pipette is the capacitance of the immersed section of the pipette tip. Its effect is reduced when the pipette is coated with an insulating agent (Penner, 1995). Therefore, in the pipette preparation steps used, the tip was dipped in a silicone-based product, Sigmacote, to minimize noise.

The criterion used to identify an appropriate pipette diameter for use with *E. aulicae* protoplasts was the ability of the cell to remain attached to the tip of the pipette. The second heater knob of the pipette puller controls pipette diameter. The setting adopted for these studies was 58 ± 1 since a lower setting, associated with larger pipette diameters, often resulted in cells being sucked into the pipette shortly after cell contact

was made. One would expect that use of an even higher setting would ensure no cell loss; however, the resultant reduction in the patch size could be detrimental to detecting channel activity. This would depend on the channel density within the membrane.

The mean pipette resistance value was 20 Mega Ω . Resistance values are commonly used in documenting pipette sizes in patch clamp studies (Brink and Fan, 1989; Caldwell et al., 1986; Garrill et al., 1992b). An investigator, when reproducing a technique from a publication, can easily determine whether the pipette size is close to a stated resistance value.

3.4.2 Pipette-Cell Contact

Protoplast movement occurred intermittently during recording sessions making cell-pipette contact often difficult to attain. *E. auilcae* protoplast attachment studies (Lake, 1994) showed that ethanol-cleaned glass coverslips, used in the recordings in this study, have been associated with high levels of cell attachment in salt solutions similar in composition to that used in patch clamp recordings. However, forces inherent to patch clamping, i.e, probing cells with pipettes and withdrawl of membrane-attached pipettes from cells, probably require the cells to be more firmly attached to their coverslips than the dislodgment protocols used in the Lake study. Since gigaseal recordings were possible with ethanol-cleaned coverslips in the recording dish no modifications were made in their preparation.

The lack of complete cell attachment to the recording dish did however, affect another aspect of patch clamping data collection. Four major pipette-membrane configurations are possible in patch clamping. These include 'whole cell', 'cell-attached',

'inside-out' and 'outside-out'. The latter two involve the removal of a patch of membrane from the cell. Both require the cell to remain stationary while the pipette is pulled away from the cell. As stated above (section 3.3.2), after a gigaseal is attained, the cells remain attached to the pipette even when it is removed from the bath solution. Until protocols are developed for improved adhesion of protoplasts to recording dishes, patch clamp recording using 'inside-out' and 'outside-out' modes is not possible. Therefore, in this preliminary study of *E. auilcae* protoplast ion channels only 'whole-cell' and 'cell-attached' recording configurations were investigated.

3.4.3 'Whole-cell' Recordings

Early studies performed in our laboratory were in the whole cell configuration (Hicks and Murrin, unpublished results). Using HEPES-based solutions with pH values of 7.4, depolarizing voltage-activated channels were evident. Their sensitivity to a K^+ channel blocker, tetraethylammonium (TEA^+), suggested that they are involved in potassium ion transport.

Attempts to duplicate these results were unsuccessful; no channel activity was noted, with either depolarization or hyperpolarization of the membrane, using the same HEPES-based solutions used in the early Hicks and Murrin study. Formulation changes of the recording solutions were made in an attempt to promote channel activity. A number of formulations, with sucrose as a osmotic stabilizer and different pH values, were used from which no channel activity was evident. Limited success was gained with one formulation. A discussion of its development and resultant activity follows.

In early experiments, both the pipette and bath solution pH levels was 7.4. *E. aulicae* protoplast cultures are maintained in Grace's insect tissue culture medium supplemented with 2.7% fetal calf serum. This growth medium has a pH of 6.2. Transport systems in fungi can be inhibited at internal pH levels greater than 7 (Griffin, 1994). Therefore, pH adjustments were made in an attempt to more closely reflect physiological conditions. The pH of bath and pipette solutions were changed to 6.2 and 7.0, respectively. HEPES is not an effective buffer at either of these pH levels, while MES is capable of buffering over this range and has been deemed suitable for *E. aulicae* growth at a concentration of 10 mM (Dunphy and Chadwick, 1985). Therefore, MES was substituted for HEPES in an equimolar concentration. Since *E. aulicae* can tolerate a variety of minimal media, including phosphate buffered saline, saline solution, MES-sucrose and microtubule stabilizing buffer (Lake, 1994), no further adjustments were made to the bath solution. The contents of the pipette solution were also reconsidered for their approximation of intracellular physiological conditions. No quantitative data on the cytoplasmic ion contents of *E. aulicae* exist. Using cellular ionic content information of another fungus, *Saccharomyces cerevisiae*, adjustments to the pipette solution were made. The three major cations of *S. cerevisiae* are K^+ , Mg^{2+} and Ca^{2+} at 150, 20 mM and 3 mM, respectively (Griffin, 1994). Sodium may exist in trace amounts. The 'whole-cell' HEPES formulation (Table 3.1) had a K^+ concentration of 140 mM. Since this is similar to the intracellular *S. cerevisiae* value, no change was made in its concentration. Due to the reported absence of significant sodium levels in *S. cerevisiae*, sodium was removed from the pipette MES formulation (Table 3.1). Mg^{2+} and Ca^{2+} exist in the yeast cytoplasm in a 6.7:1 ratio. Considering this information, along with the interest in keeping

the osmolality basically the same as the HEPES pipette solution, Ca^{2+} was removed and Mg^{2+} was added at 5mM in the MES formulation (Table 3.1). The early results incorporated BAPTA in the pipette solution. The same level of this free calcium chelator (Dieter et al., 1993) was used in the MES formulation.

The number of reports of 'whole-cell' recordings are few for fungal systems. *Saprolegnia* (Lew et al., 1992; Levina et al., 1994) and *Neurospora* (Levina et al., 1995) studies used the 'cell attached' recording configuration. However, 'whole-cell' recordings have been achieved in *Saccharomyces cerevisiae* (Gustin et al., 1986; Bertl et al., 1995). The MES-based pipette formulation given in Table 3.1 resembles that used by Bertl et al. (1995). The level of KCl in the MES formulation is 140 mM and is 175 mM in the Bertl et al. formulation. NaCl is absent from both formulations. MgCl_2 is present in 5 mM concentration for both formulations. CaCl_2 is absent in the MES formulation and is present at only 100 nM in the solution from Bertl et al. (1995). Both solutions have a calcium chelator present; 1mM BAPTA is in the MES solution and 1mM EGTA is in the Bertl et al. formulation. Both formulations have a pH of 7.0. The differences between the two formulations is the presence of MES in the Table 3.1 formulation and the presence of ATP in the Bertl et al. solution. Since the MES-based solution is very similar to a formulation proven to be acceptable for 'whole-cell' recording of yeast channel activity (Bertl et al., 1995), the former was investigated for its compatibility with *E. auilcae* patch clamping.

Using the MES-based recording formulations the majority of the cells showed no activity during depolarization. Only one cell responded to voltages ranging from +20 to +50 mV. This evidence of membrane depolarization-activated channels are consistent

with the Hicks and Murrin study (unpublished results). However, the inability to reproducibly detect whole-cell activity led to the rejection of this mode of patch clamp recording.

The MES-based solutions used in the 'whole-cell' recordings seemed theoretically sound. However, their formulations were based on knowledge of yeast intracellular ionic content and yeast patch clamping results. This suggests that generalizations of fungal biochemistry may not be of assistance in developing patch clamp recording solutions for *E. auilcae*.

Although very limited channel activity was recorded during the whole-cell recordings, data of resting membrane potentials (RMPs) were collected. RMP values vary according to the specific ionic concentrations in the bath and pipette solutions. One can only state that the values range from -1.4 to -23.4 mV when the bath and pipette K^+ concentrations are 5 mM and 140 mM respectively. The negative value of the voltages found in *E. auilcae* is consistent with other systems however their magnitude is much smaller. Byrne and Schultz (1994) state that nerve cell RMP's range from -40 to -90 mV. RMPs for *Neurospora crassa* have been documented by electrode implantation (Griffin, 1994). Their RMP values ranged from -170 to -230 mV. However, Lew et al. (1992) reported RMPs near 0 mV for *Saprolegnia*, with extracellular and approximate intracellular potassium ion concentrations of 100mM and 10 mM, respectively.. Inhibition of cellular respiration and substrate uptake have been linked to membrane depolarization, i.e., more positive RMP values, in *N. crassa*. Transport mechanisms may play a role in maintaining the RMP of *E. auilcae*.

3.4.4 On-cell Single Channel Studies

The inability to easily reproduce the whole-cell recording results (Hicks and Murrin, unpublished) led to a re-assessment of the approach to patch clamping *E. auilcae* protoplasts. HEPES-based recording solutions, used in the early study, did not result in any recordings with activity. Use of MES-based solutions in whole-cell recording resulted in channel activity in only 1 out of 15 cells tested, i.e., 6.7% of the time. This level of success is within the range found with other cells. Only 5% of *S. cerevisiae* experiments resulted in activity (Garrill and Davies, 1994). Perhaps with further adjustments to the solutions, this value could increase. However, lack of information on the intracellular composition of fungi, especially *E. auilcae*, was seen as a barrier to making sound decisions on pipette solution adjustments. Therefore, another patch clamping configuration was sought, in which similarity between the pipette solution and the cytoplasm would not be a critical factor.

The four main recording configurations are 'whole-cell', 'cell-attached', 'inside-out' and 'outside-out'. The latter two require cells to remain firmly attached to the bottom of the recording dish so the pipette can be withdrawn from the cell isolating a patch of membrane. As discussed earlier, *E. auilcae* protoplasts do not adhere to the glass bottom of recording dishes. Therefore, the 'inside-out' and 'outside-out' recording configurations could not be used for this study. Further work on cell attachment is required before these methods can be utilized. Therefore, by process of elimination, 'on-cell', or 'cell-attached', single channel recording was used for ion channel studies of *E. auilcae* protoplasts.

The main advantage of 'cell-attached' mode is that it does minimal damage to the biological structure of the channels while allowing low- noise recordings (Jackson, 1992).

Patch excision, not performed in 'cell-attached' mode, has been implicated in causing significant drops in open times of some channels (Trautmann and Siegelbaum, 1983). Undrovinas et al. (1995) suggest that changes in channel open times, recorded using excised patches, may be due to cytoskeletal disruption caused by the excision process. Cytoplasmic-free patches, used in 'inside-out' and 'outside-out' modes, and intra-cellular modifications, available through 'whole-cell' manipulations, help determine what channels are present in a cell. However, they may not reflect what channels are active under physiological conditions. Therefore, the information gained from 'cell-attached' mode is believed to reflect near-physiological activity.

Gigaseal formation is not necessary for reproducible single-channel recordings in fungi (Garrill et al., 1992b; Lew et al., 1992; Levina et al., 1995). Structural changes to membranes, during gigaseal formation, have been documented (Ruknudin et al., 1991) suggesting deviation from physiological conditions. However, gigaseal formation is often viewed as a requirement (Sakmann and Neher, 1995b; Hille, 1984) because it gives low-noise recording. It also ensures that the current originating from the membrane patch will be captured by the electrode and will not leak from the pipette/membrane interface (Hamill et al., 1981). Wide-range applied voltage experiments are attainable with gigaseals (Garrill and Davies, 1994). During voltage-activation experiments with *E. auilcae*, warnings of possible resistor damage to the recording equipment, manifested by the clipping light on the amplifier, accompanied sub-gigaseal recordings. Sometimes this occurred with applied voltages of only +20 or -20 mV. Therefore, without gigaseals, information gained from voltage treatments would be very limited. It was imperative that gigaseal formation was attained in *E. auilcae* 'cell-attached' recordings in order to

determine whether voltage-gated channels existed in these cells.

3.4.4.1 140 mM NaCl & 5mM KCl Solutions

The initial composition of solutions used for single channel recording were chosen on the basis of their success with animal cell studies. Modifications were made to accomodate *E. auilcae* growth parameters and improve chances of gigaseal formation. The first set of solutions tested, consisting of 140 mM NaCl and 5 mM KCl (Table 3.2). were very similar to the bath solution used by Hancock et al. (1996) for frog muscle cell recording. Since the low noise recordings documented in that paper were attained using the same equipment that the *E. auilcae* recordings were to be generated from, their solutions served as a starting point from which modifications were developed. The low K^+ concentration, 5mM, in the pipette was deemed appropriate for *E. auilcae* work. The whole-cell data of Hicks and Murrin (unpublished results) showed TEA⁺ sensitivity to an outward current suggested the presence of a K^+ channel. This information, in addition to the knowledge that a K^+ concentration gradient with a low level of K^+ outside the cell will favour outward K^+ movement (Byrne and Schultz, 1994), suggested a low level of K^+ in the pipette as a wise choice. External K^+ concentrations exceeding 10 mM and a complete lack of external K^+ have been shown to reduce outward K^+ (K^+_{out}) current (Adams and Nonner, 1990). Therefore, 5 mM K^+ was used in most *E. auilcae* patch clamping experiments.

The formulations given in Table 3.2 include modifications to accomodate *E. auilcae*. The pH was set at 6.2 and the osmolality was adjusted to 349 mOsm. Both of these physical parameter settings have been identified as being suitable for *E. auilcae*

growth (see Chapter 2). Adjustments in pH levels have previously been made to recording solutions to reflect fungal growth conditions (Garrill et al., 1992b). However, no gigaseals were formed with the solutions presented in Table 3.2. Therefore, more formulation changes to the recording solutions were required.

3.4.4.2 Sucrose & 11.5 mM KCl Recording Solutions

In an effort to develop patch solutions more closely related to growth conditions, and perhaps also, I thought, to be more conducive to gigaseal formation, the solutions listed in Table 3.3 were developed. The major component of the earlier formulation (Table 3.2) is NaCl at a concentration of 140 mM. Although NaCl is not a common ingredient in *E. aulicae* growth medium, Na⁺ serves as the cation for polyatomic phosphate and carbonate anions. In the mass fermentation medium developed for *E. aulicae* (Nolan, 1993), the Na⁺ concentration is 34.21 mM. This value includes the level of NaCl in the tryptic soy broth added to the medium. In both Grace's insect tissue culture medium and the 13 amino acid medium (see Chapter 2) the Na⁺ concentration is 11.51 mM. Therefore, a reduction in the Na⁺ concentration seemed appropriate; however, a decrease in the NaCl level would also affect the Cl⁻ level. Since the wire microelectrode used in patch clamping requires at least a 10 mM level of Cl⁻ (Penner, 1995), it seemed that decreasing the NaCl level close to 11.5 mM would not be detrimental. Solutions used in fungal patch clamping studies have a range of 0 to 12 mM Na⁺ (Caldwell et al., 1986; Bertyl and Slayman, 1992; Garrill et al., 1992a). Therefore, a reduced level of NaCl, 11.5 mM, was deemed appropriate for investigation of patch clamp suitability. In order to maintain 349 mOsm solutions for *E. aulicae*, sucrose, an osmotic stabilizer (Dunphy and

Nolan, 1979), was used in the formulation listed in Table 3.3. Although theoretically, the solution changes seemed sound, they showed no compatibility with *E. auilcae* patch clamping. No pipette or seal resistance readings could be made. Consequently, the solutions listed in Table 3.3 were deemed inappropriate. Due to the poor performance of the low level NaCl in these solutions, the concentration was restored to 140 mM for all future solution formulations.

3.4.4.3 Improving Chance of Gigaseals

The problem with the first single channel recording formulations (Table 3.2) was the inability to attain giga-seals. Changes in solution and pipette voltages have been associated with giga-seal formation. Changes in osmolality, with the pipette solution being 10% hyperosmolar relative to the bath solution, have been adopted for fungal (Levina et al., 1995) and plant studies (Assman, 1996). The potential exists for future investigation of the role of ion channel activity in osmotolerance exists based on the knowledge of the broad range osmotic tolerance of *E. auilcae* (see Chapter 2). Information on channel activity using isosmolar pipette and bath solutions would be useful as a reference point for osmolality changes. Therefore, achieving giga-seals by osmolality modifications was not considered an ideal approach.

Two approaches were investigated for their effects on giga-seal formation with *E. auilcae* protoplasts: pipette hyperpolarization and increased divalent cation levels. Hyperpolarization of the pipette during membrane contact, has been suggested by Penner (1995) for giga-seal formation. Natalia Levina (personal communication) suggested a

pipette voltage of -40 mV based on success she has had with fungal patch clamping. The second approach involves the levels of divalent cations in the solutions. Higher CaCl_2 concentrations, up to 10 mM, in the bath solution has helped with gigaseal formation with plant systems (Assmann, 1996). Higher levels of Mg^{2+} relative to Ca^{2+} have also been linked to gigaseal formation (Roger Lew, personal communication). The approach used in this study looked at 3 different divalent cation levels and two pipette voltages. The results have a small sample size and missing data points. This is a reflection of cell/pipette behaviour. Cells moving off the pipette early in the seal formation process was a common occurrence in the protoplasts during all patch clamping experiments.

Three combinations resulted in gigaseals. One, with a 2X divalent cation pipette solution combined with a 1X divalent cation bath solution and the pipette at +10 mV, had gigaseals in 3 out of 15 cells. One out of 3 cells had gigaseals using 2X divalent cation pipette and bath solutions and a pipette voltage of +10 mV. A third combination, using 5X divalent cation bath solution, 1X divalent cation pipette solution and the pipette at +10 mV, did give a gigaseal. However, the background noise associated with this combination deemed it unacceptable for future studies. Although the highest success rate, 1/3, is considerably higher than 3/15, I did not feel confident in the success rate of the 1/3 probability group. This was because of the small sample size of 3. Due to the time-intensive nature of patch clamping *E. auilcae* protoplasts, I decided to identify a gigaseal-forming protocol with the existing data. The encouraging early data, 2/3 success rate, in the final 3/15 probability group and its larger sample size led to the choice of its parameters for future studies. Therefore, use of a pipette solution with 2X divalent cations in combination with a bath solution with 1X divalent cations and a pipette set at +10 mV

was used for seal formation for *E. aulicae* protoplasts.

3.4.4.4 Formulation Changes to Reduce Channel Rundown

Having the ability to attain gigaseals allowed a major hurdle in *E. aulicae* protoplast patch clamping to be crossed. However, with the initiation of data collection one other obstacle became apparent. A decay in activity, commonly referred to as 'run-down' (Rorsman and Trube, 1990), was noted in some recordings. Fig. 3.8 and Fig. 3.9 show reduced activity with time. The magnitudes of their current traces differ considerably even though they resulted from identical recording conditions. The reason for the differences is not known. The data are presented as the current activity recorded over the 10 episodes. When dealing with channel rundown, presenting the data in terms of channel activity per unit time would be ideal. An investigator using pCLAMP software must be able to clearly identify the number of channels present in order to generate such a figure. The nature of ion channel activity in *E. aulicae* does not lend itself to this type of analysis (see section 4.4.3.2). Therefore the rundown figures used in this document do not supply channel activity per unit time information.

The major problem with run-down activity is that it complicates channel characterization. One method of classifying channels depends on the use of specific blockers that reduce activity. Using channel blockers on a cell type prone to 'run-down', an investigator would not be able to determine whether a reduction in activity is due to the blocker or due to 'run-down'. This could result in incorrect characterization of channels. *E. aulicae* protoplasts, during 'cell-attached' recording adhere to the pipette when it is removed from solution. It is impossible to record the activity of the same cell before and

after the addition of a blocker. This is because the original pipette would have to be removed and replaced with a blocker-containing solution; the original cell would be lost during the manipulation. Therefore, it was imperative to find a solution adjustment that would eliminate 'run-down'. Channel activity in excised membrane patches can be restored when ATP is added (Mislner et al., 1986). Since a major advantage of 'cell-attached' recordings is the ability to identify activity at near-physiological conditions, substituting ATP with an energy source common to protoplast growth medium seemed logical. ATP-free, glucose-containing solutions have been used in patch clamp studies (Undrovinas et al., 1995). Three monosaccharides, glucose, fructose and mannose are utilized by species of Entomophthorales (Latgé, 1975). Both glucose and fructose are present in the 13 amino acid medium (see Chapter 2) at concentrations of 3.8 and 2.2 mM respectively. Therefore these two sugars were added to the solutions at these concentrations (Table 3.5). The resultant curves showed low noise recordings with no evidence of 'run-down'. Therefore these solutions were adopted for all future studies of *E. aulicae* protoplast single channel recordings.

3.4.5 Setting Recording Period Guidelines

The length of time *E. aulicae* protoplasts are present in the bath solution appears to affect gigaseal formation. The best chance of getting a gigaseal occurred when the cells had been in the solution for 30 to 90 minutes. Outside of this time frame large numbers of vacuoles were present indicating cellular stress. It is therefore recommended that patch clamping of cells occurs 30 to 90 minutes after introduction of the recording bath solution. This is suggested in order to improve gigaseal formation and allow the

investigator to record signals during a period of minimal cellular stress.

3.5 *Summary*

A protocol was developed for ion channel studies of *E. aulicae* protoplasts. Reproducible, low-noise recordings were attained with membrane/pipette gigaseals using a 'cell-attached' recording configuration. The protocol involves the use of borosilicate glass pipettes that are heat polished and silicone-coated. An appropriate pipette size for patch clamp recording imparts a resistance value of 20 Mega Ω when contacting the recording bath solution. The pipette solution consists of the following components: 140 mM NaCl, 5 mM KCl, 2 mM CaCl₂, 2.4 mM MgCl₂•6H₂O, 10 mM MES, 3.8 mM glucose, 2.2 mM fructose, 29.8 mM sucrose, final pH of 6.2. The bath recording solution contains 140 mM NaCl, 5 mM KCl, 1 mM CaCl₂, 1.2 mM MgCl₂•6H₂O, 10 mM MES, 3.8 mM glucose, 2.2 mM fructose, 36 mM sucrose and had a final pH of 6.2. Recommended recording times are 30 to 90 minutes after the cells are suspended in the bath solution.

Fig. 3.1: Patch clamp recording equipment. **a**, Nicolet Model 310 digital oscilloscope; **b**, List patch clamp probe and controller L/M-EPC 7 (Medical Systems Corp.); **c**, TL-1 interface (Axon Instruments); **d**, Zeiss IM-35 inverted microscope; **e**, 35mm camera; **f**, pipette holder; **g**, manual pipette manipulation controls; **h**, vibration isolation table; **i**, Faraday cage; **j**, Zeiss motorized pipette micromanipulator.



Fig. 3.2: Orientation of patch clamp recording equipment. **a**, bridge holder; **b**, agar bridge; **c**, cell suspension; **d**, recording dish; **e**, pipette filled with pipette solution; **f**, pipette holder.

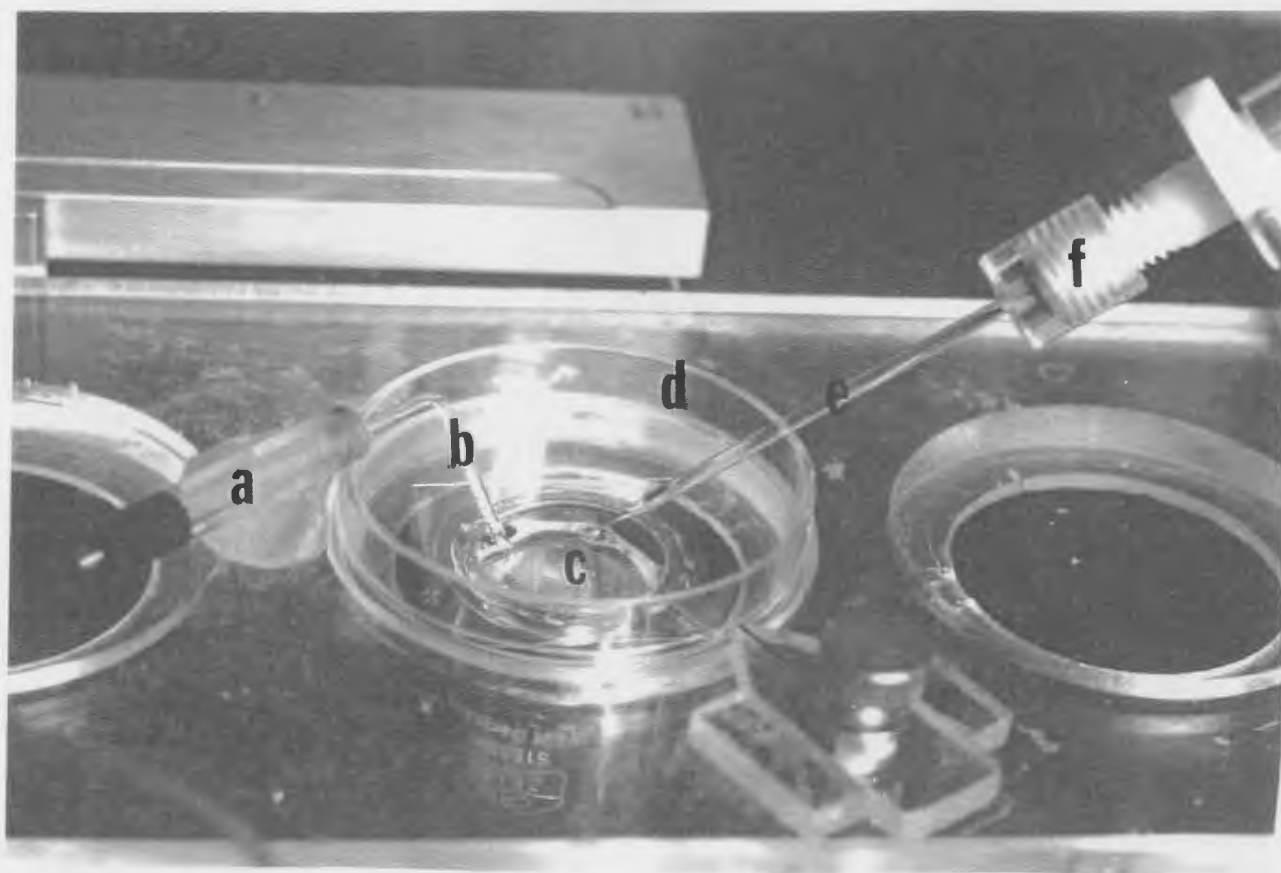


Fig. 3.3: *Entomophaga aulicae* protoplast (**a**) with an attached recording pipette (**b**). The magnification bar is approximately 10 μ m.

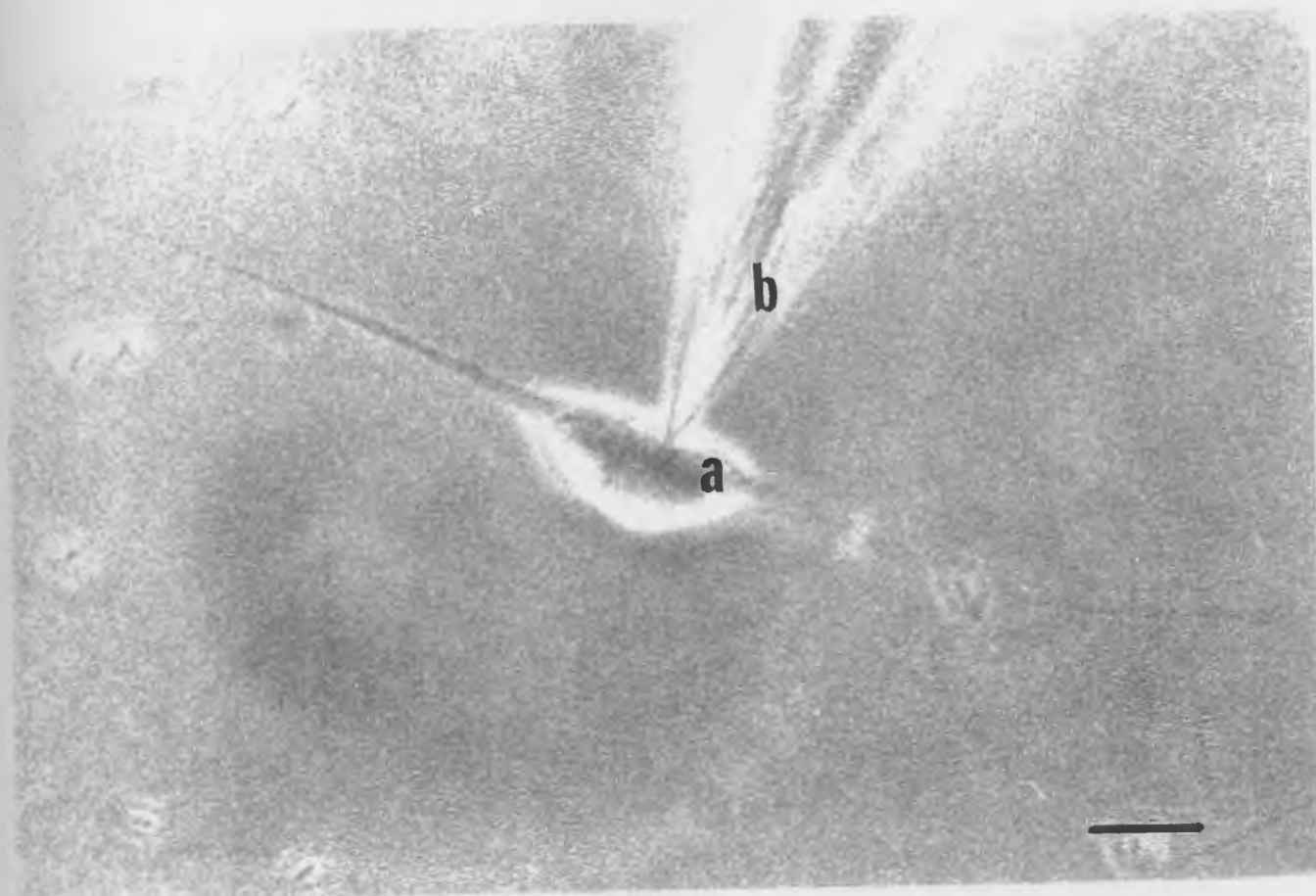
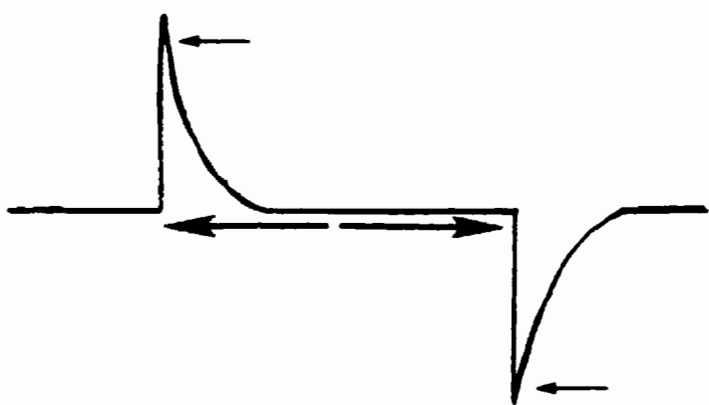
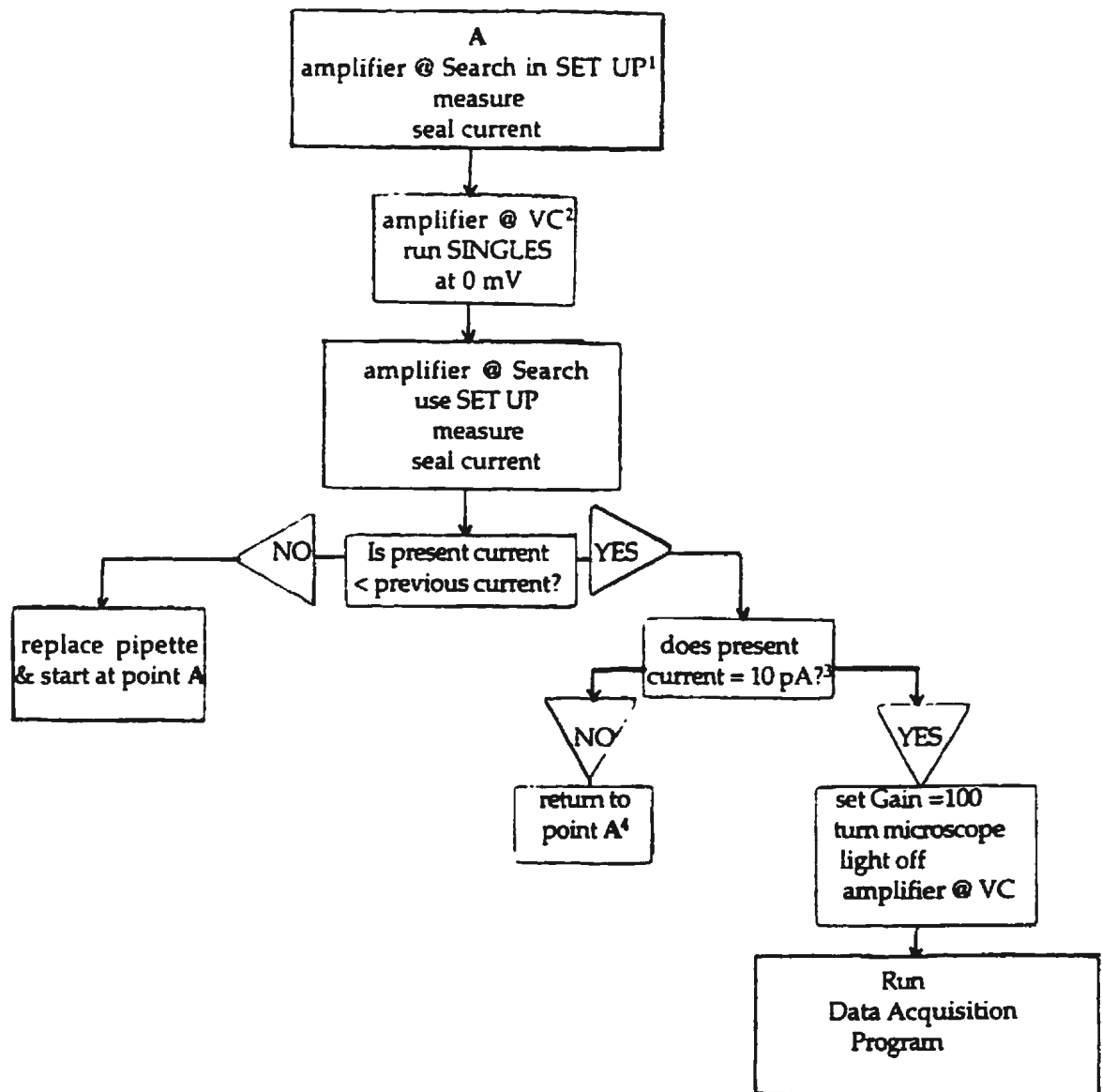


Fig. 3.4: Oscilloscope pattern indicating attainment of 'whole cell' recording configuration. Large arrows indicate period of applied voltage. Small arrows indicate transient current spikes.





¹ data acquisition program see Appendix 1

² voltage clamp

³ using Eqn. 3.3 this results in a gigaseal

⁴ repeat this NO loop for a maximum of 3 times
after the third time, prepare a new pipette and start at A

Fig. 3.5: Method used in monitoring seal formation and initiating data acquisition for single channel on cell recordings.

Fig. 3.6: Whole-cell recordings. **a**, depolarized cell with no discernible activity in voltages ranging from -70 to +50 mV. **b**, depolarized cell with channel activity in the last 4 episodes which correspond to voltages of +20 mV to +50 mV. **c**, hyperpolarized cell with no discernible activity in the range of -70 to -160 mV.

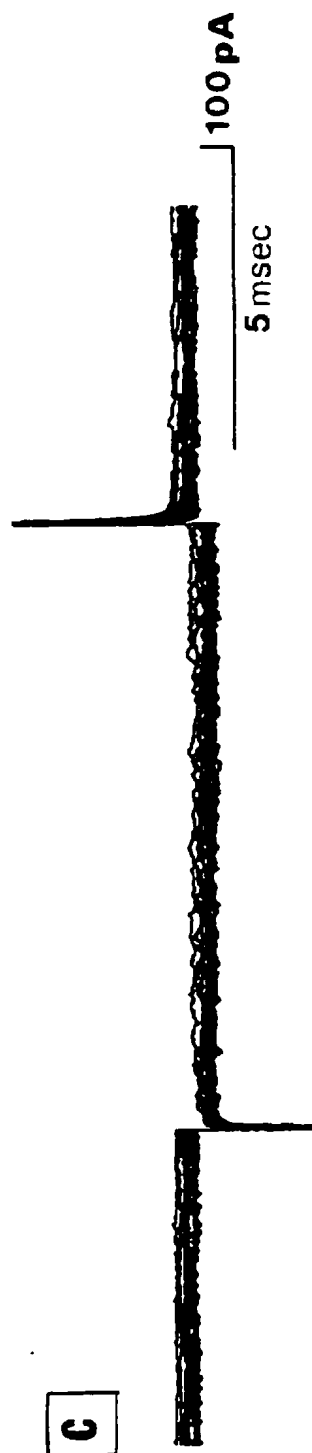
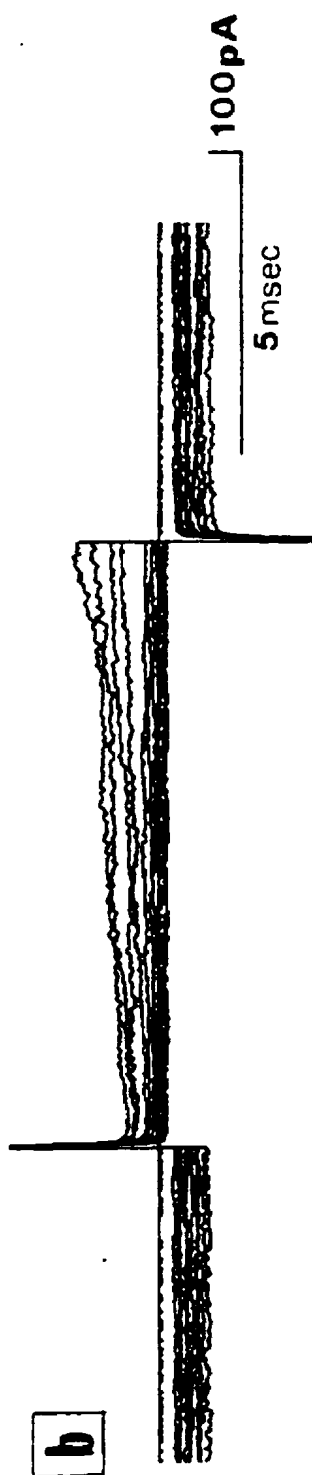
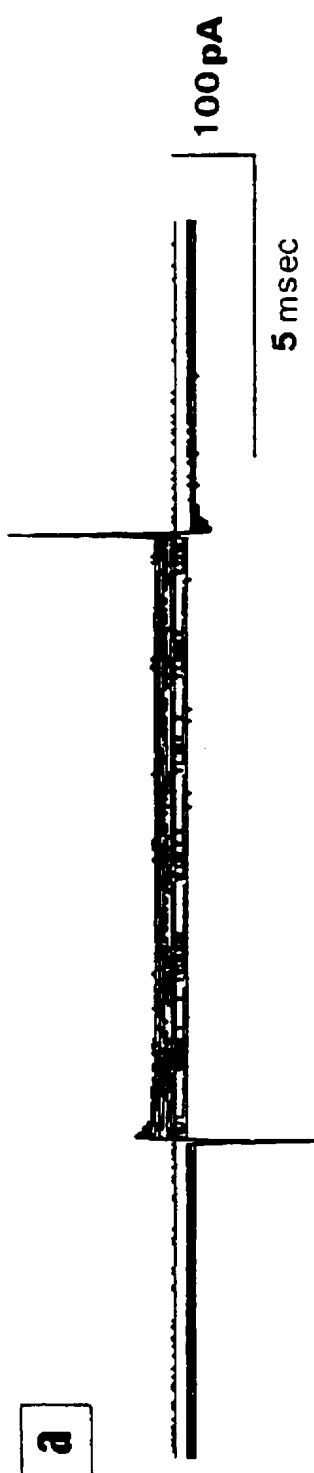


Fig. 3.7: Single channel recordings in cell attached configuration showing recording noise associated with the use of 5X divalent cation bath solution, 1X divalent cation pipette solution and a pipette voltage of +10 mV. Representative recordings. episodes 1, 5 and 10, are shown.

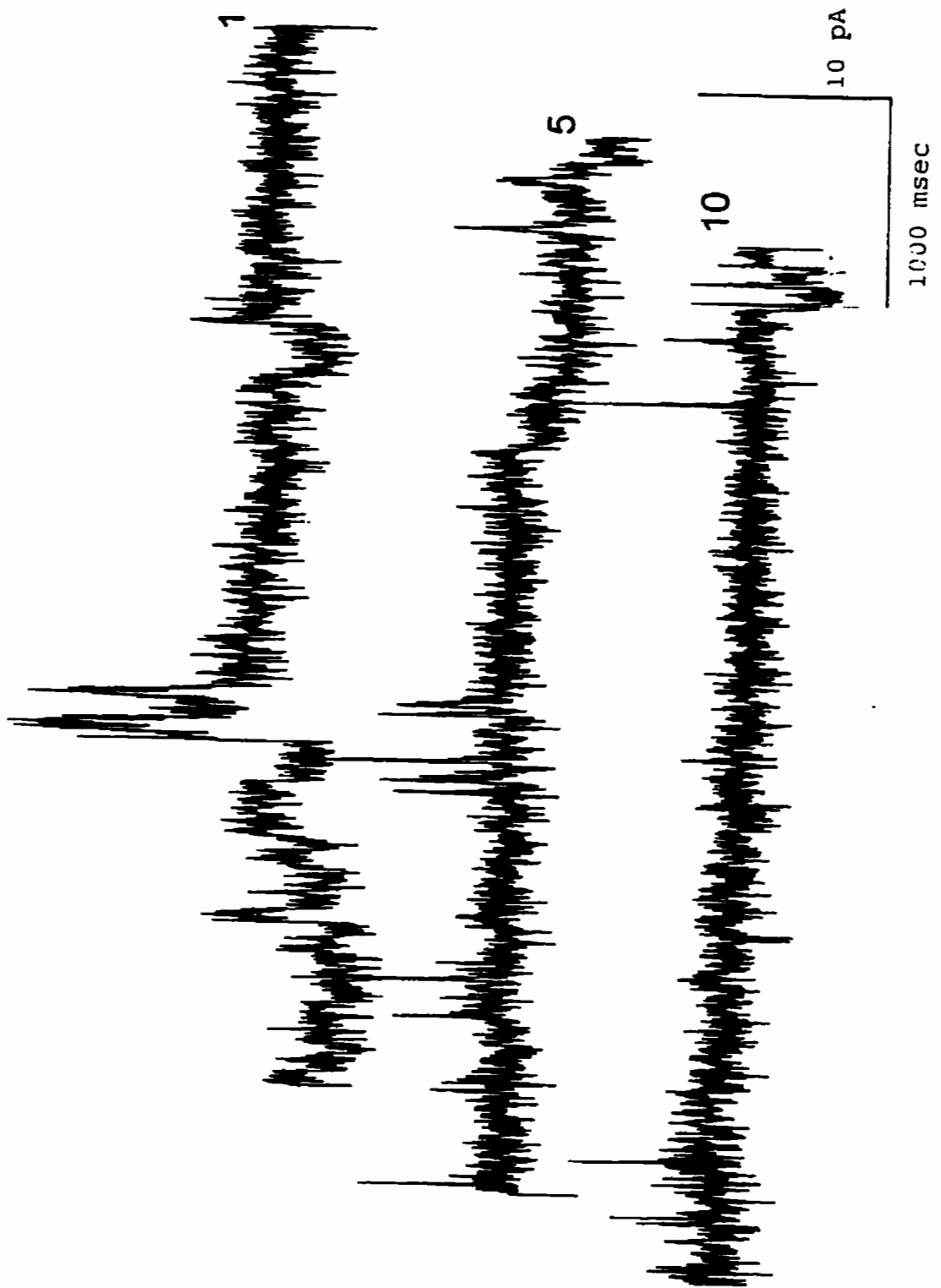


Fig. 3.8: Single channel recordings in cell attached configuration showing evidence of run-down in channel activity in solutions without glucose and fructose. High amplitude current is present in episodes 1 and 2 followed by a more uniform level of activity in the following episodes. Episode number is found in the right-hand end of each trace. The time period between the start of each episode is 10 seconds.

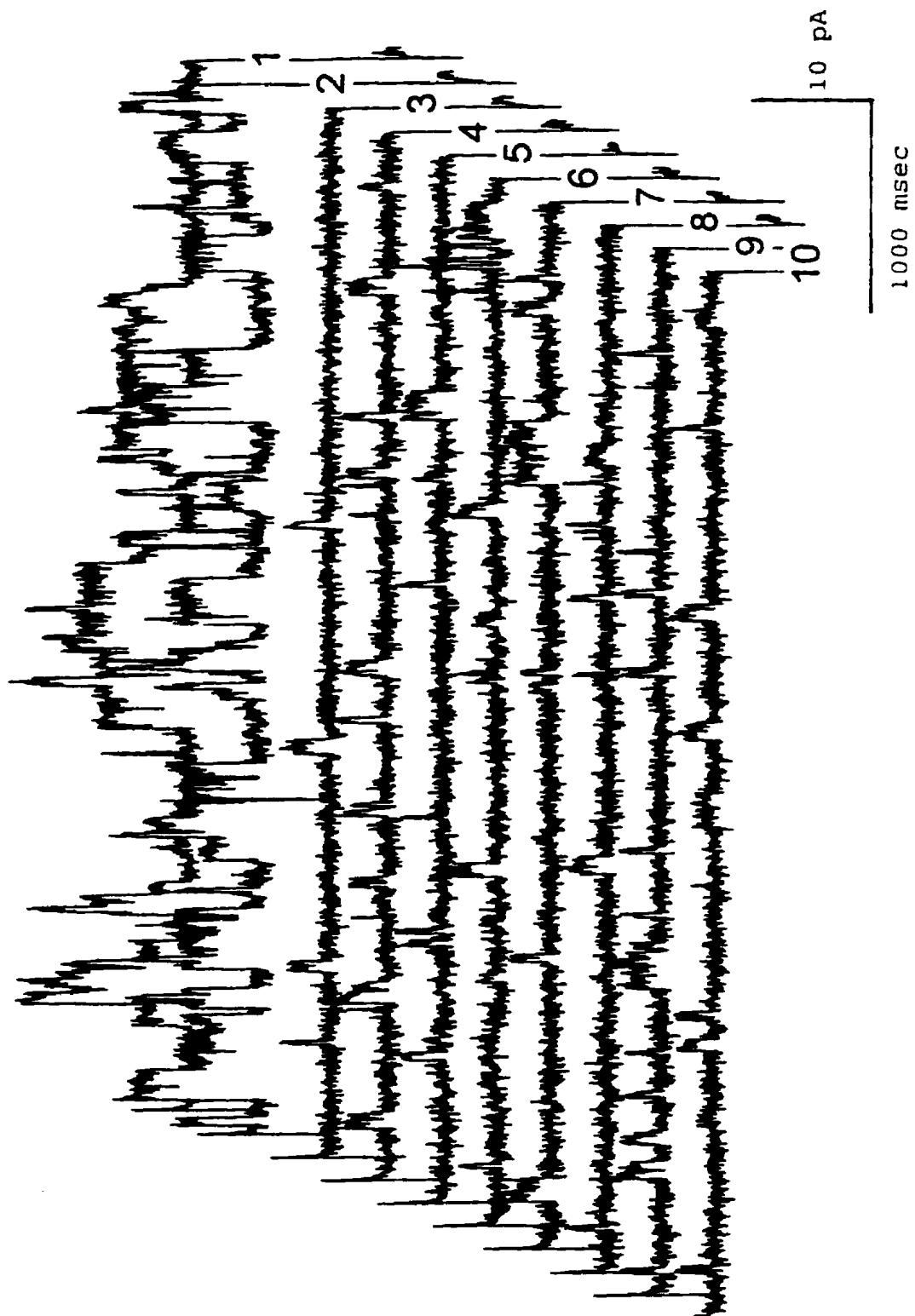


Fig. 3.9: Single channel recordings in cell attached configuration showing evidence of run-down in channel activity in solutions without glucose and fructose. There are high amplitude current in episodes 1, 2 and 4 followed by very limited activity. Episode numbers are located at the right side of each trace. The time period between the start of each episode is 10 seconds.

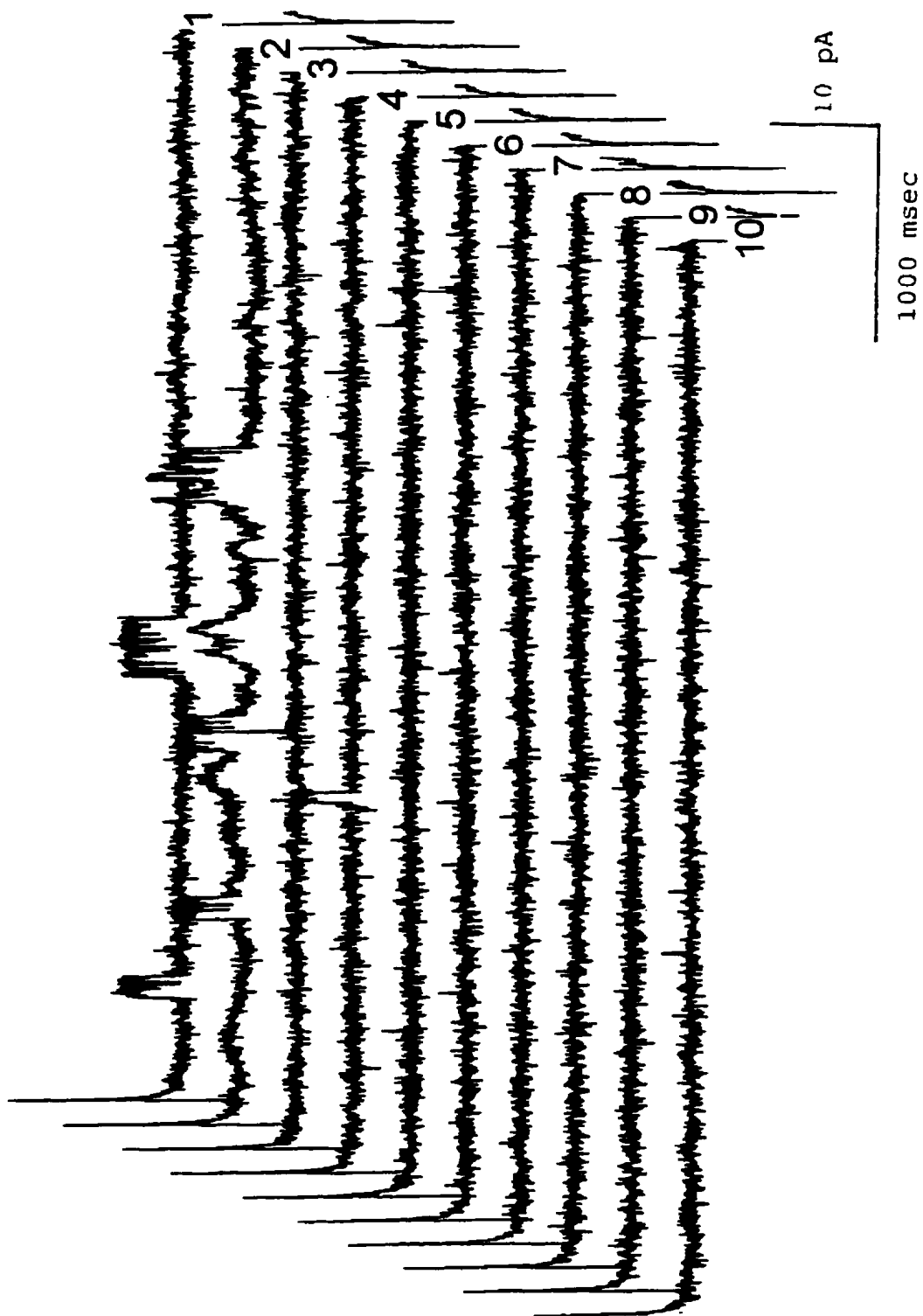


Fig. 3.10: Single channel recordings in cell attached configuration showing no evidence of run-down in channel activity in solutions without glucose and fructose. Episode numbers are located at the right side of each trace.

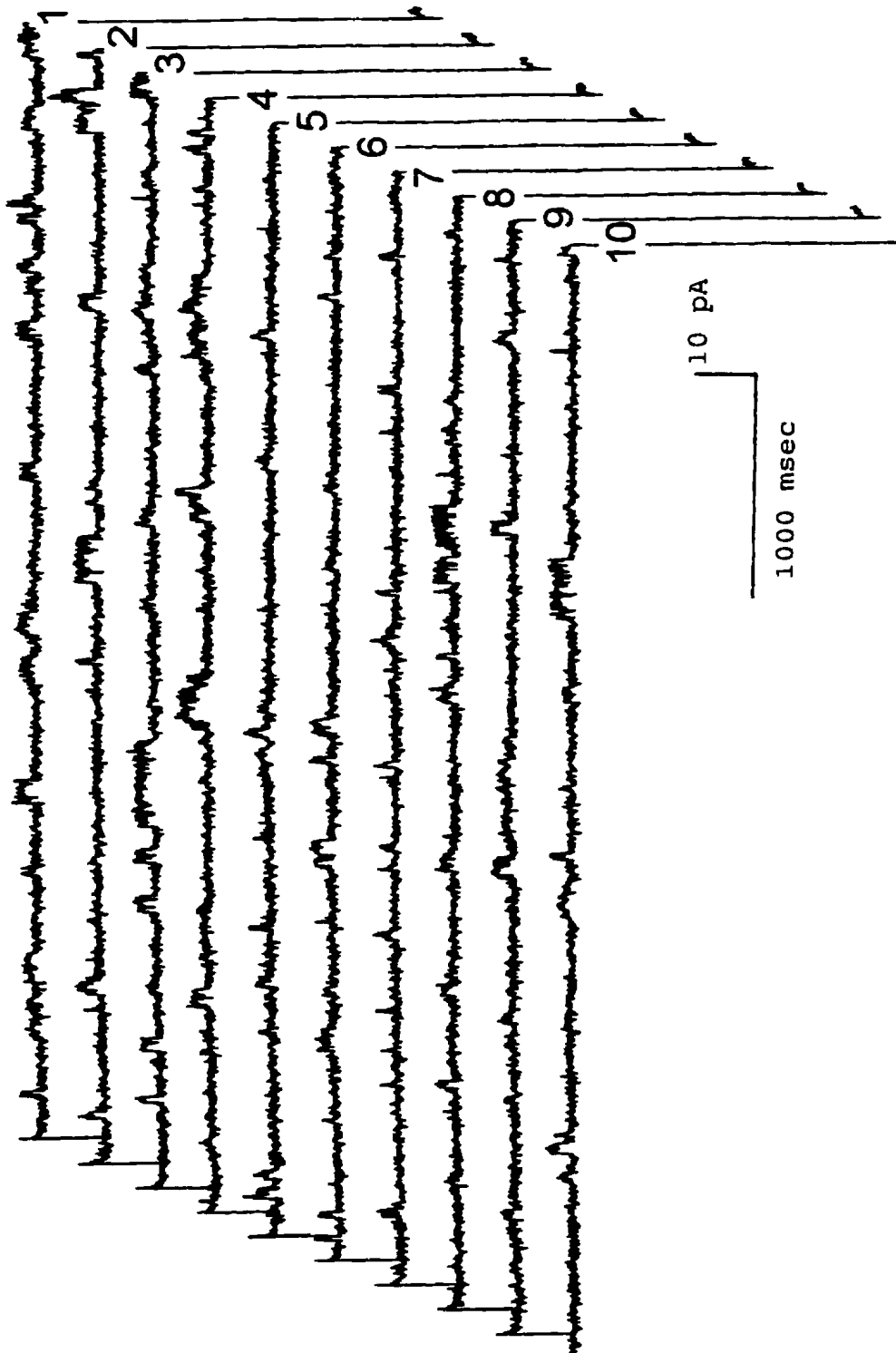
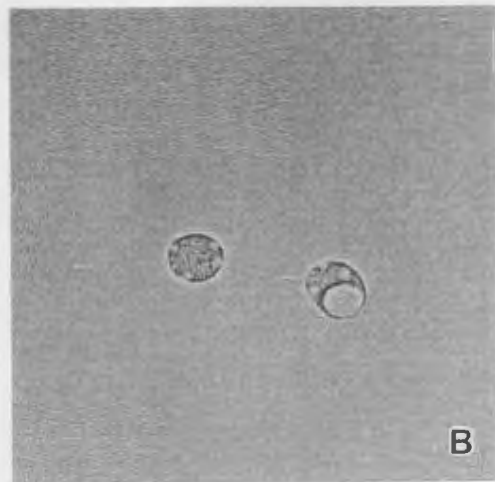
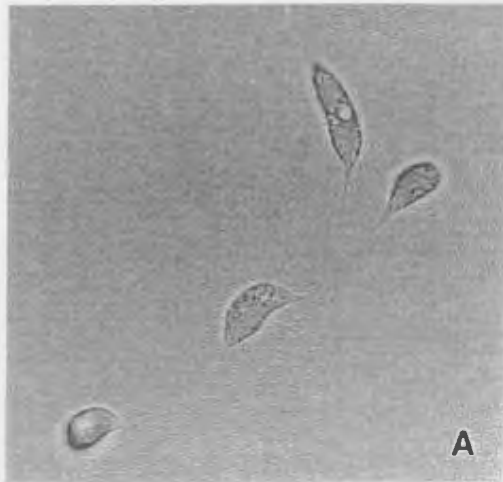


Fig. 3.11: Morphological changes in *Entomophaga aulicae* protoplasts with time when suspended in recording bath solution. **A**, spindle-shaped cells with low numbers of small vacuoles in cells 50 min. after suspension in solution. **B** and **C**, round cells with large vacuoles in cells 120 and 150 min., respectively, after exposure to bath solution. **D**, rounded cells with large vacuoles 9 minutes after suspension in bath solution. Magnification bar represents 50 μ m.



Chapter 4

Potassium ion channels in protoplasts of *Entomophaga aulicae*.

4.1 Introduction

Since the introduction of patch clamp technology ion channel activity has been studied in a number of systems. Early studies investigated mammalian, squid, frog and snail cells (Hille, 1984). More recently, the techniques have been used with non-animal systems including algae (Lew et al., 1990), bacteria (Buechner et al., 1990), plants (Fairley and Walker, 1989) and fungi (Caldwell et al., 1986; Garrill et al., 1992a & 1992b; Levina et al., 1994 & 1995). A major challenge in adapting the patch clamp technique to these organisms is the establishment of a gigaseal. The inability to form high resistance seals has been reported by investigators in a number of fields (Elzenga et al., 1991; Saimi et al., 1992; Lew et al., 1992). The main obstacle for high level pipette/membrane seals with plant and fungal cells is the existence of a cell wall. Protocols for enzymatic digestion of wall material have been developed for specific cellular systems (Garrill et al., 1992b; Barbara et al., 1994).

One does not need to apply wall-degrading enzymes for *E. aulicae* to form protoplasts; they form spontaneously *in vivo* (Tyrrell, 1977) and in artificial medium (Nolan, 1985). Transmission electron microscope and fluorescent microscopy studies have not detected any cell wall on these protoplasts (Murrin and Nolan, 1987; Beauvais et al., 1989). Chitin and β -glucans are major components of fungal cell walls (Gooday and Gow, 1990). *E. aulicae* possesses a protoplast-specific chitin synthase inhibitor and has low levels of glucan synthase activity (Beauvais and Latgé, 1991). Ease of protoplast

propagation and the lack of a cell wall make *E. auilcae* an attractive candidate for patch clamp studies.

Voltage-activated K^+ channels, cation-selective stretch-activated channels and anion-selective channels have been identified in fungal plasma membranes (Garrill, 1994). Calcium-transporting stretch-activated channels are involved in hyphal tip growth of *Saprolegnia ferax* (Garrill, 1992b). In yeast, osmoregulation may involve stretch-activated channels (Gustin et al., 1988) and voltage-activated channels (Bertl and Slayman, 1992). A depolarization-activated K^+ channel identified in *Saccharomyces cerevisiae* is believed to be involved in balancing charge movements during transport (Bertl et al., 1993).

Ion channel studies can be performed in a number of recording configurations. 'Whole cell', 'cell-attached' and excised patches in 'outside-out' or 'inside-out' orientation are the major configurations. An early study of *E. auilcae* protoplasts using whole cell recordings (Hicks and Murrin, unpublished results) showed the presence of outward rectifying voltage-activated channel activity. The channels were present only during depolarizing voltages. Tetraethylammonium ion (TEA^+), a potassium ion channel blocker (Begenisich, 1994), when added to the bath solution reduced activity of the outward current. This early work suggested that *E. auilcae* protoplasts may have outward rectifying, voltage-activated potassium ion (K_O^+) channels. Pharmacological channel blockers have been known to behave differently in different biological systems (Swandulla and Chow, 1992). Therefore a more rigorous study of channel characterization was required to confirm the preliminary results.

This chapter documents the characterization of ion channel activity in *E. aulicae* protoplasts using the methodology presented in Chapter 3. Briefly, it entails recording in the 'cell-attached' mode using recording solutions with osmolality and pH levels equivalent to those of *in vitro* growth conditions. Bath and pipette solutions used were identified in Chapter 3 for being associated with acceptable chances of gigaseal formation and good quality, consistent recordings.

The approaches used for data analysis, as well as channel characterization, are presented. Mean current amplitude values were used to determine the current-voltage relationship of the voltage-activated channels. Two K^+ channel blockers, TEA⁺ and barium ion (Ba^{2+}), were used in channel characterization. The reduction in activity associated with these blockers suggest that these channels are indeed involved with K^+ transport. The current-voltage pattern was sensitive to elevated levels of K^+ applied to the exterior of the cell. This serves as further evidence that *E. aulicae* protoplasts contain K^+ channels.

4.2 Materials and Methods

4.2.1 Culture Preparation

Protoplasts of *Entomophaga aulicae* (isolate FPMI 893) were maintained at 20°C in Grace's insect tissue culture medium (Canadian Life Technologies, Inc.) supplemented with 2.7% fetal calf serum (Canadian Life Technologies, Inc.).

Culture dishes for cell recording were prepared from 35x10 mm Petri dishes (Becton Dickson Labware). A 15mm diameter circular disk was excised from the bottom of each dish and discarded. Glass coverslips, 22x22 mm, were ethanol cleaned. Prior to

assembly, the culture dishes, coverslips and a syringe filled with valve lubricant/sealant (Dow Corning 111 Compound) were UV sterilized. The coverslip was mounted on the exterior of the dish bottom covering the excised area with a thin layer of sealant. The assembled dishes were UV sterilized prior to use.

A 24-hour protoplast culture was transferred to a 15 ml conical centrifuge, centrifuged at 150xG for 5 minutes and the pellet resuspended in the appropriate recording bath solution. Approximately 30 minutes after introduction of the bath solution, an aliquot of the cell suspension was transferred to the coverslip section of a prepared culture dish.

4.2.2 Recording Methods

All preparation and experimentation was performed at room temperature. Agar bridges were prepared from glass capillary tubes (Drummond Scientific Co.) bent at a 90° angle. They were filled with a solution consisting of 2%(w/w) agar (Difco Laboratories) prepared in the same formulation of recording bath solution used for the cell suspension. The bridge holder was filled with the same bath solution passed through a 0.22 µm syringe filter.

Patch pipettes were made from fiber-filled borosilicate glass capillary tubes (World Precision Instruments, Inc., Narco Scientific). They were cut on a two stage vertical puller (Narishige Model PP-83, Japan). The pipettes were heat polished by positioning them close to a heated wire. The pipettes were backfilled using a finely tapered syringe filled with 0.22 µm filter sterilized pipette solution. More detail on the

backfilling technique can be found in section 3.2.2. The tips were dipped in Sigmacote (Sigma Chemical Co.) and mounted on the pipette holder.

The hardware used for all recordings consisted of a Zeiss IM-35 inverted microscope, Zeiss micromanipulator, List patch clamp probe and controller L/M-EPC7 (Medical Systems Corp.) with a 10 kHz filter setting, TL-1 Interface (Axon Instruments, Inc.), and a Nicolet Model 310 digital oscilloscope. An IBM-compatible Impulse computer with a Samsung monitor was used to control and record data acquisition. Refer to Figs. 3.1 and 3.2 for equipment orientation.

The methodology used for monitoring gigaseal formation is as stated in section 3.2.2.5 and 3.2.2.7. All of the data presented in this chapter are from gigaseal levels of pipette/membrane resistance.

Single channel currents were recorded in the 'cell-attached' recording configuration

4.2.3 Ramp voltage studies

Bath and pipette solution formulations used in ramp experiments are found below in Table 4.1.

The data acquisition protocol, Ramp 5S, used pClamp Clampex software (Axon Instruments Inc.). The parameters of Ramp 5S are listed in Appendix 1. The program runs a repetitive cycle in which the membrane is subjected to programmed voltages for 5 seconds followed by a 5 second period at the resting membrane potential (RMP). In Ramp5S the voltage protocol is referred to as a ramp. In this study a voltage ramp from 100 mV hyperpolarized to 100 mV depolarized was applied for 5 sec. Data are collected

at the voltages between these specified limits. The ramp is repeated every 10 sec. Deviations from the linear baseline represent activity. This allows one to scan a broad range of voltages for channel activity in a short time period.

Table 4.1: Patch clamp recording solutions used in Ramp voltage studies of *E. aulicae* protoplasts.

Chemical	Bath Solution	Pipette Solution
NaCl	140 mM	140 mM
KCl	5 mM	5 mM
CaCl ₂	1 mM	2 mM
MgCl ₂ •6H ₂ O	1.2 mM	2.4 mM
¹ MES	10 mM	10 mM
glucose	3.8 mM	3.8 mM
fructose	2.2 mM	2.2 mM
sucrose	36 mM	29.8 mM
final pH	6.2	6.2

¹MES = 2 N-morpholino ethanesulfonic acid

4.2.4 Hyperpolarization studies

The recording solutions used for monitoring channel activity during membrane hyperpolarization are listed in Table 4.1.

The parameters for the pClamp data acquisition protocol, Singles, are listed in Appendix 1. For hyperpolarization studies the Singles program holds the membrane at a specified voltage below its RMP for a period of 5 seconds. This is followed by a 10 second period with no applied voltage, i.e., at RMP. This is repeated 10 times at the same voltages. Current fluctuations from the flat baseline represent channel openings. Activity above the baseline represents outward movement of cations from the cell; inward movement is characterized by activity below the baseline.

4.2.5 Depolarization studies

4.2.5.1 Channel recordings

Table 4.1 lists the solutions used for membrane depolarization recordings.

The Singles pClamp data acquisition protocol was used in these studies. The acquisition parameters are listed in Appendix 1. Data are acquired in a similar fashion to that stated in section 4.2.4 with the exception of the applied voltages. In the case of depolarization, the voltages used in the program were in the positive mV range.

4.2.5.2 Analysis of Multiple Current Level Recordings

Data analysis consisted of first using pClamp's Fetchan Demohist program (see Appendix 2) with visual validation of channel activity to extract an idealized plot of the data. This entailed setting a baseline, i.e. closed channel level, for the plotted data and then setting a level representing open channel activity. Individual open and closed events were visually scrutinized for acceptance. If the program did not detect obvious channel activity or recorded false openings, the baseline and/or level settings were adjusted until

channel detections were deemed acceptable. The program compiled an events list from the idealized plot and these data were stored in separate files in ASCII format.

To facilitate further data analysis, amplitude values from the idealized plot events list were binned for graphical representation as histograms using pStat (see Appendix 2 for parameter settings). Several approaches were then attempted to analyze data in histogram format including 1. pStat's Gaussian fit command, 2. pStat's arithmetic mean, 3. the "findmean" program and 4. the use of Origin software to perform weighted mean calculations.

The mean current amplitude value was determined by using the weighted average calculation as defined by Sokal and Rohlf (1995). The use of the weighted mean is appropriate with histograms, i.e. binned data. It is the same as determining the number of values in a bin and multiplying them by the mean bin value. This is repeated for all of the bins. The sum of these products is then divided by the total number of data points. Its calculation is as follows:

$$\text{Amp} = \frac{\Sigma(\text{amp} \cdot n)}{\Sigma n} \quad (\text{Eq'n. 4.1})$$

where

amp = current amplitude (pA)

n = # of events having an amplitude value.

The multichannel analysis program, 'findmean', was retrieved from the internet. It is a MS-DOS program and was found through a document (Ramanan et al., 1996) in a

patch clamping website. It was received through ftp from patch.pnb.sunysb.edu (129.49.110.105) and loaded on an IBM-compatible computer for use.

4.2.5.3 *Current-voltage relationship*

Mean current amplitude values (I) were calculated using equation 4.1. They were plotted against the applied voltage (V) from which the data were collected. Linear regression of the values was used to calculate the slope of the I/V plot. The slope value represents the membrane conductance with the units in picoSiemens (pS).

4.2.5.4 *Channel blockers*

In order to block K⁺ channel activity, 5mM Ba Cl₂ or 10 mM TEA Cl were added to the pipette . The pipette and bath recording solutions used in channel blocking experiments are as listed in Table 4.2.

Data acquisition was performed with the same set-up as stated in section 4.2.5.1. Membrane depolarization was performed using the Singles protocol.

Data analysis was based on visual inspection of the channel recordings only. Comparisons based on the level of activity were made between recordings with and without the presence of channel blockers. Numerical analysis was not performed because of some difficulty with baseline drift.

Table 4.2: Patch clamp recording solutions for channel blocker studies in protoplasts of *Entomophaga aulicae*.

Chemical	Bath Solution	Control Pipette Solution	Ba ²⁺ Pipette Solution	¹ TEA ⁺ Pipette Solution
NaCl	140 mM	140 mM	140 mM	140 mM
KCl	5 mM	5 mM	5 mM	5 mM
CaCl ₂	1 mM	2 mM	2 mM	2 mM
MgCl ₂ 6H ₂ O	1.2 mM	2.4 mM	2.4 mM	2.4 mM
MES	10 mM	10 mM	10 mM	10 mM
glucose	3.8 mM	3.8 mM	3.8 mM	3.8 mM
fructose	2.2 mM	2.2 mM	2.2 mM	2.2 mM
sucrose	36 mM	29.8 mM	14.8 mM	19.8 mM
BaCl ₂ 2H ₂ O	-	-	5 mM	-
² TEA Cl	-	-	-	10 mM
final pH	6.2	6.2	6.2	6.2

¹TEA⁺ = tetraethylammonium ion

²TEA Cl = tetraethylammonium chloride

4.2.5.5 Effect of elevated K⁺ levels on conductance

In order to compare the effects of elevated K⁺ on channel activity, data collected under 'control' conditions were required. For this study, 'control' conditions are those identified in Chapter 3 of this document, i.e., the protocol deemed most suited for *E.*

aulicae ion channel studies. 'Control' conditions differ from elevated K^+ levels only by the recording solution formulations. Control potassium levels were 5mM, and elevated levels were 60 and 140 mM. 'Control' bath and pipette solutions used in this study are listed in Table 4.1. The solutions with different K^+ levels are listed below in Table 4.3.

Mean current amplitude values were determined using the same methodology stated in section 4.2.5.2 . Membrane conductance was calculated in the same manner stated in section 4.2.5.3.

Table 4.3: Patch clamp recording solution formulations for studying the effects of elevated potassium ion levels on channel activity.

Chemical	60 mM K^+	60 mM K^+	140 mM K^+	140 mM K^+
	Bath Solution	Pipette Solution	Bath Solution	Pipette Solution
NaCl	85 mM	85 mM	5 mM	5 mM
KCl	60 mM	60 mM	140 mM	140 mM
CaCl ₂	1 mM	2 mM	1 mM	2 mM
MgCl ₂ 6H ₂ O	1.2 mM	2.4 mM	1.2 mM	2.4 mM
MES	10 mM	10 mM	10 mM	10 mM
glucose	3.8 mM	3.8 mM	3.8 mM	3.8 mM
fructose	2.2 mM	2.2 mM	2.2 mM	2.2 mM
sucrose	36 mM	29.8 mM	36 mM	29.8 mM
final pH	6.2	6.2	6.2	6.2

4.3 Results

4.3.1 Ramp voltage studies

Ramp voltages, in which the membrane is subjected briefly to voltages ranging from -100 mV to +100 mV, were used to identify the voltage activation range. The Ramp5S protocol used in this study runs 10 episodes consisting of 5 seconds of ramping voltage followed by 10 seconds at the RMP. Ramp experiments were performed on approximately 15 cells. In all cases channel activity showed a high level of variability. In a typical recording from one cell, an episode's channel pattern would be restricted to negative voltages, i.e., hyperpolarization (Fig. 4.1). The next episode, recorded only 10 seconds later, showed very little activity (Fig. 4.2). This was followed by activity with only positive voltages (Fig. 4.3). This pattern seemed to be random; depolarization activity did not always occur after hyperpolarization-activated signals.

4.3.2 Hyperpolarization studies

Hyperpolarization resulted in sporadic current patterns (Figs. 4.4 and 4.5) during which delayed, short-lived, inward ion movement patterns were common (n=18 cells). The hyperpolarization-generated patterns were, in general, spiky and did not reach easily discernible plateau amplitudes.

4.3.3 Depolarization studies

4.3.3.1 Channel recordings

Depolarization studies resulted in easily discernible channel recordings when the membrane was subjected to voltages in the +60 to +100 mV range (Fig. 4.6) (n=34 cells). The current pattern of ion transport across *E. aulicae* protoplast membranes indicates multiple current channel activity, i.e., a number of channel amplitudes were present. Three current amplitudes, 3.13, 5.83 and 7.71 pA, are identified in Fig. 4.7a to serve as a scale for this recording of one episode. Fig. 4.7b is a histogram of the current amplitudes from 10 episodes, one of which is found in Fig. 4.7a. No pattern of clusters at equidistant amplitudes is discernible in Fig. 4.7b. In fact it was not found in any of the recordings.

4.3.3.2 Analysis of Multiple Current Level Recordings

Analysis of multiple current channel recordings is a complex issue. A multichannel data analysis program found on the internet, 'findmean', and its corresponding journal publication (Ramanan et al., 1992) were investigated for their potential use in analyzing the *E. aulicae* channel data. The program requires information on a number of parameters before data analysis can proceed. The investigator must supply the program with a value for the number of channels present. This was unknown in the collected recordings. Probabilities and meantime data information was also required. I can only assume that these last two parameters were referring to channel open times. I was therefore unable to supply the required information which resulted in the inability to use this software program to analyze the data.

The data collected by visually validating channel openings (i.e. the events lists from the idealized plots) were compiled in histogram format from which the mean current amplitude values were calculated. I found the application of pSTAT's histogram generation and Gaussian fit functions to the data to be of little value. A correct fit of a Gaussian equation to a histogram allows one to extract a mean value of the histogram plot. A poorly fitting equation results in lack of confidence in the derived value of the mean. Fig. 4.8 shows an amplitude histogram with a Gaussian fit. Large discrepancies exist between the Gaussian equation and the actual histogram values. The difference between a theoretical value, in this case generated from a Gaussian equation, and an actual value, in this case an amplitude histogram value, is known as a residual. It is used to assess closeness of fit between theoretical and true values. Fig. 4.9 shows the residual plot for the amplitude data of Fig. 4.8. Because the pattern of residuals does not form a regular band about the x axis, we conclude that a normal distribution is not a good model for the data. The closeness of fit of a Gaussian equation can be subjective. If one chose to accept the Gaussian fitting standards of the pCLAMP program for *E. auilcae* ion channel activity another problem can arise. Multiphasic curve fitting would be required to cover the multiple levels of current activity. The curve fitting program allows one to have a maximum of 4 curves. In some instances the *E. auilcae* current amplitudes showed more than 4 peaks.

pSTAT offers information on collected data without invoking the Gaussian fit command. One of the values generated is the arithmetic mean. Fig. 4.10 shows an amplitude histogram of channel activity. Visual inspection of this graph suggests that the mean current amplitude is approximately 4.5 pA. The pSTAT's arithmetic mean value of

the same data is 2.36 ± 2.45 pA (Table 4.4). The large discrepancy resulted in abandoning this approach for determining mean current amplitude values.

Use of the weighted average formula (Eq'n. 4.1) for determining mean amplitude values was deemed appropriate. Use of the formula resulted in a mean value of 4.60 pA for the data presented in Fig. 4.10 which is more credible than pSTAT's generated 2.36 pA. This resulted in the adoption of the weighted mean formula for all calculations of mean amplitude.


Table 4.4: The pSTAT-generated information on the amplitude values represented in Fig. 4.10. Note the value for the amplitude arithmetic mean value of 2.36 pA indicated by the arrowhead.

General information for file L6301C16.EVL

Number of events 3434
 Total record time in file 39.033 s
 Number of conductance levels 1

Level 1 amplitude data

Bin distribution mode: **Standard**

Arithmetic mean (S.D.) 2.36 \pm 2.45 pA 
 Histogram area 34.72 event-pA
 Fitting range area 34.72 event-pA
 Fit area as % of data area .. 100.0 %
 Number of outliers 0

4.3.3.3 Current-voltage relationship

I/V plots were based on mean amplitude values derived from ion channel recordings performed at different voltages. Fig. 4.11 shows channel activity at different voltages. The amplitude histograms and mean amplitude values derived from Fig. 4.11 data are represented in Fig. 4.12. The resultant I/V plot, based on a number of cell recordings is found in Fig. 4.13. The slope of the I/V curve gives a conductance value of 31 pSiemens (pS).

4.3.3.4 Channel blockers

Use of two K^+ channel blockers, TEA⁺ and barium, resulted in reduced ion channel activity (n=2 and 4 cells, respectively). Fig. 4.14 shows typical channel activity when no blockers were present. Channel openings are easily recognized as plateau-forming patterns. Use of both barium and TEA⁺ resulted in major reductions in activity (Figs. 4.15 & 4.16 respectively). Unfortunately high levels of baseline drift occurred, and precluded numerical analysis of the data. However, figures such as 4.15 and 4.16 allow for visual assessment of channel activity. The presence of background noise and non-horizontal baselines masks possible brief openings since the latter, if present, have low amplitude values. The effects of these channel blockers on channel activity suggest that K^+ channels exist in *E. aulicae* protoplast membranes.

4.3.3.5 Effect of elevated K^+ levels on conductance

The effects of elevated levels of K^+ on membrane conductance are found in Fig. 4.17. Control recordings of *E. aulicae* protoplast ion channels used 5 mM K^+ in the

recording solutions. The resultant conductance value is 31 pS. The I/V slope was reduced to 10.6 pS and -20.1 pS with K⁺ concentrations of 60 mM and 140 mM respectively. This sensitivity to K⁺ concentrations suggests that there are K⁺ ion channels in *E. auilcae*. The negative value of the conductance with 140 mM potassium means that the channels are less conductive at the higher voltages. Negative conductance values have not been found in the literature. However, the values generated from the 60 and 140 mM K⁺ are based on only one recording per voltage.

4.4 Discussion

The identification of voltage-activated channels from the 'whole-cell' recordings (Hicks and Murrin, unpublished results) warranted further investigation using single channel signals. With the protocol developed for attaining gigaseal recordings from *E. auilcae* protoplasts, documented in Chapter 3, ion channel studies were initiated. Voltage-activated channels have been found in fungi (Garrill, 1994). Gigaseals, attained with *E. auilcae* protoplasts (see Chapter 3), allow the investigator to acquire data over a broad range of voltages. This initial study of ion channels in protoplasts of *E. auilcae* deals with channels sensitive to changes in voltage.

4.4.1 Ramp voltage studies

Ramp voltage experiments are commonly used in patch clamp experiments (Sakmann and Neher, 1995a; Hancock et al., 1996). They allow

the investigator to examine the effects of a broad range of voltages on channel activity. The data collected in the -100mV to +100 mV range in this study showed no consistent pattern. The high level of variability and apparent unpredictable nature of the ion current pattern generated from ramp voltage runs led us to discontinue this approach. With such a high level of variability channel characterization using specific blockers could not be done. A reduction in activity or a shift from hyperpolarization sensitivity to depolarization activation may falsely be attributed to channel blockage.

4.4.2 Hyperpolarization studies

Hyperpolarization-sensitive channels are present in the plasma membrane of plants (Roberts and Tester, 1995) and animals (Hancock et al., 1996) and in vacuolar membranes of fungi (Bertl and Slayman, 1992). K⁺ channels sensitive to both positive and negative voltages have been identified in yeast plasma membranes (Ramirez et al., 1989).

Membrane hyperpolarization of *E. auilcae* protoplasts did elicit a response; however, the recorded data showed sporadic activity. No channel activity was recorded during whole-cell hyperpolarization of *E. auilcae* protoplasts in the earlier study (Hicks and Murrin, unpublished data). This suggests that hyperpolarization-activated channels may not function during normal physiological conditions. The current pattern may have been caused by undue application of negative voltage to the membrane. The absence of hyperpolarized-activated channel activity suggests that *E. auilcae* protoplasts do not contain the same type of channels found in the plasma membrane of *S. cerevisiae*

(Ramirez et al., 1989). No tonoplast studies have been performed on *E. aulicae*. It is therefore unclear as to whether *E. aulicae* cells contain hyperpolarization-sensitive channels similar to those found by Bertl and Slayman (1992) in *S. cerevisiae*.

4.4.3 Depolarization studies

4.4.3.1 Channel recordings

Depolarizing voltage-activated channels with outward currents are present in *E. aulicae* protoplasts. Channel activity shows openings of non-equidistant current amplitude. Depolarization-sensitive K^+ channels are present in the plasma membrane of *Saccharomyces cerevisiae* (Gustin et al., 1986; Bertl et al., 1993). However the *S. cerevisiae* recordings showed open channel current flow at easily discernible amplitudes; they did not exhibit multiple current channel openings with numerous current amplitudes. Multiple current channel openings have been found in stretch-activated channels of an oomycete *Saprolegnia ferax* (Lew et al., 1992).

4.4.3.2 Analysis of Multiple current Level Recordings

Analysis of multiple current channel recordings is a complex issue. A number of software packages are available for recordings with openings at a single current amplitude value. They include pCLAMP by Axon Instruments, CED 1401 by Cambridge Electronic Design and VCAN by Strathclyde Electrophysiology Software (Dempster, 1993). However, commercially available software packages for ion channel behaviour are not suitable for data containing non-equidistant multiple amplitudes (VanDongen, 1996). At

least three multichannel analysis programs do exist. They are TRANSIT (Van Dongen, 1996), "findmean" by S.V. Ramanan and ADAM by Dabrowski (Ramanan et al., 1996). The documentation for the "findmean" program (Ramanan et al., 1992) and its MS-DOS program required knowledge of parameters not calculated by the program and therefore unknown to the investigator. The general acceptance of use of these programs by researchers actively engaged in patch clamping is unknown. General patch-clamp reference books (Sakmann and Neher, 1995a; Hille, 1992) do not discuss the use of these programs, no doubt due to their lack of discussion of multichannel analysis.

Based on widespread use and acceptance of pCLAMP software as a standard for ion channel analysis (Dempster, 1993) and its availability, it was employed in multichannel analysis. The Fetchan program of the pCLAMP software system was used to detect channel openings. Although this software allows for automated measurement of channel amplitudes, one cannot solely rely on the resultant data (Heinemann, 1995). Subtle errors, which may go undetected, may occur if a flaw in the automated method is present. Visual inspection by the investigator validating current amplitudes is an accepted approach (Heinemann, 1995; Dempster, 1993) and was incorporated in all of the data collected. Although this is introducing a subjective view to the information collected, one must acknowledge the ability of the human eye to effectively discriminate pattern from background noise. Also, it seems that experimenter subjectivity is inherent in patch clamp data analysis. Visual inspection is used to check current amplitude values in manual data analysis too. Therefore, the approach used in this study is considered valid.

Since pCLAMP comes with a statistical package, pSTAT, it was initially used in determining mean channel amplitude values. However, my own confidence in the ability

of this program to analyze multichannel records was low. The standard approach to determining current amplitude is to use the current amplitude histogram plot and, have a Gaussian equation fit it (Colquhoun and Sigworth, 1995). The theoretical mean of the equation, μ , is then used as the mean amplitude value. However, with the multichannel recordings generated, fitting one Gaussian equation to an all-points amplitude histogram proved to be inaccurate.

pSTAT offers another means of determining mean amplitude. Without invoking any curve-fitting to the amplitude histogram data, some numerical information on the data is available. One such parameter available is the arithmetic mean. Its accuracy was questionable and it was therefore deemed inappropriate for use.

A weighted average formula (Eqn.4.1; Sokal and Rohlf, 1995) was used for determining mean amplitude. Using this formula, mean amplitude calculations were in agreement with visual estimations from amplitude histograms. Therefore, it was used in all future calculations.

4.4.3.3 Current-voltage relationship

Ion channels are characterized by their current-voltage relationship (Hamill et al., 1981). With information on mean amplitude values and their associated voltages, a current-voltage (I-V) plot can be made. The slope of the I-V curve for *E. auilcae* gave a conductance value of 31 pS. Gustin et al. (1986) reported a conductance of 20.5 pS for outward rectifying potassium ion channels in the plasma membrane of *Saccharomyces cerevisiae*. Conductance values reported for inward rectifying potassium ion channels include the whole cell value of 47.8nS for *Saprolegnia* (Lew et al., 1992), and single

channel values of 30 and 65 pS in the alga *Mougeotia* (Lew et al., 1990) and 28pS and 11.4 pS for frog muscle (Hancock et al., 1996).

Channel conductances have a broad range. K^+ channels have been shown to range from 2 to 200 pS (Moczydlowski et al., 1988). Since the conductance values depend on the ionic content of the recording solutions used, it is difficult to state whether the conductance values are due solely to channel type. I-V plots and their resultant conductance values are, however, still commonly used in publications for channel characterization. Comparison of conductance values, using identical recording solutions for a particular channel, would help determine the similarity of the channels in other systems. However, based on the number of recording formulations investigated for this study, adoption of reported formulations may not result in compatibility.

4.4.3.4 Channel blockers

Channels can also be characterized by their sensitivity to specific agents. One such chemical, TEA⁺ has been identified as a K^+ ion channel blocker. It can block channels when applied externally as well as internally (Hille, 1984). Another blocker, barium (Ba^{2+}), blocks K^+ channels when applied externally (Hurst et al., 1995; Armstrong et al., 1982). In order to monitor the effects of these blockers on channel activity, an applied voltage of +80 mV was used since it always evoked discernible channel openings in *E. aulicae* protoplasts. The concentrations of the blockers used in the solutions, 5 mM of Ba^{2+} and 10 mM of TEA⁺, have been used in *Saprolegnia* studies (Lew et al., 1990). Since the *E. aulicae* protoplasts remain attached to pipettes when they are removed for replacement, recordings from a cell before and after application of a blocker were not

possible. All of the recordings using blockers had high levels of baseline drift in the first 1-2 seconds of recording. This made use of the Fetchan event detection system unsuitable for use. Manual baseline adjustments in the non-linear drifting regions were difficult to control and believed to result in inaccurate data. Therefore, numerical summation of the effects of blockers was not possible. This left visual assessment of channel activity as the only means of determining the effect of the blockers on channel activity. Use of Ba^{2+} and TEA^{+} caused major reductions in the activity. This consistent, marked, reduction suggests that the major depolarization-gated channel activity is involved in K^{+} transport.

The effects of Ba^{2+} and TEA^{+} on channel activity are consistent with those found by Lew et al. (1990) on K^{+} channels. When these two blockers were used in identifying channels in the algal cells no activity was noted. Depolarization-activated channels of *S. cerevisiae* have been blocked by using Ba^{2+} and TEA^{+} (Gustin et al., 1986).

With the identification of the protoplast channels as K^{+} , based on blocking agents, further confirmation was required. Although a large selection of pharmacological agents have been identified as K^{+} channel blockers, their behaviour may vary with different systems (Swandulla and Chow, 1992). Therefore, another approach for confirmation of channel identity was sought.

4.4.3.5 Effect of elevated K^{+} levels on conductance

Increasing extracellular K^{+} concentration has been associated with increasing inward K^{+} current (Vonbeckerath et al., 1996) resulting in higher conductance levels. The amplitude of the current is affected by the ion gradient. Since membrane depolarization of *E. auilcae* protoplasts show outward ion movement, use of higher levels

of extracellular K^+ should diminish the current amplitude if the channels are indeed K^+ . This would result in a lowered conductance level with higher K^+ concentration in the extracellular solutions. The data collected support the K^+ classification of the channel. Higher levels of external K^+ caused a drastic reduction in channel conductance. With 5 mM K^+ the conductance was 31 pS. The I-V slope was reduced to 10.6 pS and -20.1 pS with K^+ concentrations of 60 mM and 140 mM respectively. This indicates a sensitivity to K^+ , and, serves as further evidence of the identification of the major *E. aulicae* channels as K^+ . However, the results at higher K^+ levels are based on one recording at each voltage. Further data collection with recording solutions of 60 and 140 mM K^+ is required to confirm the preliminary results obtained.

4.4.4 Suggested roles of identified channels

Outward-rectifying, depolarization-activated K^+ channels, similar to those identified in *E. aulicae* have been found in the plasma membrane of the yeast *S. cerevisiae* (Gustin et al., 1986; Bertl et al., 1993). Suggested roles for the existence of these channels are maintenance of membrane potential, osmoregulation and charge balancing during transport.

The role of voltage-dependent channels in the maintenance of membrane potential has been suggested by Gustin et al. (1986). Fungi have an ATP- H^+ pump in their plasma membrane (Griffin, 1994). It is believed that this pump, in addition to ion channel openings, functions in the regulation of cell membrane potential.

In order for *E. aulicae* protoplasts to survive osmoticum ranging from 0 to 550 mOsm (Chapter 2) a transport mechanism must be involved. K^+ channels, classified as

stretch-activated, have been associated with regulating cell volume (Sarkadi and Parker, 1991). Osmotic stress in yeast caused by the addition of NaCl to the medium causes a significant drop in the cytoplasmic K^+ level, an increase in Na^+ levels and an increase in glycerol production (Sunder et al., 1996). The total cationic level in the cytoplasm of the yeast was not significantly affected by the extracellular addition of NaCl. This suggests that the cytoplasmic charge remained unchanged, and, that the expulsion of K^+ was involved in charge balancing to compensate for intake of Na^+ . Regulatory volume decrease (RVD) in kidney cells is also associated with cellular K^+ loss (Roy and Banderli, 1994). Membrane hyperpolarization followed by depolarization occurs during RVD in these cells. If a similar change in membrane potential occurs in *E. aulicae* during osmotic stress, the depolarization may activate the K^+ channels present.

4.5 Summary

Outward-rectifying, depolarization-activated K^+ channels have been identified in *E. aulicae* protoplasts. The current-voltage relationship of these channels shows a conductance of 30.1 pS during 'cell-attached' patch clamp recording using a pipette solution of 5 mM K^+ . Channel characterization was based on the effects of channel blockers. Activity was sharply reduced with the addition of K^+ -specific channel blockers, Ba^{2+} and TEA^+ . Membrane conductance was sensitive to extracellularly-applied elevated levels of K^+ . Suggested roles for these channels include maintenance of membrane potential, charge balancing and osmotic regulation.

Figs. 4.1-4.3: Single channel recordings in cell attached configuration during a 5 second ramp from hyperpolarizing 100 mV to depolarizing 100 mV. The figures are from recordings from the same cell over a period of 45 seconds. **Fig. 4.1** shows activity associated with the negative voltages, i.e., hyperpolarization sensitive.

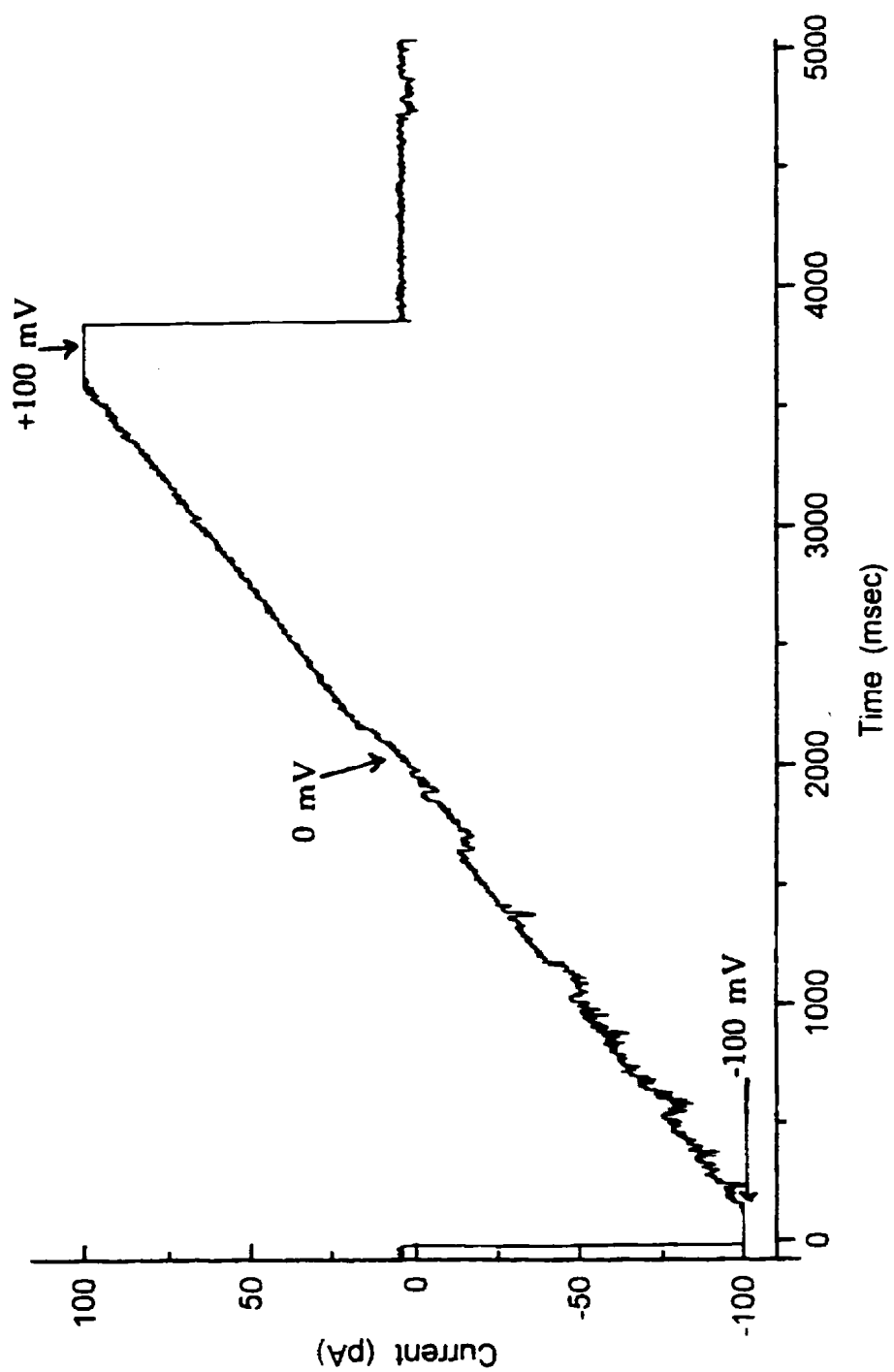


Fig. 4.2 : Single channel recording in cell attached configuration showing ramp voltage activity in the episode following Fig. 4.1. Very little activity is present over the -100 mV to +100 mV range.

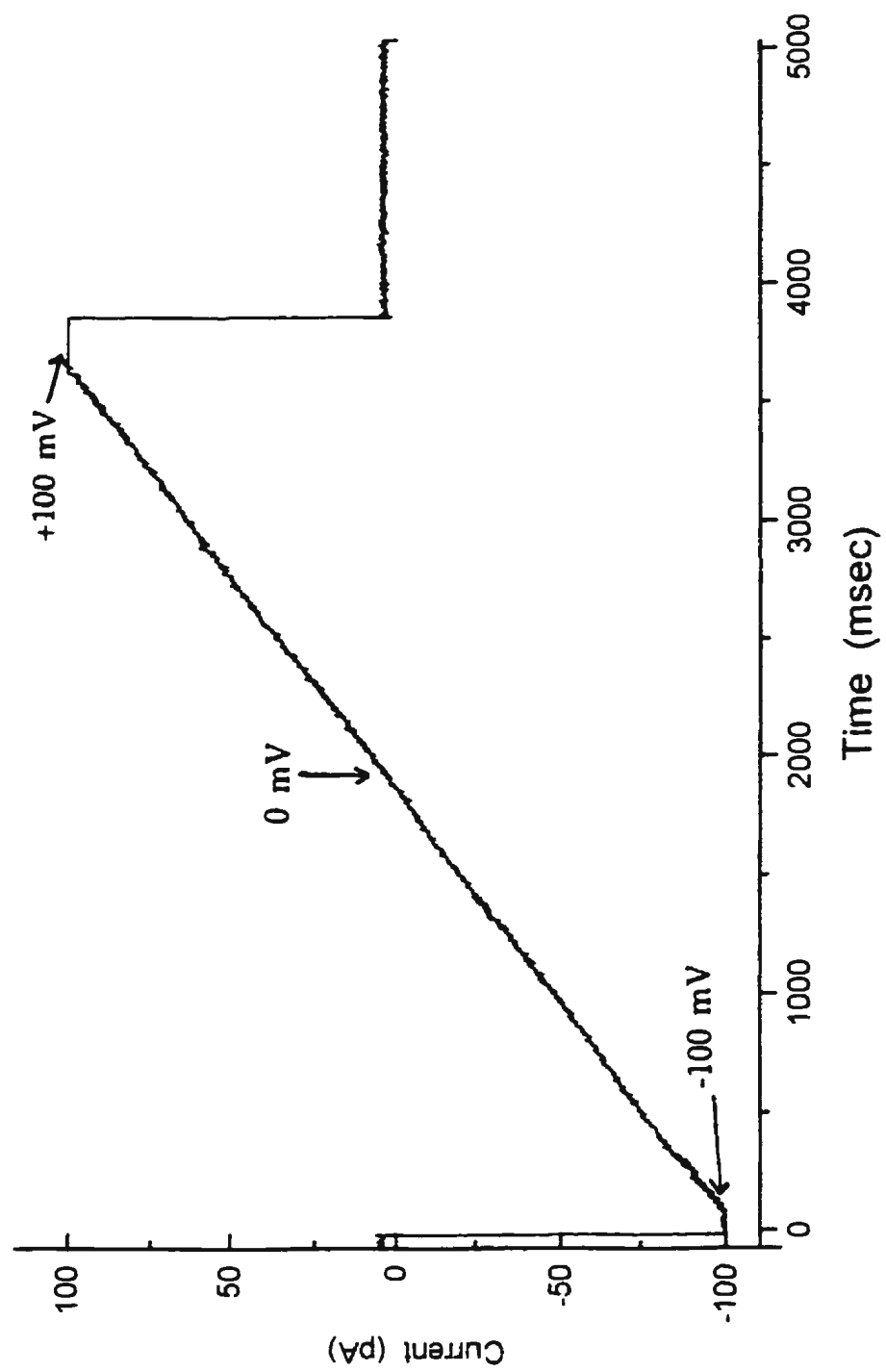
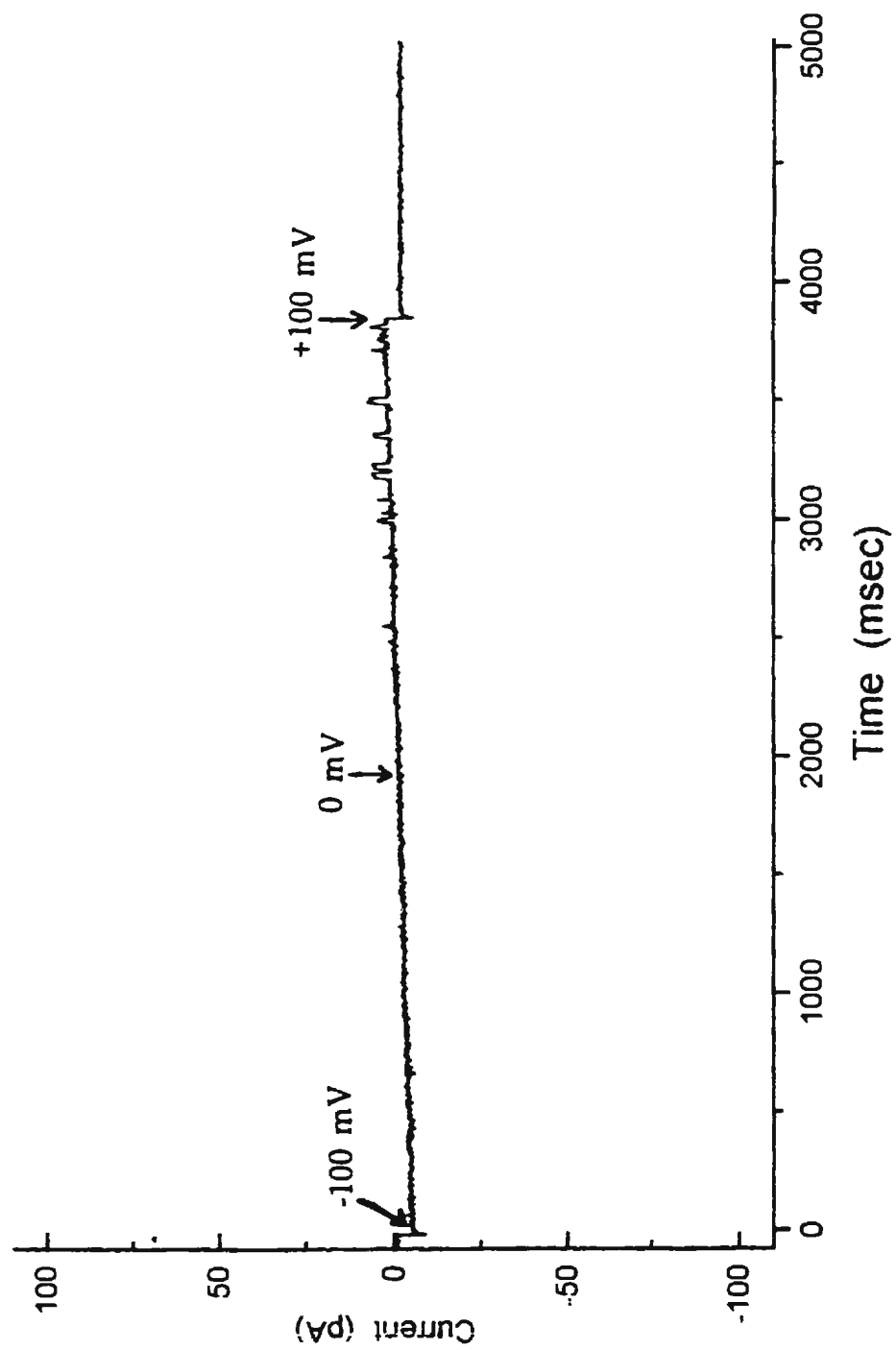


Fig. 4.3 : Single channel recording in cell attached configuration showing ramp voltage recording of the episode following Figs. 4.1 and 4.2. Channel activity at the positive voltages is evident.



Figs. 4.4: Single channel recordings in cell attached configuration. Hyperpolarization-activated currents begin during episode 2 and carry over through to the middle of episode 8. Activity in episode 1 and beyond episode 8 is not easily discernible from background noise.

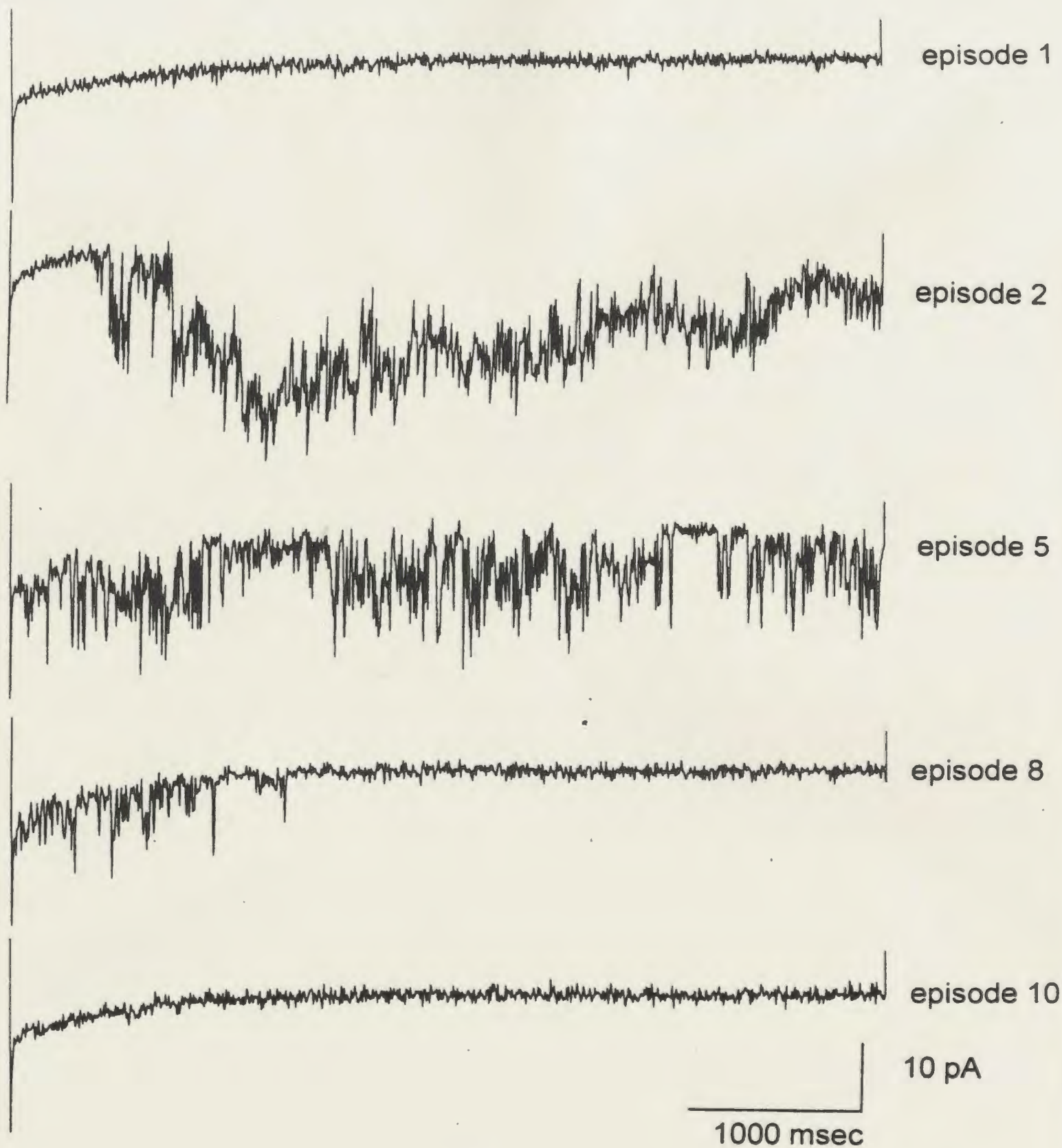


Fig. 4.5: Single channel recordings in cell attached configuration with membrane hyperpolarization resulting in sporadic activity. This series of episodes shows limited activity in the first and fourth episode with no discernible activity by episode 7. The unlevel baseline in episode 10 makes the identification of channel openings difficult.

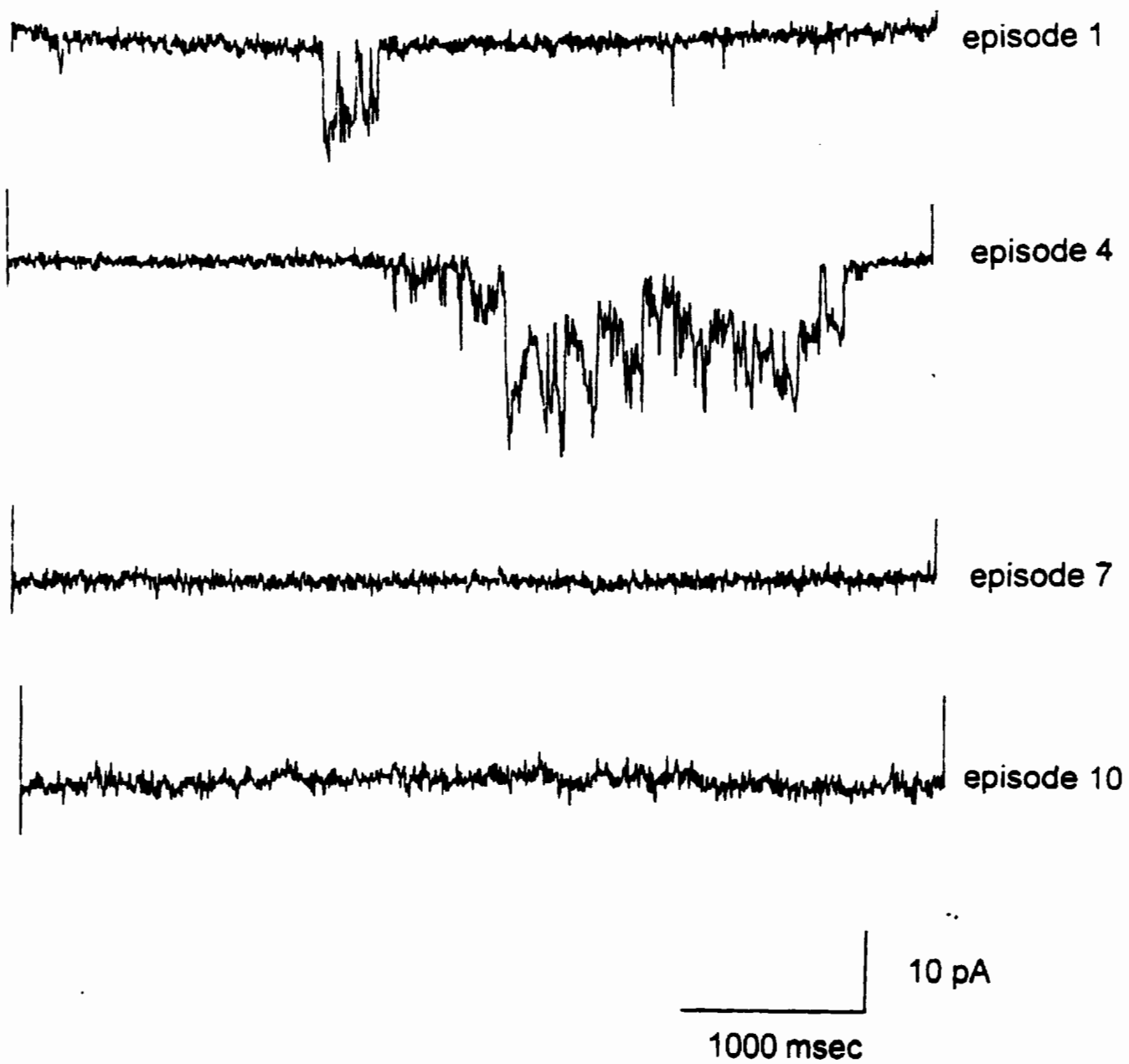
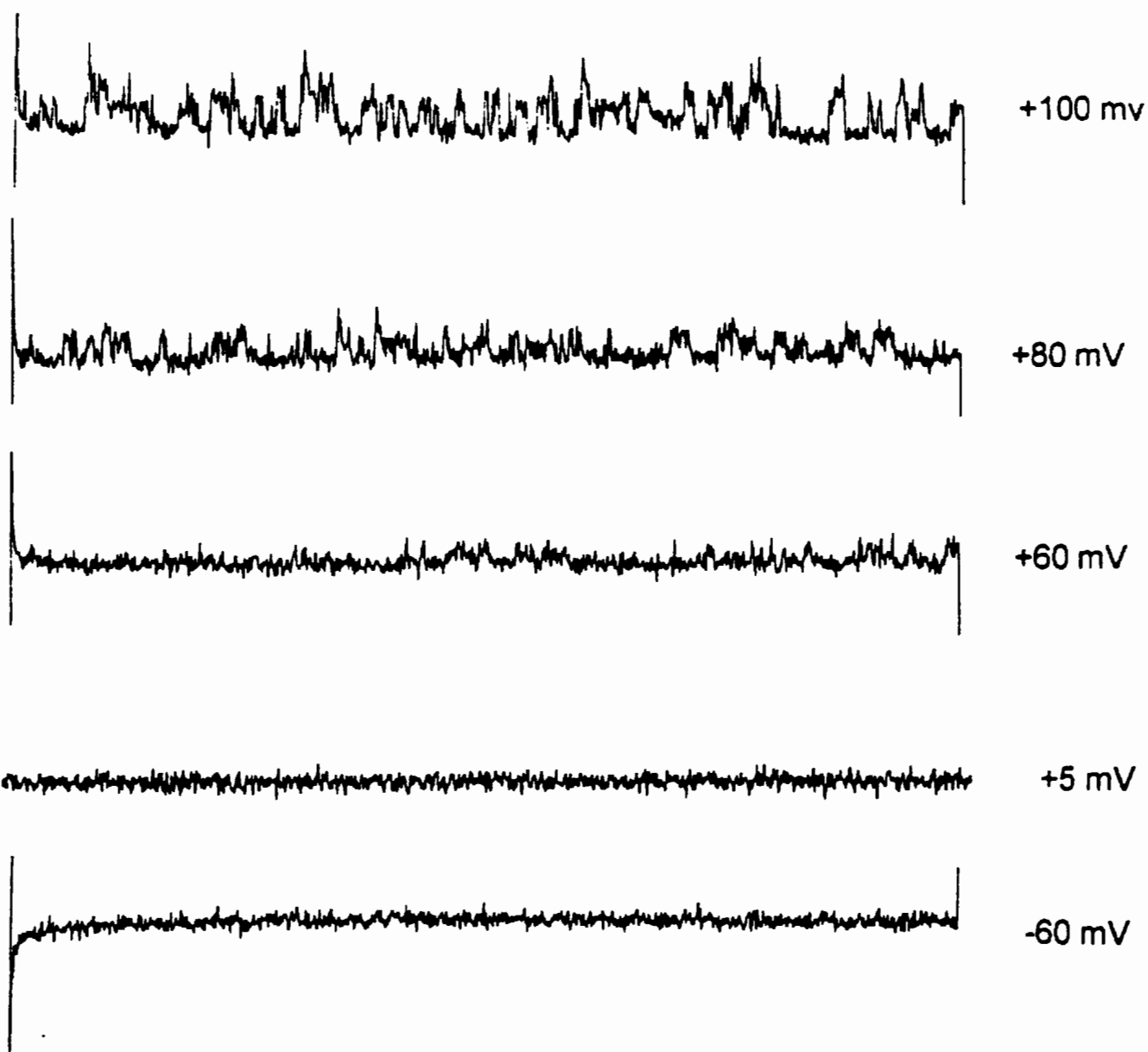


Fig. 4.6: Single channel recordings in cell attached configuration showing evidence of depolarized voltage-activated channels in *E. auilcae* protoplasts. Outward current is discernible in voltages ranging from +60 to +100 mV.



10 pA
1000 msec

Fig. 4.7a: Single channel recording in cell attached configuration during membrane depolarization. Multiple current channel activity is evident in voltage-activated channel openings. This trace, resulting from membrane depolarization at +100 mV, shows amplitude values of some of the channel openings.

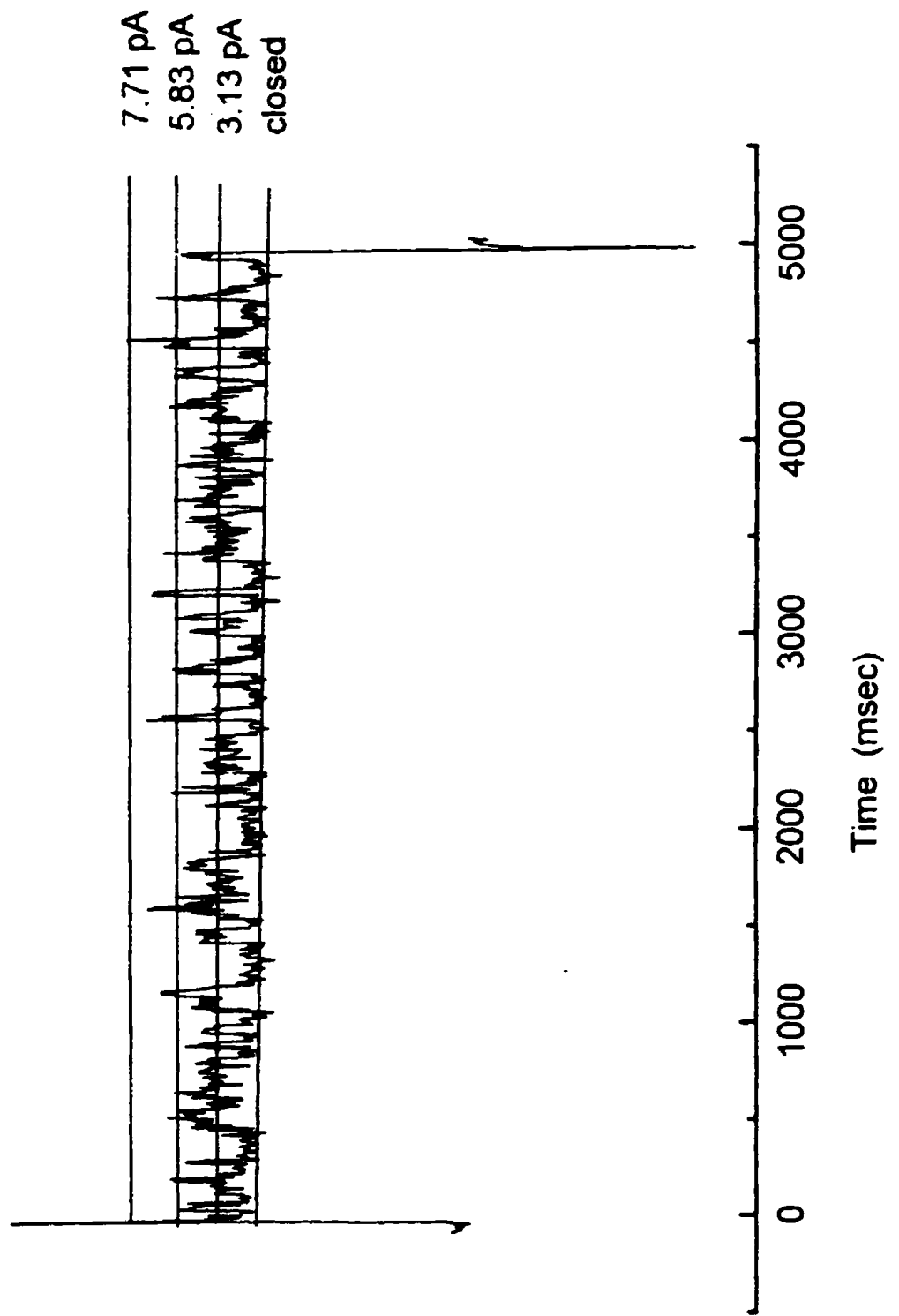


Fig. 4.7b: Current amplitude histogram of all 10 episodes from which Fig. 4.7a is one.

Histogram was generated using pClamp pStat program from Fetchan Demohist idealized events list of single channel recordings from a membrane depolarization at +100 mV.

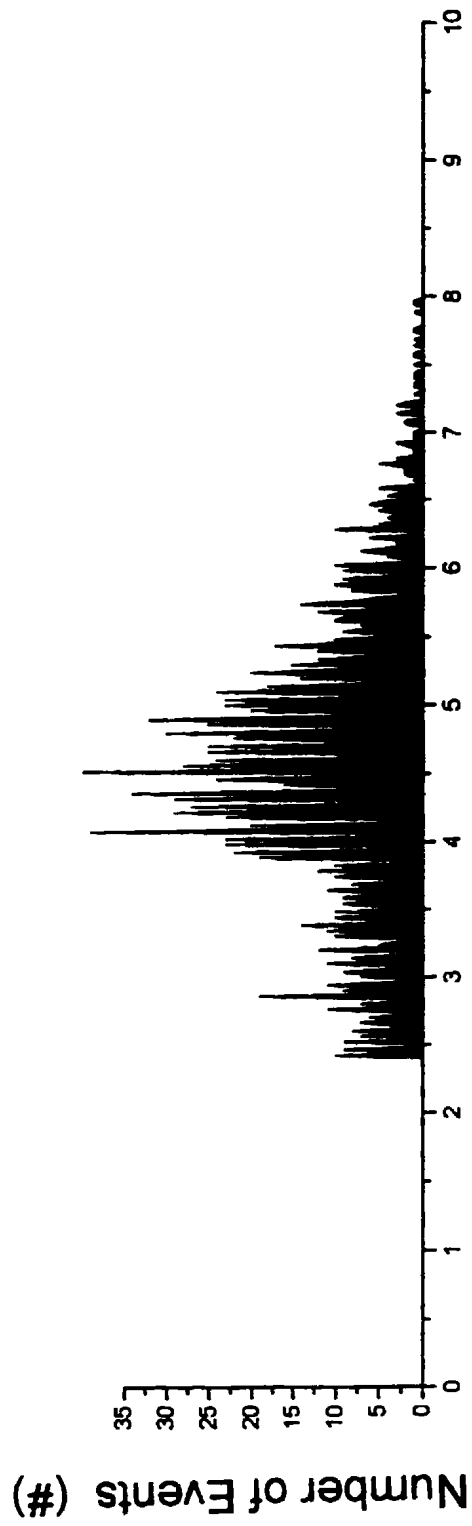


Fig. 4.8: Current amplitude histogram generated by pClamp pStat program from Fetchan Demohist idealized events list of single channel recordings from a membrane depolarized cell. The solid line represents a pStat generated Gaussian equation fit to the data. (A residuals plot for the line of fit and data is given in Fig. 4.9.)

1048 Events
103 Bins
5 N/div

$\mu_1=108.24$
 $\mu_1=4.08$
 $\sigma_1=1.28$

Level 1 ampl
Histogram

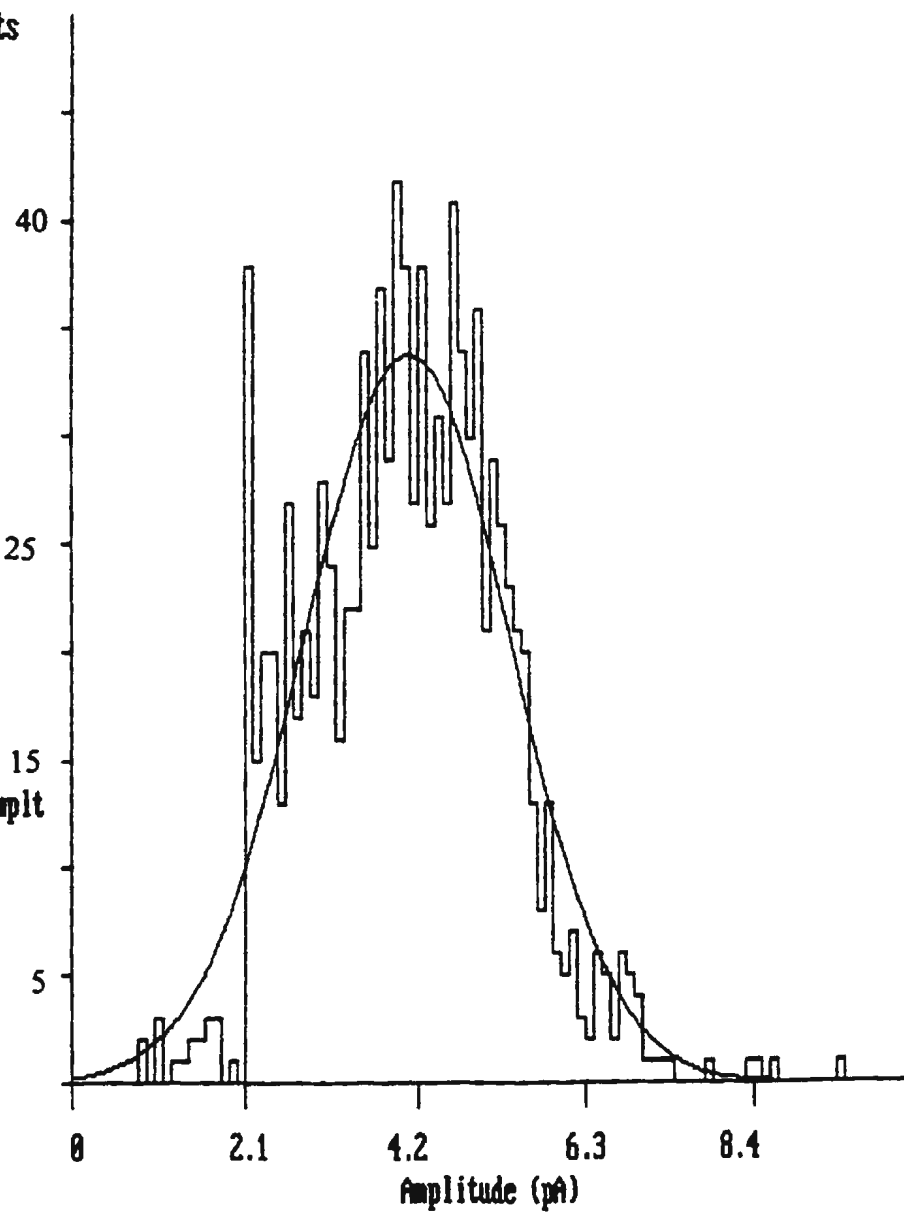


Fig. 4.9: The residuals plot of the theoretical Gaussian fit and the actual data shown in Fig. 4.8. The absence of a regular banding pattern about the x axis suggests a poor fit.

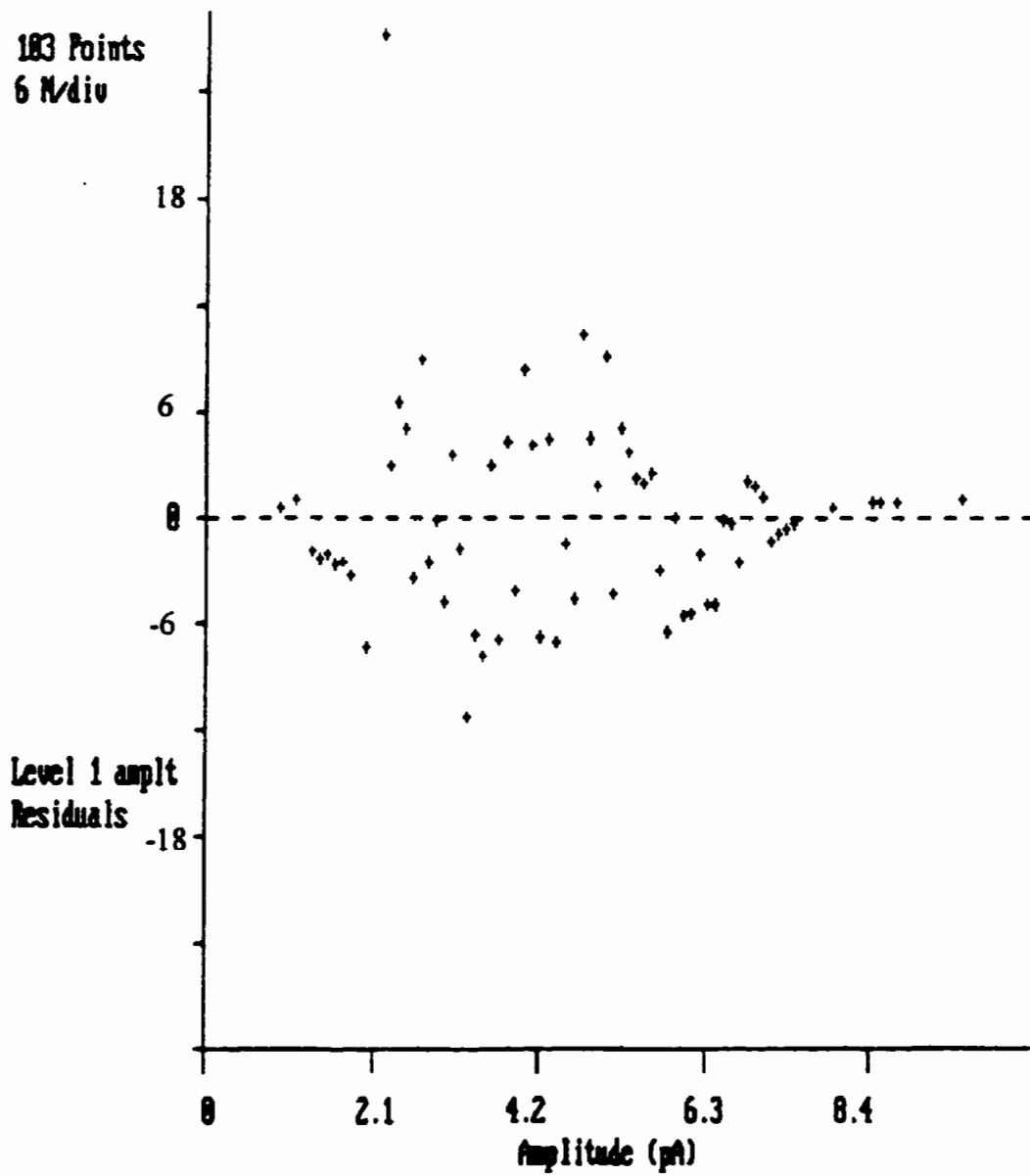


Fig. 4.10: Current amplitude histogram generated by pClamp pStat program from Fetchan Demohist idealized events list of single channel recordings from a membrane depolarized cell. Data used to generate this histogram were used to calculate the arithmetic mean using the pStat software program (See Table 4.4.)

1736 Events
400 Bins
5 N/div

Level 1 amplt
Histogram

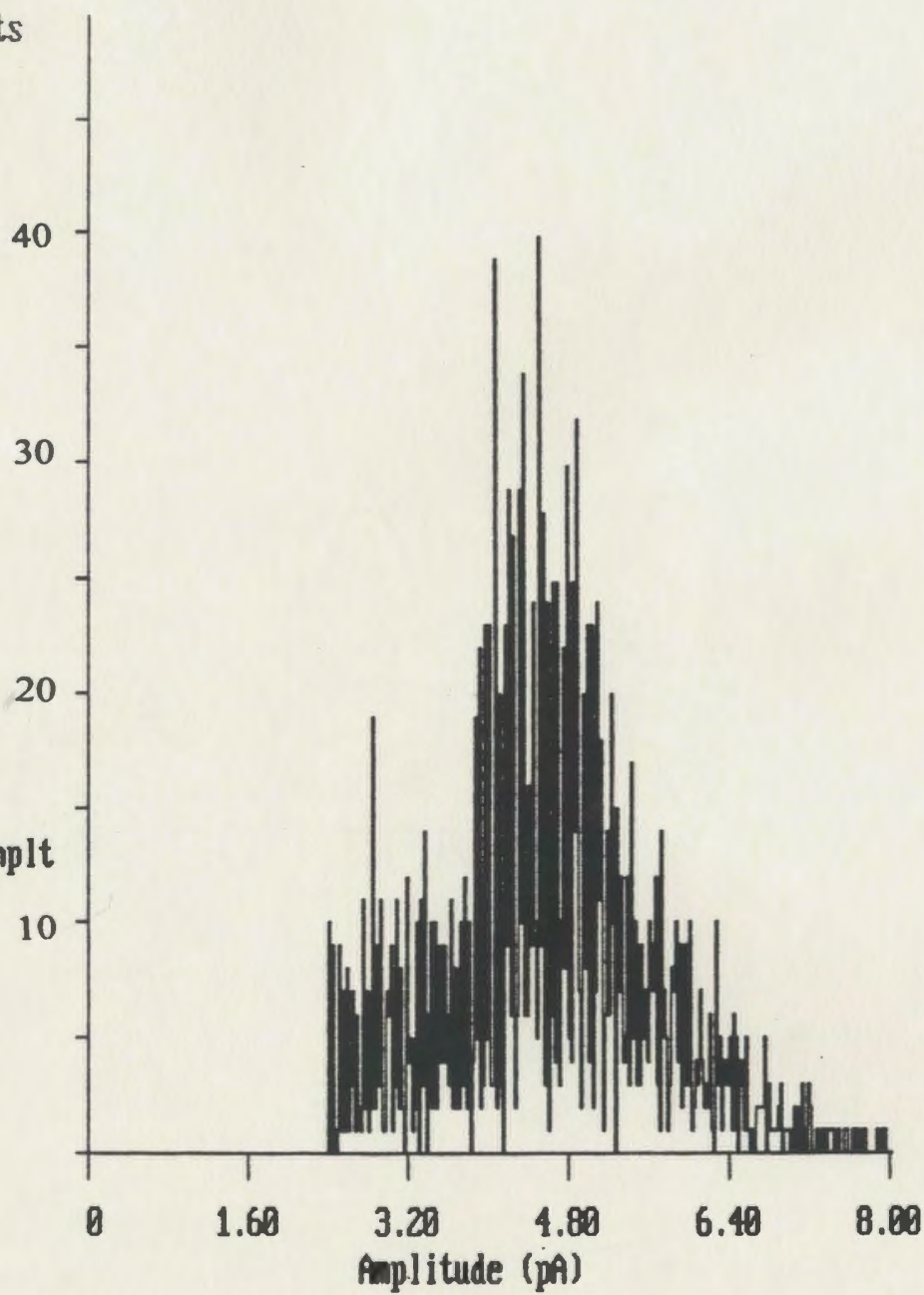


Fig. 4.11: Single channel recording in cell attached configuration during membrane depolarization. Representative recordings at +60, +80 and +100 mV.

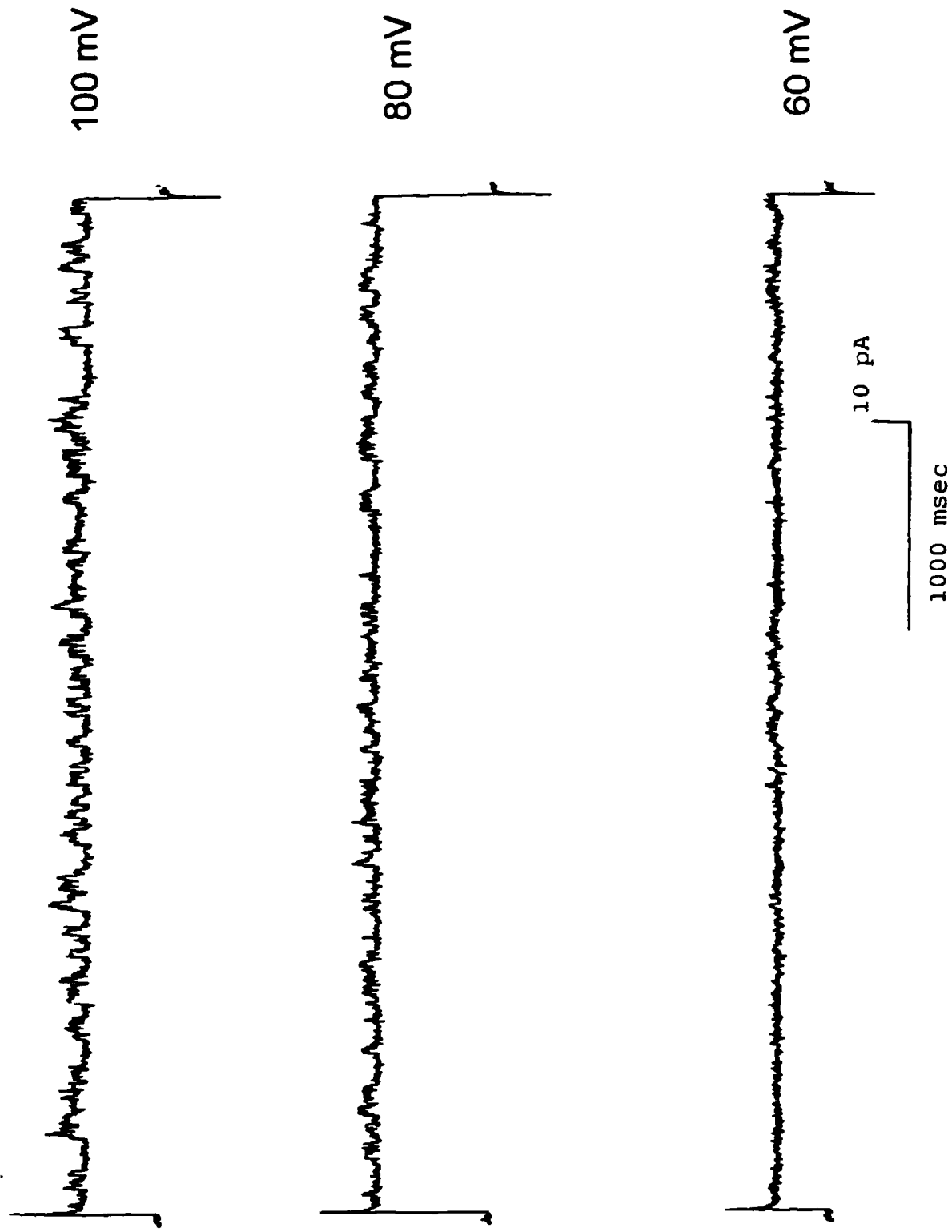


Fig. 4.12: Amplitude histograms of the recordings represented in Fig. 4.11 and their mean amplitude values. The current amplitude values were determined using pClamp's Fetchan Demohist program and validation of channel openings by visual inspection. The bin size is 0.1 pA. The weighted mean formula (Eqn. 4.1) was used in calculating the mean values.

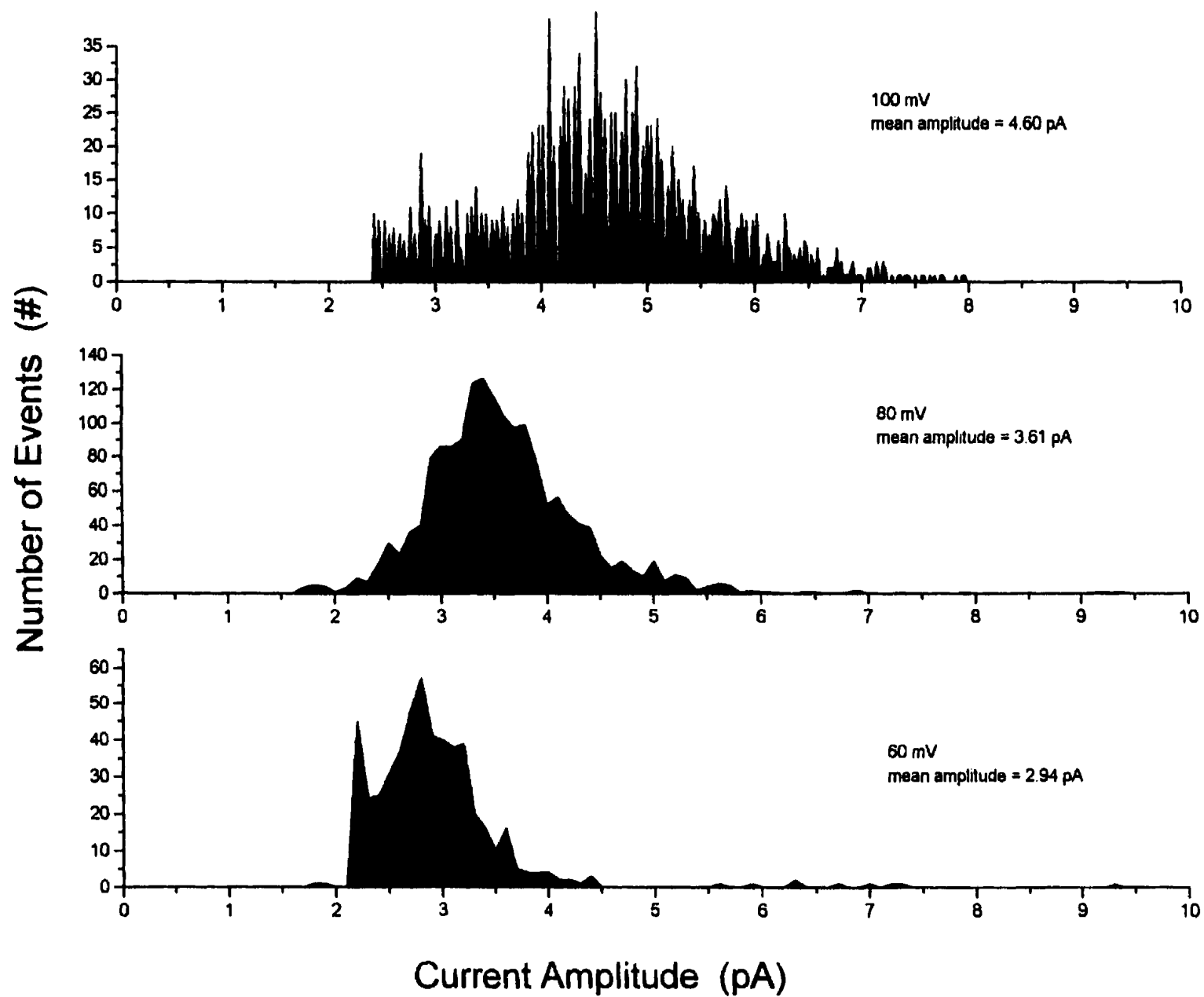


Fig. 4.13: Current-voltage relationship of *E. auilcae* protoplasts with a conductance of 31 pS. Each point is the mean of 3 to 6 recordings. The error bars indicate the standard deviation. Linear regression was used to determine the straight line fit.

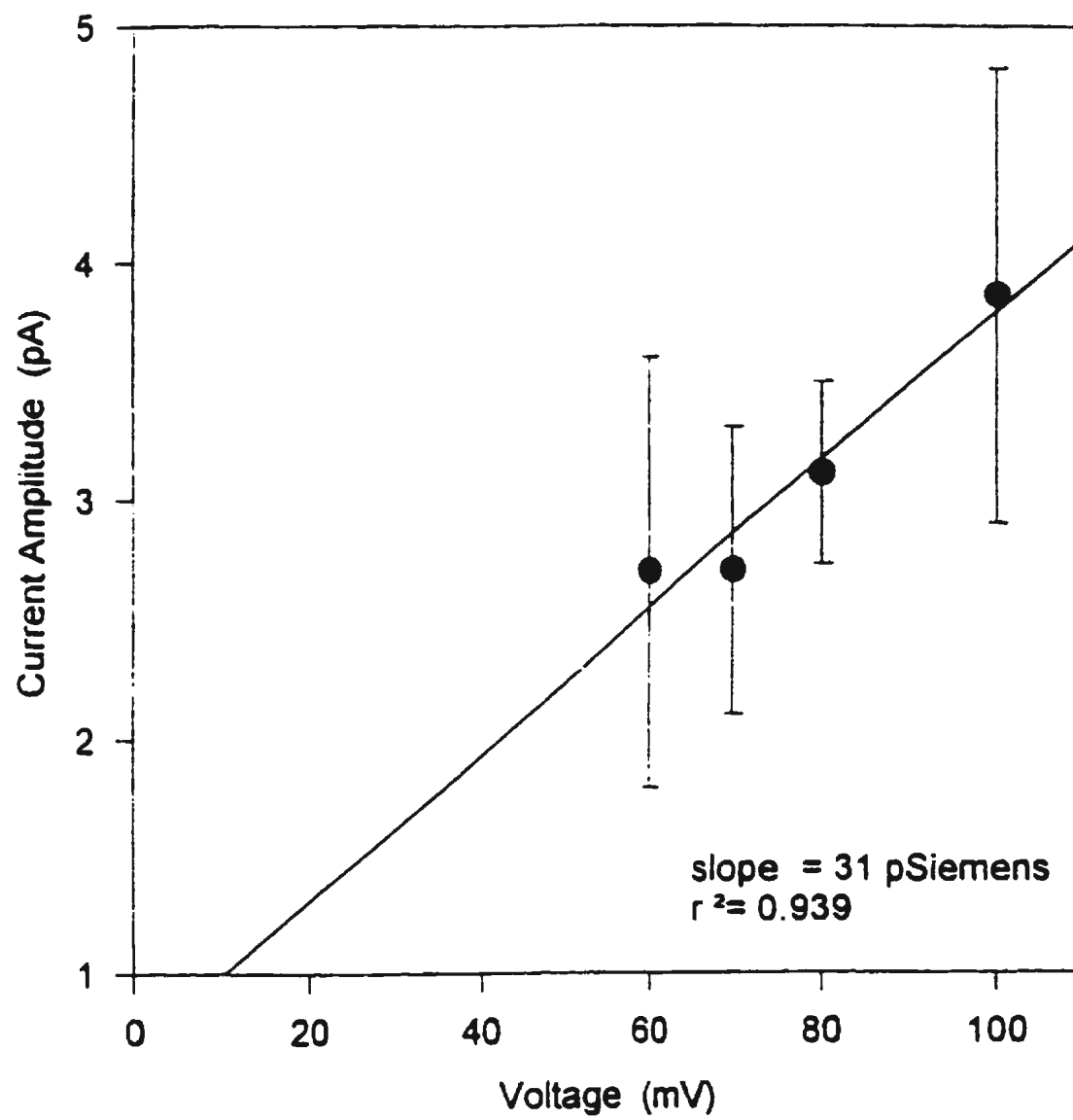


Fig. 4.14: Single channel recordings in cell attached configuration during membrane depolarization at +80 mV with no blockers present. The 5 traces are from different cells. They are from the 5th episode of a 10 episode run and are representative of the activity present.

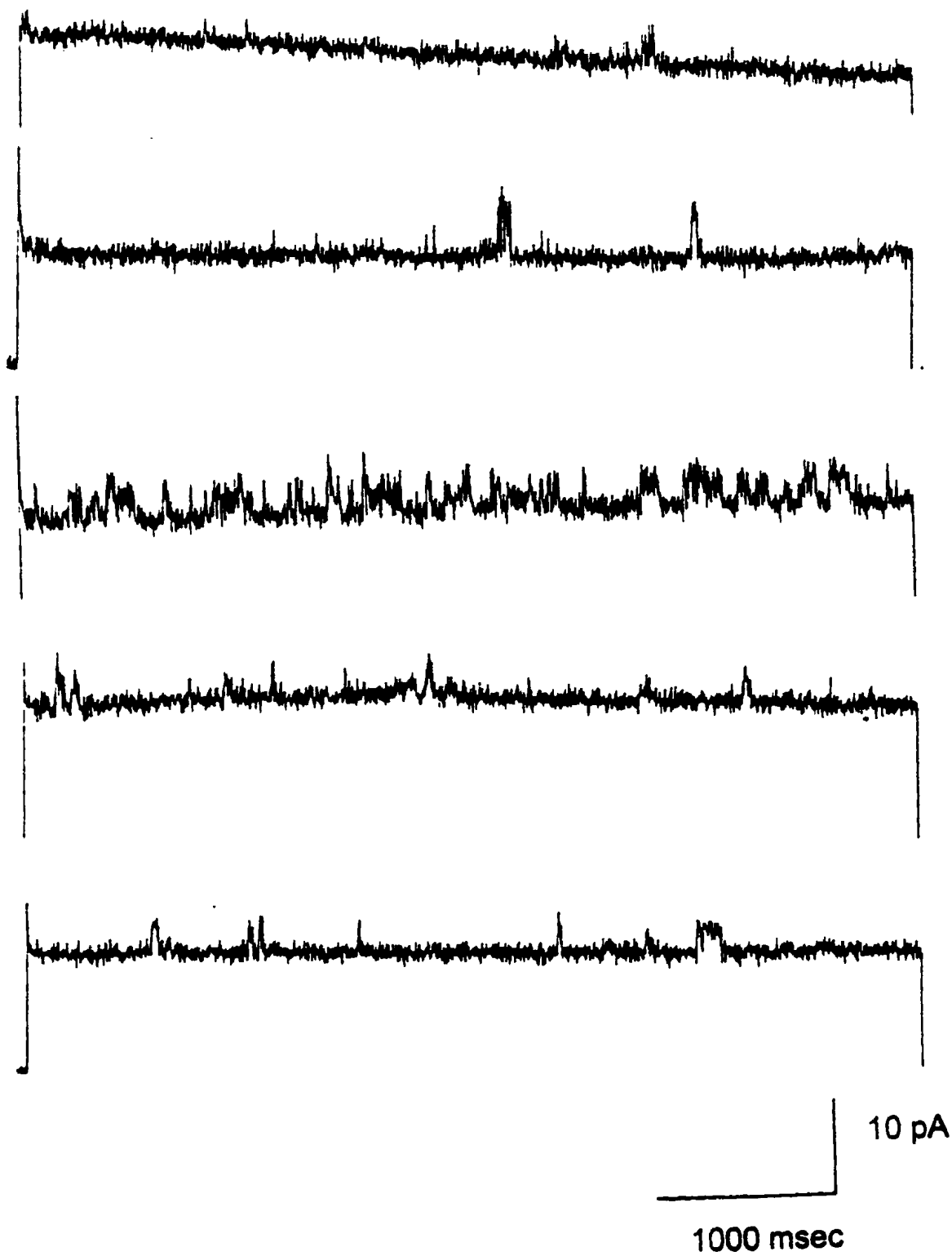


Fig. 4.15: Single channel recording in cell attached configuration during membrane depolarization. Representative channel activity in +80 mV with 5 mM Ba²⁺ present in the pipette solution. Each trace is from a different cell.

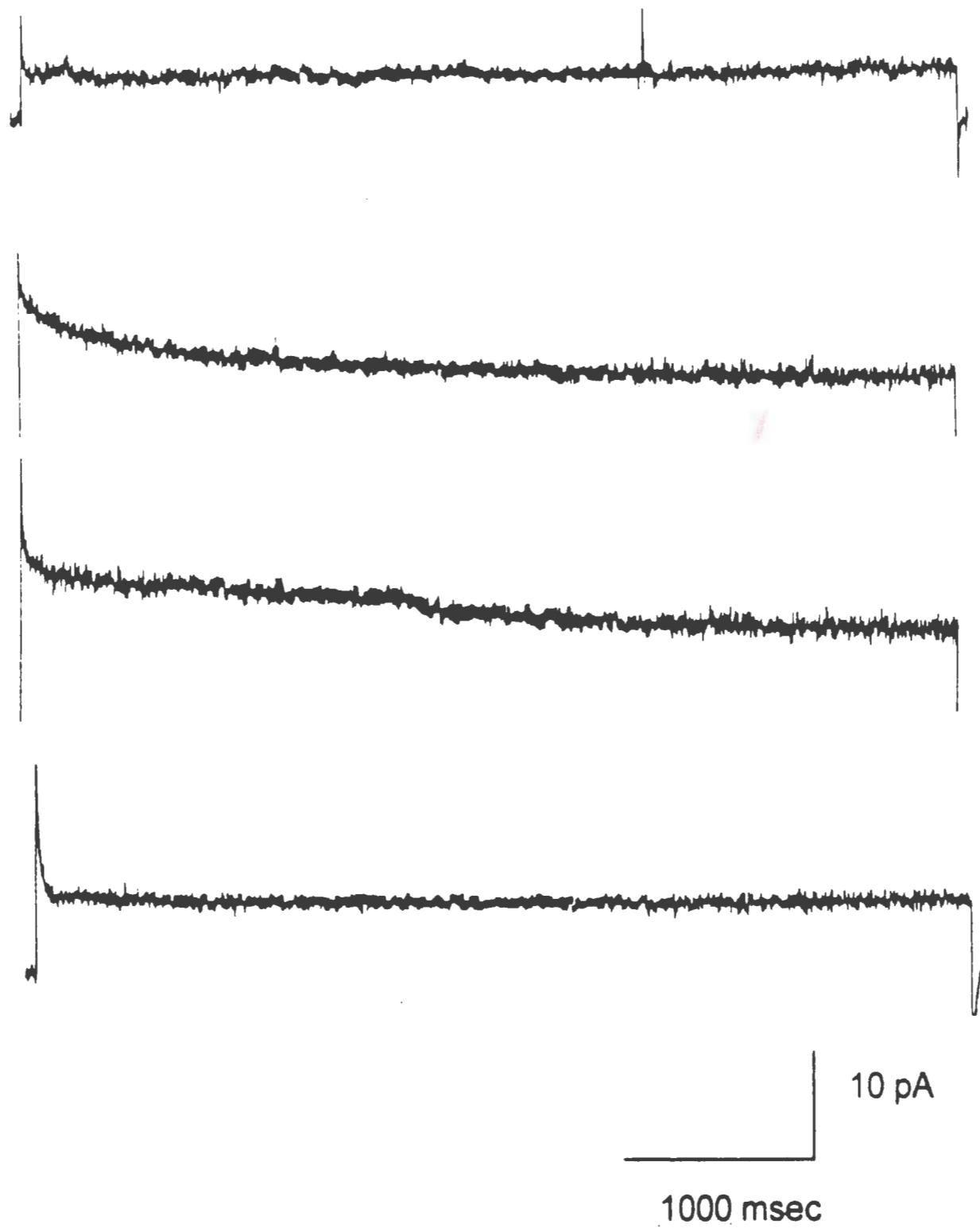


Fig. 4.16: Single channel recordings in cell attached configuration during membrane depolarization. Representative channel activity in +80 mV with 10 mM TEA⁺ present in the pipette solution. The two recordings are from different cells.

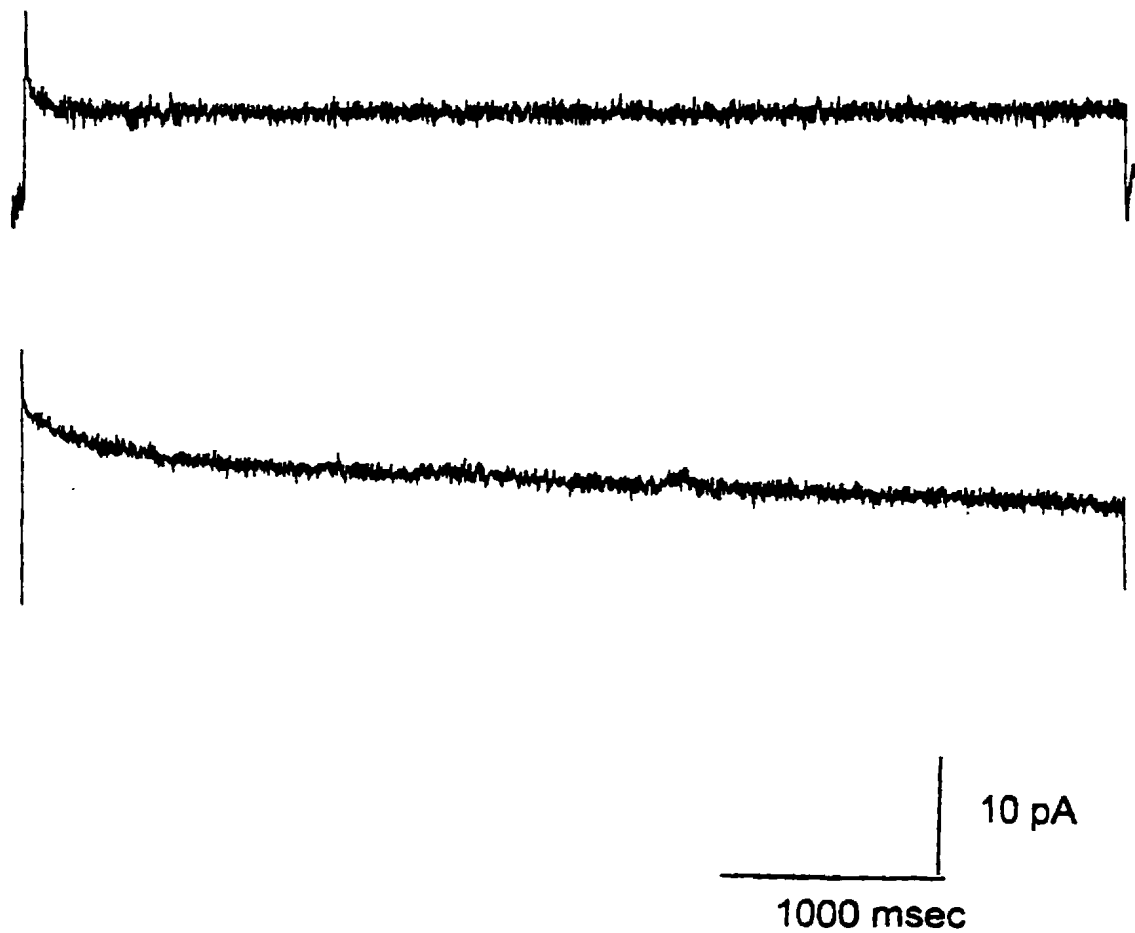
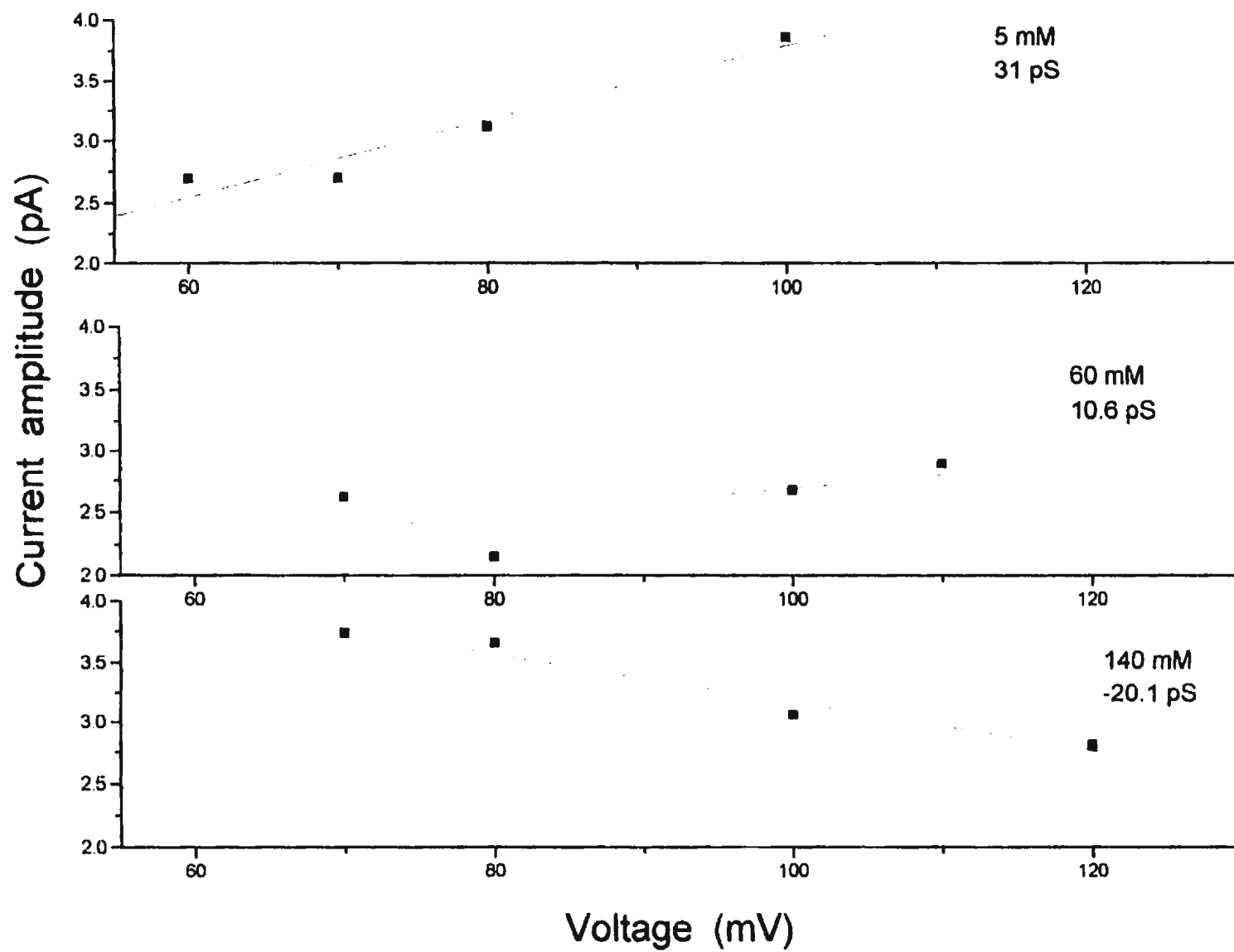


Fig.4.17: The effect of K^+ concentration on the current-amplitude relationship. The conductance is 31 pS with 5 mM K^+ , 10.6 pS with 60 mM K^+ and -20.1 pS with 140 mM K^+ . Each value in the 60 and 140 mM graphs represent data from one recording. The 5 mM data points are the mean of 3 to 6 recordings. The K^+ levels stated were present in both bath and pipette solution.



Chapter 5

Conclusions and Future Research

5.1 Summary and Discussion of Findings

The effects on *Entomophaga* species of changes in the physical parameters tested, pH and osmolality, showed broad range tolerance. *E. maimaiga* showed no significant difference in growth in 350 mOsm medium ranging in pH from 5.8 to 7.1. At a pH level of 5.5 growth was adversely affected. No difference in growth was found in pH 6.2 media ranging in osmolality from 250 to 400 mOsm. Further investigation of osmotic tolerance showed that *E. maimaiga* and *E. aulicae* protoplasts are capable of surviving one hour treatments in solutions ranging in osmolality from 0 to 550 mOsm.

This study into the effects of pH and osmolality was undertaken to identify media parameters suitable for *E. maimaiga* protoplast growth. The results suggest that a medium with an osmolality of 350 mOsm and a pH range from 5.8 to 7.1 is acceptable for growth. Also, a medium of pH 6.2 and an osmolality range of 250 to 400 mOsm is acceptable. The medium developed for mass fermentation of *E. aulicae* (Nolan, 1993) has a pH of 6.2 and an osmolality of 349 mOsm. Based on these two physical parameters, the Nolan medium should sustain *E. maimaiga* protoplast growth. Early studies with the Nolan formulation support this (Murrin and Houston, unpublished results); *E. maimaiga* protoplasts did grow and produce stable hyphal bodies. However, the lag phase of *E. maimaiga* growth was several days. Further adjustments in the medium formulation may be required to reduce the lag period. A reduction in production time would be beneficial for industrial mass production of hyphal bodies. Knowledge of the pH and osmotic

tolerance of the protoplasts, documented in this thesis, may be of assistance when modifying the fermenter formula.

The ability of both *E. aulicae* and *E. maimaiga* protoplasts to survive solutions ranging from distilled water to an osmolality of 550 mOsm suggests that these cells are very capable of regulating water uptake. The mechanism by which this occurs in these wall-free protoplasts is unclear and warrants further investigation. Since osmoregulation involves ion transport, one way to investigate the mechanics of protoplast osmotolerance is by using the patch clamp technique.

The approach taken to identify parameters for *E. aulicae* protoplast patch clamping was to incorporate near-physiological conditions and attain gigaseal membrane/pipette resistance. The developed protocol involves the following conditions: a) 'cell-attached' recording configuration; b) a pipette that has been heat polished, silicone-coated and has a final size that imparts 20 Mega Ω of resistance; c) a pipette solution consisting of 140 mM NaCl, 5 mM KCl, 2 mM CaCl₂, 2.4 mM MgCl₂•6H₂O, 10 mM MES, 3.8 mM glucose, 2.2 mM fructose, 29.8 mM sucrose and a final pH of 6.2; d) a bath solution consisting of 140 mM NaCl, 5 mM KCl, 1 mM CaCl₂, 1.2 mM MgCl₂•6H₂O, 10 mM MES, 3.8 mM glucose, 2.2 mM fructose, 36 mM sucrose and a final pH of 6.2; e) patch clamp recordings taken 30 to 90 minutes after the cells are introduced to the bath solution. Channel activity recorded under these conditions had low levels of noise, was reproducible and showed no evidence of channel run-down.

The suggested method for data analysis of the *E. aulicae* protoplast multiple current amplitude channel recordings is composed of three parts. It uses a combination of commercially available computer programs, visual validation by the investigator and

implementation of a mathematical computation. Channel openings are detected with the pCLAMP Fetchan program. If the resultant current amplitudes do not reflect values discernible by visual inspection, the Fetchan parameters are adjusted and the program re-initiated. Mean amplitude values are determined by calculating their weighted mean using an established formula (Sokal and Rohlf, 1995).

The identification of voltage-gated K^+ channels in *E. auilcae* protoplasts was based on the use of two K^+ channel blockers, TEA⁺ and Ba²⁺. Their presence caused major reductions in channel activity. Further evidence of the K^+ classification of these channels is based on the effect of elevated K^+ levels on membrane conductance. With 5 mM K^+ the conductance was 31 pS. This value changed to 10.6 and -20.1 pS with K^+ levels of 60 and 140 mM respectively.

The role of these voltage-activated channels in *E. auilcae* protoplasts is unclear. They may be involved in the maintenance of membrane potential (Gustin et al., 1986). They could also be involved in osmotic regulation by the fungus. Swelling-activated K^+ channels have been closely associated with calcium-activated channels (Sarkadi and Parker, 1991). The latter have been found in the oomycete *Saprolegnia* (Garrill et al., 1992a and 1992b). Stretch-activated K^+ channels have been identified with cell volume regulation (Sarkadi and Parker, 1991). Membrane depolarization and K^+ efflux occurs during regulatory volume decrease in kidney cells (Roy and Banderali, 1994). The K^+ channels found in *E. auilcae* may also be involved in charge balance. Cells exposed to high levels of NaCl lower their K^+ content while Na⁺ uptake occurs (Sunder et al., 1996).

Since *Entomophaga* protoplasts are capable of surviving osmolalities ranging from 0 to 550 mOsm a mechanism for ion transport must exist. Further investigation is

required to determine the role of the identified channels.

5.2 Future Research

The conductance values of the 60 mM and 140 mM K⁺ solutions are based on a small sample size. In order to confirm the effects of elevated K⁺ levels, future work should involve the repetition of these experiments and a re-calculation of the conductance values.

The cytoskeleton has been shown to play a direct role in ion channel activity. The use of cytochalasin D (CD), an inhibitor of actin polymerization, affects open channel characteristics of a sodium ion channel in mammalian heart cells (Undrovinas et al., 1995). 'Inside-out' patch clamp recordings have been shown to affect ion channel behaviour as well. Mechanical disruption of the cytoskeleton during patch excision and/or lack of cytoskeletal cytoplasmic requirements may account for this (Undrovinas et al., 1995). Some ion channels are not affected by patch excision suggesting that they are unaffected by cytoskeletal-channel interactions (Duszyk et al., 1995).

In order to further characterize the K⁺ channels of *E. aulicae*, the role of the cytoskeleton should be investigated. Patch excision experiments are expected to be difficult to attain with the protoplasts due to their inability to firmly adhere to the bottom of a recording dish. However, cell attached recording, identified as the appropriate recording configuration for *E. aulicae* protoplasts (see Chapter 3), can be used for investigating the effect of actin on channel activity. Delivery of CD to the cytoplasm is attainable by dissolving it in dimethyl sulfoxide (DMSO) and adding it to the pipette and bath recording solutions. The information gained would help in determining the role the

cytoskeleton plays in the behaviour of the ion channels found in *E. auilcae*.

With the protocols developed for *E. auilcae* protoplast patch clamping and data analysis, the question of osmoregulation can be addressed. K^+ transport has been shown to be affected when changes in cell volume occur (Delpire and Gullans, 1994; Sarkadi and Parker, 1991). Researchers interested in fungal tip growth have investigated stretch-activated channels (Lew et al., 1992; Levina et al., 1994 and 1995). This requires monitoring the degree of negative pressure delivered in the pipette to cause stretching of the membrane. Although this approach is useful, it is restricted to investigating only increases in cell volume. It would not be useful in cell shrinkage studies. *E. auilcae* protoplasts are capable of surviving solutions having an osmolality level of at least 550 mOsm. Based on other cell systems (Hoffmann, 1992), the potential exists that protoplast cell shrinkage will occur at some level of osmolality. Therefore, experimentation accommodating cell volume decrease is of interest. It is proposed that the effect of osmolality on ion channel activity be investigated by adjusting the osmolality of the pipette solutions. It is suggested that the formulation of the bath solution, having an osmolality of 349 mOsm, remain the same as identified in section 5.1. This would allow the investigator to record the effect of different osmolalities on channel activity immediately after a patch of membrane is exposed to the pipette-delivered test osmolality solution.

Information on the effect of osmolality on cell volume would be useful in investigating the mechanism of protoplast osmoregulation. The volume of spherical cells can easily be determined using a microscope with digital video imaging equipment and software (Delpire and Gullans, 1994). The radius of the cell can be determined and the

volume calculated using the equation $V = 4/3 \pi r^3$ where V is volume and r is radius. However since, under normal physiological conditions, *E. aulicae* protoplasts are spindle-shaped cells with tapered extensions accurate volume measurements using the above-mentioned technique is not possible (Lamb and Murrin, unpublished results). Volumes of irregular-shaped cells can be determined by flow cytometry. The resistance cells impart when passing through an orifice is proportional to their volume. The compatibility of *E. aulicae* protoplasts to volume measurements using this type of equipment needs to be investigated. If cell volumes can be determined, then the effects of osmolality on protoplast cell volume should be determined by measuring their volume in solutions of different osmolalities. Cells subjected to low osmolalities swell and then decrease their volume (Hoffmann, 1992). It would be of interest to monitor protoplast volume changes over time to document their behaviour at different osmolalities.

The osmotic tolerance tests of *E. maimaiga* and *E. aulicae* used cell morphology to assess the effects of osmolality (Chapter 2). At low osmolalities all of the cells were round. This indicates microtubule depolymerization. Documentation of the cytoskeletal changes in protoplasts due to changes in osmolalities would supply further information on protoplast osmoregulation. This could be attained by employing fluorescent microscopy techniques using actin and microtubule-specific fluorescent probes.

The effects of osmolality on ion channel behaviour, cell volume and the cytoskeleton would aid in determining the mechanisms used in *E. aulicae* protoplast osmoregulation. The approaches outlined above are suggested for future research in these areas.

References

- Adams, D.J. and W. Nonner. 1990. Voltage-dependent potassium channel: gating, ion permeation and block. In "Potassium Channels : Structure, Classification, Function and Therapeutic Potential" N.S. Cook, ed. John Wiley and Sons, New York.
- Armstrong, C.M., R.P. Swenson Jr. and S.R. Taylor. 1982. Block of squid axon K⁺ channels by internally and externally applied barium ions. *J. Gen. Physiol.* **80**:663-682.
- Arnold, W.N. 1981. Physical aspects of yeast cell envelope. In "Yeast Cell Envelopes: Biochemistry, and Ultrastructure" Volume 1. W.N. Arnold, ed. CRC Press, Florida.
- Assmann, S.M. "Patch Clamping Plant Cells: Tips and Tricks" Focus on Methods #016. <http://www.axonet.com/pub/tech/focus> (02 Apr 1996)
- Axonet "Does the command potential control the pipette tip potential, the transmembrane potential, or both?" Q&A #013. <http://www.axonet.com/pub/tech/focus> (27 Feb 1996).
- Barbara, J.-G., H. Stoeckel and K. Takeda. 1994. Hyperpolarization-activated inward chloride current in protoplasts from suspension-cultured carrot cells. *Protoplasma* **180**:136-144.
- Beauvais, A. 1989. Les polysaccharides de la paroi fongique: regulation de leur synthese et ses implications immunologiques. PhD thesis. University of Paris 6.
- Beauvais, A., J.P. Latgé, A.Vey and M.C. Prevost. 1989. The role of surface components of the entomopathogenic fungus *Entomophaga aulicae* in the cellular immune

- response of *Galleria mellonella* (Lepidoptera). *J. Gen. Microbiol.* **135**:489-498.
- Beauvais, A. and J.P. Latgé. 1991. Modulation of glucan and chitin synthesis. In "Fungal Cell Wall and Immune Response". J.P. Latgé and D. Boucias, eds. pp. 97-110. Springer-Verlag, Berlin.
- Begenisich, T. 1994. Permeation properties of cloned K⁺ channels. In "Handbook of Membrane Channels, Molecular and Cellular Physiology" C. Peracchia, ed. Academic Press, San Diego.
- Bertl, A. and C.L. Slayman. 1992. Complex modulation of cation channels in the tonoplast and plasma membrane of *Saccharomyces cerevisiae* : single-channel studies. *J. Exp. Biol.* **172**:271-287.
- Bertl, A., C.L. Slayman and D. Gradmann. 1993. Gating and conductance in an outward-rectifying K⁺ channel from the plasma membrane of *Saccharomyces cerevisiae*. *J. Memb. Biol.* **132**:183-199.
- Bertl, A., J.A. Anderson, C.L. Slayman and R.F. Gaber. 1995. Use of *Saccharomyces cerevisiae* for patch-clamp analysis of heterologous membrane proteins: characterization of Kat 1, an inward-rectifying channel from *Arabidopsis thaliana*, and comparison with endogenous yeast channels and carriers. *Proc. Natl. Acad. Sci.* **92**:2710-2705.
- Boulton, A.A. 1965. Some observations on the chemistry and morphology of the membranes released from yeast protoplasts by osmotic shock. *Exp. Cell Res.* **37**:343-359.
- Brink, P.R. and S. Fan. 1989. Patch clamp recordings from membranes which contain gap junction channels. *Biophys. J.* **56**:579-593.

- Buechner, M. A.H. Delcour, B. Martinac, J.Adler and C. Kung. 1990. Ion channel activities in the *Escherichia coli* outer membrane. *Biochim. Biophys.* **1024**:111-121.
- Butt, T.M., A.E. Hajek and R.A. Humber. 1994. The effect of temperature on growth and survival of protoplasts of the gypsy moth pathogen *Entomophaga maimaiga*. *J. Invertebr. Pathol.* **64**, 74-75.
- Byrne, J.H. and S.G. Schultz. 1994. "An Introduction to Membrane Transport and Bioelectricity : Foundations of General Physiology and Electrochemical Signaling". Raven Press, New York.
- Caldwell, J.H., J. Van Brunt and F.M. Harold. 1986. Calcium-dependent anion channel in the water mold, *Blastocladiella emersonii*. *J. Membr. Biol.* **89**:85-97.
- Cavalie, A., R. Grantyn and H.D. Lux. 1992. Fabrication of patch clamp pipettes. In "Practical Electrophysiological Methods. A guide for *in vitro* studies in vertebrate neurobiology" H. Kettermann and R. Grantyn, eds. Wiley Liss, New York.
- Chen, T.Y. and C. Miller. 1996. Nonequilibrium gating and voltage dependence of the ClC-0 Cl channel. *J. Gen. Phys.* **108**: 237-250.
- Colquhoun, D. and F.J. Sigworth. 1995. Fitting and statistical analysis of single-channel records. In "Single-Channel Recording" Second edition. B. Sakman and E. Neher,eds. Plenum Press, New York.
- Delpire, E. and S.R. Gullans. 1994. Cell volume and K⁺ transport during differentiation of mouse erythroleukemia cells. *Am. J. Physiol* **266**:C515-C523.
- Dempster, J. 1993. "Computer Analysis of Electrophysiological Signals" Biological techniques Series. Academic Press, London.

- Dieter, P., E. Fitzke and J. Duyster. 1993. Bapta induces a decrease of intracellular free calcium and a translocation and inactivation of protein-kinase-c in macrophages. *Biol. Chem.* **374**:171-174.
- Dunphy, G.B. and R.A. Nolan. 1979. Effects of physical factors on protoplasts of *Entomophthora egressa*. *Mycologia* **71**:589-603.
- Dunphy, G.B., and Nolan, R.A. 1982. Simplified growth media for *Entomophthora egressa* protoplasts. *Can. J. Microbiol.* **28**, 815-821.
- Dunphy, G.B. and J.M. Chadwick 1985. Influence of physical factors and selected media on the growth of *Entomophthora egressa* protoplasts isolated from spruce budworm larvae. *Mycologia* **77**: 887-893.
- Duszyk, M., D. Liu, B. Kamosinska, A.S. French and S.F.P. Man. 1995. Characterization and regulation of a chloride channel from bovine tracheal epithelium. *J. Physiol.* **489**: 81-93.
- Elinder, F., M. Madeja and P. Arhem. 1996. Surface-charges of K⁺ channels-effects of strontium on 5 cloned channels expressed in *Xenopus* oocytes. *J. Gen. Physiol.* **108**: 325-332.
- Elzenga, J.T.M., C.P. Keller, E. Van Volkenburg. 1991. Patch clamping protoplasts from vascular plants; method for the quick isolation of protoplasts having a high success rate of gigaseal formation. *Plant Physiol.* **97**: 1573-1575.
- Fairley, K.A. and N.A. Walker. 1989. Patch clamping corn protoplasts; gigaseal frequency is not improved by Congo Red inhibitor of cell wall generation. *Protoplasma* **153**:111-116.

- Farkas, V. 1985. The fungal cell wall. In "Fungal Protoplasts Applications in Biochemistry and Genetics" J.F. Peberdy and L. Ferenczy, eds. Marcel Dekker, Inc. New York.
- Garrill, A. 1994. Transport. In "The Growing Fungus" N.A.R. Gow and G.M. Gadd eds., Chapman & Hall, London.
- Garrill, A., S.L. Jackson, R.R. Lew and I.B. Heath. 1992a. Ion channel activity and tip growth: tip localization stretch-activated channels generate an essential Ca^{2+} gradient in the oomycete *Saprolegnia ferax*. *Eur. J. Cell. Biol.* **60**:358-365.
- Garrill, A., R.R. Lew and I.B. Heath. 1992b. Stretch-activated Ca^{2+} and Ca^{2+} -activated K^{+} channels in the hyphal tip plasma membrane of the oomycete *Saprolegnia ferax*. *J. Cell Sci.* **107**:127-134.
- Garrill, A. and J.M. Davies. 1994. Patch clamping fungal membranes: a new perspective on ion transport. *Mycol. Res.* **98**: 257-263.
- Gaymard, F., M. Cerutti, C. Horeau, G. Lemailliet, S. Urbach, M. Ravallec, G. Devauchelle, H. Sentenac and J.B. Thibaud. 1996. The baculovirus /insect cell system as an alternative to *Xenopus* oocytes-first characterization of the Akt1 K^{+} channel from *Arabidopsis thaliana*. *J. Biol. Chem.* **271**: 22863-22870.
- Gooday, G.W. and N.A.R. Gow. 1990. Enzymology of tip growth in fungi. In "Tip Growth in Plant and Fungal Cells". I.B. Heath, ed. Academic Press, Inc. USA.
- Griffin, D.H. 1994. "Fungal Physiology" Wiley-Liss, Inc. New York.
- Gustin, M.C., B. Martinac, Y. Saimi, M.R. Culbertson and C. Kung. 1986. Ion channels in yeast. *Science* **233**: 1195-1197.

- Hajek, A.E., Humber, R.A., Elkinton, J.S., May, B., Walsh, S.R.A., and Silver, J.C. 1990. Allozyme and restriction fragment length polymorphism analyses confirm *Entomophaga maimaiga* responsible for 1989 epizootics in North American gypsy moth populations. *Proc. Natl. Acad. Sci.* **87**, 6979-6982.
- Hajek, A.E. and R.S. Soper. 1992. Temporal dynamics of *Entomophaga maimaiga* after death of gypsy moth (Lepidoptera: Lymantriidae) larval hosts. *Environ. Entomol.* **21**:129-135.
- Hancock, S., F.L. Moddy-Corbett and N.S. Virgo. 1996. Potassium inward rectifier and acetylcholine receptor channels in embryonic *Xenopus* muscle cells in culture. *J. Neurobiol.* **29**:354-366.
- Hamill, O.P., A. Marty, E. Neher, B. Sakmann and F. J. Sigworth. 1981. Improved patch clamp techniques for high resolution current recording from cells and cell-free membrane patches. In "Single-Channel Recordings" Second edition. B. Sakmann and E. Neher eds. Plenum Press, New York.
- Heinemann, S.H. 1995. Guide to data acquisition. In "Single-Channel Recording" Second edition. B. Sakman and E. Neher, eds. Plenum Press, New York.
- Hille, B. 1984. "Ionic Channels of Excitable Membranes". Sinauer Assoc. Inc., Sunderland, Mass.
- Hille, B. 1992. "Ionic Channels of Excitable Membranes" Second edition. Sinauer Assoc. Inc., Sunderland, Mass.
- Hoffmann, E. K. 1992. Cell swelling and volume regulation. *Can. J. Physiol. Pharmacol.* **70**:310-313.
- Hoffmann, E.K. and L.O. Simonsen. 1989. Membrane mechanisms in volume and pH

- regulation in vertebrate cells. *Physiol. Rev.* **69**:315-382.
- Hurst, R.S., R. Latorre, L.Toro and E. Stefani. 1995. External barium block of shaker potassium channels: evidence of two binding sites. *J. Gen. Physiol.* **106**:1069-1085.
- Jackson, M.B. 1992. Cell-attached patch clamp. In "Practical Electrophysiological methods: A Guide for *in vitro* studies in Vertebrate Neurobiology" H. Kettenbaum and R. Grantyn, eds. Wiley-Liss, New York.
- Jackson, S.L. and I.B. Heath. 1993. Roles of calcium ions in hyphal tip growth. *Micro. Rev.* **57**: 367-382.
- Kropf, D.L. 1994. Cytoskeletal control of cell polarity in a plant zygote. *Develop. Biol.* **165**:361-371.
- Lacey, L.A., and Goettel, M.S. 1995. Current developments in microbial control of insect pests and prospects for the early 21st century. *Entomophaga* **40**, 3-27.
- Lake, N. 1994. Attachment and scanning electron microscopy of protoplasts of the insect-pathogenic fungus, *Entomophaga aulicae*. BSc (Honors) thesis. Dept. of Biology, Memorial University of Newfoundland.
- Latgé, J.-P. 1975. Croissance et sporulation de 6 espèces d'Entomophthorales. Influence de la nutrition carbonée. *Entomophaga* **20**:201-207.
- Levina, N.N., R.R. Lew and I.B. Heath. 1994. Cytoskeleton regulation of ionic channel distribution in the tip-growing organism *Saprolegnia ferax*. *J. Cell Sci.* **107**:127-134.
- Levina, N.N., R.R. Lew, G.J. Hyde and I.B. Heath. 1995. The roles of Ca²⁺ and plasma

- membrane ion channels in hyphal tip growth of *Neurospora crassa*. *J. Cell Sci.* **108**: 3405-3417.
- Lew, R.R., B.S. Serlin, C.L. Schauf and M.E. Stockton. 1990. Red light regulates calcium-activated channels in *Mougeotia* plasma membrane. *Plant Physiol.* **92**: 822-830.
- Lew, R.R., A. Garrill, L. Covic, I.B. Heath and B.S. Serlin. 1992. Novel ion channels in the protists, *Mougeotia* and *Saprolegnia*, using sub-gigaseals. *FEBS* **310**:219-222.
- Misler, S., L.C. Falke, K. Gillkiss and M.L. McDaniel. 1986. A metabolite- regulated potassium channel in rat pancreatic B cells. *Proc. Natl. Acad. Sci. USA* **83**:7119-7123.
- Moczydlowski, E., K. Lucchesi and A. Ravindran. 1988. An emerging pharmacology of peptide toxins targeted against potassium channels. *J. Membr. Biol.* **105**:95-111.
- Murrin, F., J. Holtby, R.A. Nolan and W.S. Davidson. 1986. The genome of *Entomophaga aulicae* : base composition and size. *Exp. Mycol.* **10**:67-75.
- Murrin, F. and R.A. Nolan. 1987. Ultrastructure of the infection of spruce budworm larvae by the fungus *Entomophaga aulicae*. *Can. J. Bot.* **65**:1694-1706.
- Murrin, F., W. Newcomb and I.B. Heath. 1988. The ultrastructure and timing of events in the nuclear cycle of the fungus *Entomophaga aulicae*. *J. Cell Sci.* **90**:501-516.
- Neher, E. 1992. Ion channels for communication between and within cells. *Science* **256**:498-502.
- Neher, E. and B. Sakmann. 1976. Single channel currents recorded from membrane of

- denervated frog muscle fibers. *Nature* **260**:799-802.
- Neher, E. and B. Sakmann. 1992. The patch clamp technique. *Sci. Amer.* **266** (March): 44-51.
- Nolan, R.A. 1985. Protoplasts of Entomophthorales. In "Fungal Protoplasts Applications in Biochemistry and Genetics" J.F. Peberdy and L. Ferenczy, eds. Marcel Dekker, Inc. New York.
- Nolan, R.A. 1993. An inexpensive medium for mass fermentation production of *Entomophaga aulicae* hyphal bodies competent to form conidia. *Can. J. Microbiol.* **39**:588-593.
- Otvos, I.S., MacLeod, D.M., and Tyrrell, D. 1973. Two species of *Entomophthora* pathogenic to eastern hemlock looper (Lepidoptera: Geometridae) in Newfoundland. *Can. Entomol.* **105**,1435-1441.
- Penner, R. 1995. A practical guide to patch clamping. In "Single-Channel Recording" B. Sakmann and E. Neher, eds. Plenum Press, New York.
- Pierce, S.K. and A.P. Politis. 1990. Ca²⁺-activated cell volume recovery mechanisms. *Ann. Rev. Physiol.* **52**:27-42.
- Rae, J.L. and R. Levis. "A Technique for Ultra Low-Noise Single-Channel Recording Using an Axopatch 200A, Quartz Pipettes and Silicone Fluid" Focus on Methods #013. <http://www.axonet.com/pub/tech/focus> (27 Feb 1996).
- Ramanan, S.V., S.F. Fan, P.R.Brink. 1992. Model invariant methods for extracting single-channel mean open and closed times for heterogeneous channel records. *J. Neuro. Meth.* **42**:91-103.

- Ramanan, S.V., P.R. Brink and R.T. Mathias. 1996. "Analysis of Multichannel records" Focus on Methods #024. <http://www.axonet.com/pub/tech/focus> (26 Feb. 1996).
- Ramirez, J.A., V. Vacata, J.H. McKusker, J.E. Haber, R.K. Mortimer, W.G. Owen and H. Lecar. 1989. ATP-sensitive K^+ channels in a plasma membrane H^+ -ATPase mutant of the yeast *Saccharomyces cerevisiae*. *Proc. Natl. Acad. Sci. USA* **86**: 7866-7870.
- Rhodes, A., and Fletcher, D.L. 1966. "Principles of Industrial Microbiology" Pergamon Press, Oxford.
- Roberts, S. K. and M. Tester. 1995. Inward and outward K^+ selective currents in the plasma membrane of protoplasts from maize root cortex and stele. *Plant J.* **8**: 811-825.
- Rorsman, P. and G. Trube. 1990. Biophysics and physiology of ATP-regulated K^+ channels (K_{ATP}) In "Potassium Channels; structure, classification function and therapeutic potential" N.S. Cook,ed. John Wiley & Sons, New York.
- Roy, G. and U. Banderali. 1994. Channels for ions and amino acids in kidney cultured cells (MDCK) during volume regulation. *J. Exp. Zoo.* **268**: 121- 126.
- Ruknudin, A. M.J. Song and F. Sachs. 1991. The ultrastructure of patch-clamped membranes: a study using high voltage electron microscopy. *J. Cell Biol.* **112**: 125-134.
- Saimi, Y., B. Martinac, A.H. Delcour, P.V. Minorsky, M.C. Gustin, M.R. Culbertson, J. Adler and C. Kung. 1992. Patch clamp studies of microbial ion channel. *Meth. Enzymol.* **207**: 681-691.
- Sakmann, B. and E. Neher. 1995a. "Single-Channel Recording" Second Edition.

Plenum Press, New York.

Sakmann, B. and E. Neher. 1995b. Geometric parameters of pipettes and membrane patches. In "Single-Channel Recording" Second Edition. Plenum Press, New York.

Sarkadi, B. and J.C. Parker. 1991. Activation of ion transport pathways by changes in cell volume. *Biochem. Biophys. Acta.* **1071**:407-427.

Serrano, R. 1977. Energy requirements for maltose transport in yeast. *Eur.J. Biochem* **80**: 97-102.

Sokal, R.R., and F.J. Rohlf. 1995. "Biometry. The Principles and Practice of Statistics in Biological Research" p.501 W.H. Freeman and Co., New York.

Soper, R.S., M. Shimanzu, R.A. Humber, and A.E. Hajek. 1988. Isolation and characterization of *Entomophaga maimaiga* sp nov., a fungal pathogen of gypsy moth, *Lymantria dispar*, from Japan. *J. Invertebr. Pathol.* **51**,229-241.

Sunder, S., A.J. Singh, S. Gills and B. Singh. 1996. Regulation of intracellular level of Na⁺, K⁺ and glycerol in *Saccharomyces cerevisiae* under osmotic stress. *Mol. Cell. Biochem.* **96**:121-124.

Swandulla, D. and R.H. Chow. 1992. Recording solutions for isolating specific ionic channel currents. In "Practical Electrophysiological Methods. A Guide for *in vitro* studies in vertebrate neurobiology" H.Kettermann and R. Grantyn, eds. Wiley Liss, New York.

Tang, .M., A. Ruknudin, W.P. Yang, S.Y. Shaw, A. Knickerbocker and S. Kurtz. 1995. Functional expression of a vertebrate inwardly rectifying K⁺ channel in yeast. *Mol. Biol. Cell* **6**: 1231-1240.

- Taylor, R.S. 1992. The microtubule cytoskeleton in protoplasts of the fungus *Entomophaga aulicae*: a computer-aided 3-D reconstruction. BSc(Honors)thesis. Dept. of Biology, Memorial University of Newfoundland.
- Trautmann, A. and S.A. Siegelbaum. 1983. The influence of membrane isolation on single acetylcholine-channel current in rat myotubes. In "Single-Channel Recording" B. Sakmann and E. Neher, eds. Plenum Press, New York.
- Tyrrell, D. 1977. Occurrence of protoplasts in the natural life cycle of *Entomophthora egressa*. *Exp. Mycol.* **1**, 259-263.
- Tyrrell, D. 1988. Survival of *Entomophaga aulicae* in dried insect larvae. *J. Invertebr. Pathol.* **52**:185-186.
- Undrovinas, A.I., G.S. Shander and J.C. Makielski. 1995. Cytoskeleton modulates gating of voltage-dependent sodium channel in heart. *Am. J. Physiol. Heart Circ. Physiol.* **38**:H203-H214.
- Vandenberg, J.D. and R.S. Soper. 1975. Isolation and identification of *Entomophthora* spp. Fres.(Phycomycetes: Entomophthales) from the spruce budworm *Choristoneura fumiferana* Clems. (Lepidoptera: Tortricidae). *J.N.Y. Entomol. Soc.* **83**, 254-255.
- Van Dongen, A.M.J. 1996. A new algorithm for idealized single ion channel data containing multiple unknown conductance levels. *Biophys. J.* **70**:1303-1315.
- Vonbeckerath, N., M. Dittrich, H.G. Klieber and J. Daut. 1996. Inwardly rectifying K⁺ channels in freshly dissociated coronary endothelial cells from guinea pig heart. *J. Physiol.* **491**:357-365.

Yu, W.P., M.E. Grunwald and K.W. Yau. 1996. Molecular cloning, functional expression and chromosomal localization of a human homolog of the cyclic nucleotide-gated ion channel of retinal cone photoreceptors. *FEBS* **393**: 211-215.

Zhou, X.L. and C. Kung. 1992. A mechanosensitive ion channel in *Schizosaccharomyces pombe*. *EMBO Journal* **11**:2869-2875.

Appendix 1

Data Acquisition Parameters

Ramp5S -100 to +100mV Data Acquisition Parameters

Acquisition

1	Number of trials to perform (-1 for continuous)
Number of runs/trial (runs are averaged)	
10	Number of episodes/run (if no conditioning pulses)
0	Perform interepisode data write: 0·No, 1·Yes
1	Starting episode number (normally 1)
4	Number of 512-sample segments/episode (1..4)
1	Number of channels to sample (1..4)
0	Trigger mode: 0·External, 2·Space bar, 3·Ext
10	Time between start of episodes (s) (0 for max. rate)
2500	First clock interval (samples 1-1024) (³ 0μs)
0	Second clock interval (samples 1025-2048)(0 to use 1 st clock)
0	Delay between scope trigger and episode start (ms)

Subtraction

0	Number of P/N sub-pulses: 0·None, -N·Add, +N·Subtract
0	ADC channel number
0	Subpulse holding amplitude (mV)
0	Settling time after change of holding amplitude (ms)
0	Time interval between sub-pulses (ms)

Waveform on analog output channel #0

0	Holding amplitude (mV)
1	A Epoch type: 1·Step, 2·Ramp
-100*	Amplitude initial value (mV)
0	Amplitude increment (mV)
50	Duration initial value (samples)
0	Duration increment (samples)
2	B Epoch type: 1·Step, 2·Ramp

100*	Amplitude initial value (mV)
0	Amplitude increment (mV)
1500	Duration initial value (samples)
0	Duration increment (samples)
1	C Epoch type: 1-Step, 2-Ramp
0	Amplitude initial value (mV)
0	Amplitude increment (mV)
0	Duration initial value (samples)
0	Duration increment (samples)
1	D Epoch type: 1-Step, 2-Ramp
0	Amplitude initial value (mV)
0	Amplitude increment (mV)
0	Duration initial value (samples)
0	Duration increment (samples)
0	Inter-episode amplitude: 0-Holding, 1-Last epoch amplitude

Triggger outputs

-10	Duration and polarity of pulse on trigger channel #1 (samples)
100	Sample number at which to start pulse
-20	Duration and polarity of pulse on trigger channel #2 (samples)
150	Sample number at which to start pulse
1	First episode at which trigger channels #1 and #2 fire
12	Last episode at which trigger channels #1 and #2 fire

Conditioning train

0	Number of pulses in train (0 for none)
0	Pre-conditioning pulse duration (ms)
0	Pre-conditioning pulse amplitude (mV)
0	Conditioning pulse duration (ms)
0	Conditioning pulse amplitude (mV)
0	Post-conditioning train duration (ms)
0	Post-conditioning train amplitude (mV)

Display data

1	ADC ch.#15: amplification factor (not 0)
0	display offset: fraction of full screen
1	ADC ch.#14: amplification factor (not 0)
0	display offset: fraction of full screen
1	ADC ch.#13: amplification factor (not 0)

0 display offset: fraction of full screen
 1 ADC ch.#12: amplification factor (not 0)
 0 display offset: fraction of full screen
 0 Segment number to display (0..4) (0 for all)
 0 Skip factor: plot every Nth point (1..4)
 0 Display averaged data: 0·After each episode, N·After each N runs
 0 Autoerase: 0·No, 1·Yes
 1 Graph Style: 0·Points, 1·Lines

Units of measure

pA ADC ch. #15
 mV ADC ch. #14
 mV ADC ch. #13
 mV ADC ch. #12
 mV DAC ch. #0 (command)

Peak detection

0 Search mode: 0·None, 1·A, 2·B, 3·C, 4·D, 5·All, 6·Use sample #
 0 Optional sample number to measure, negative for negative peaks
 0 Channel number to search
 0 Number of samples averaged in search (1-20) (0 for default 5)
 0 Baseline: 0·Average first 24 samples, 1·Average interval A
 0 Display: 0·Screen, 1·File & screen

Hardware configuration

-50 DAC ch. #0: gain from DAC to cell (mV @ cell/ V @ DAC)
 -0.1 ADC ch. #15: gain from cell to ADC (V @ ADC/ pA @ cell)
 10 ADC range, ±V
 10 DAC range, ±V
 3 Autosample Axopatch1: 0·Manual, 1·Yes, 2·Yes(inverted), 3·Disabled
 1 Gain multiplier
 100000 Filter cutoff frequency

* values given for a -100 to +100mV ramp.

Singles Data Acquisition Parameters

Acquisition		
1	Number of trials to perform (-1 for continuous)	1
Number of runs/trial (runs are averaged)		
10	Number of episodes/run (if no conditioning pulses)	
0	Perform interepisode data write: 0-No, 1-Yes	
1	Starting episode number (normally 1)	
4	Number of 512-sample segments/episode (1..4)	
1	Number of channels to sample (1..4)	
0	Trigger mode: 0-External, 2-Space bar, 3-Ext	
10	Time between start of episodes (s) (0 for max. rate)	
2500	First clock interval (samples 1-1024) ($\approx 0\mu\text{s}$)	
0	Second clock interval (samples 1025-2048)(0 to use 1 st clock)	
0	Delay between scope trigger and episode start (ms)	
Subtraction		
0	Number of P/N sub-pulses: 0-None, -N-Add, +N-Subtract	
0	ADC channel number	
0	Subpulse holding amplitude (mV)	
0	Settling time after change of holding amplitude (ms)	
0	Time interval between sub-pulses (ms)	
Waveform on analog output channel #0		
0	Holding amplitude (mV)	
1	A Epoch type: 1-Step, 2-Ramp	
80**	Amplitude initial value (mV)	
0	Amplitude increment (mV)	

2000	Duration initial value (samples)
0	Duration increment (samples)
1	B Epoch type: 1-Step, 2-Ramp
0	Amplitude initial value (mV)
0	Amplitude increment (mV)
0	Duration initial value (samples)
0	Duration increment (samples)
1	C Epoch type: 1-Step, 2-Ramp
0	Amplitude initial value (mV)
0	Amplitude increment (mV)
0	Duration initial value (samples)
0	Duration increment (samples)
1	D Epoch type: 1-Step, 2-Ramp
0	Amplitude initial value (mV)
0	Amplitude increment (mV)
0	Duration initial value (samples)
0	Duration increment (samples)
0	Inter-episode amplitude: 0-Holding, 1-Last epoch amplitude

Trigger outputs

-10	Duration and polarity of pulse on trigger channel #1 (samples)
100	Sample number at which to start pulse
-20	Duration and polarity of pulse on trigger channel #2 (samples)
150	Sample number at which to start pulse
1	First episode at which trigger channels #1 and #2 fire
12	Last episode at which trigger channels #1 and #2 fire

Conditioning train

0	Number of pulses in train (0 for none)
0	Pre-conditioning pulse duration (ms)
0	Pre-conditioning pulse amplitude (mV)
0	Conditioning pulse duration (ms)
0	Conditioning pulse amplitude (mV)
0	Post-conditioning train duration (ms)
0	Post-conditioning train amplitude (mV)

Display data

1	ADC ch.#15: amplification factor (not 0)
0	display offset: fraction of full screen

1 ADC ch.#14: amplification factor (not 0)
 0 display offset: fraction of full screen
 1 ADC ch.#13: amplification factor (not 0)
 0 display offset: fraction of full screen
 1 ADC ch.#12: amplification factor (not 0)
 0 display offset: fraction of full screen
 0 Segment number to display (0..4) (0 for all)
 0 Skip factor: plot every Nth point (1..4)
 0 Display averaged data: 0·After each episode, N·After each N runs
 0 Autoerase: 0·No, 1·Yes
 0 Graph Style: 0·Points, 1·Lines

Units of measure

pA ADC ch. #15
 mV ADC ch. #14
 mV ADC ch. #13
 mV ADC ch. #12
 mV DAC ch. #0 (command)

Peak detection

0 Search mode: 0·None, 1·A, 2·B, 3·C, 4·D, 5·All, 6·Use sample #
 0 Optional sample number to measure, negative for negative peaks
 0 Channel number to search
 0 Number of samples averaged in search (1-20) (0 for default 5)
 0 Baseline: 0·Average first 24 samples, 1·Average interval A
 0 Display: 0·Screen, 1·File & screen

Hardware configuration

-50 DAC ch. #0: gain from DAC to cell (mV @ cell/ V @ DAC)
 -0.1 ADC ch. #15: gain from cell to ADC (V @ ADC/ pA @ cell)
 10 ADC range, ±V
 10 DAC range, ±V
 3 Autosample Axopatch1: 0·Manual, 1·Yes, 2·Yes(inverted), 3·Disabled
 1 Gain multiplier
 100000 Filter cutoff frequency

** Value changed to reflect desired voltage; example given for +80mV

Set-Up Data Acquisition Parameters

Acquisition

-1	Number of trials to perform (-1 for continuous)
1	Number of runs/trial (runs are averaged)
1	Number of episodes/run (if no conditioning pulses)
0	Perform interepisode data write: 0·No, 1·Yes
1	Starting episode number (normally 1)
2	Number of 512-sample segments/episode (1..4)
1	Number of channels to sample (1..4)
0	Trigger mode: 0·External, 2·Space bar, 3·Ext
1	Time between start of episodes (s) (0 for max. rate)
20	First clock interval (samples 1-1024) ($3\ 0\mu\text{s}$)
0	Second clock interval (samples 1025-2048)(0 to use 1st clock)
0	Delay between scope trigger and episode start (ms)

Subtraction

0	Number of P/N sub-pulses: 0·None, -N·Add, +N·Subtract
0	ADC channel number
0	Subpulse holding amplitude (mV)
0	Settling time after change of holding amplitude (ms)
0	Time interval between sub-pulses (ms)

Waveform on analog output channel #0

0	Holding amplitude (mV)
1	A Epoch type: 1·Step, 2·Ramp
0	Amplitude initial value (mV)
0	Amplitude increment (mV)
250	Duration initial value (samples)
0	Duration increment (samples)
1	B Epoch type: 1·Step, 2·Ramp
10	Amplitude initial value (mV)
0	Amplitude increment (mV)
500	Duration initial value (samples)
0	Duration increment (samples)
1	C Epoch type: 1·Step, 2·Ramp
0	Amplitude initial value (mV)
0	Amplitude increment (mV)

200	Duration initial value (samples)
0	Duration increment (samples)
1	D Epoch type: 1·Step, 2·Ramp
0	Amplitude initial value (mV)
0	Amplitude increment (mV)
50	Duration initial value (samples)
0	Duration increment (samples)
0	Inter-episode amplitude: 0·Holding, 1·Last epoch amplitude
Triggger outputs	
0	Duration and polarity of pulse on trigger channel #1 (samples)
100	Sample number at which to start pulse
0	Duration and polarity of pulse on trigger channel #2 (samples)
150	Sample number at which to start pulse
1	First episode at which trigger channels #1 and #2 fire
12	Last episode at which trigger channels #1 and #2 fire
Conditioning train	
0	Number of pulses in train (0 for none)
0	Pre-conditioning pulse duration (ms)
0	Pre-conditioning pulse amplitude (mV)
0	Conditioning pulse duration (ms)
0	Conditioning pulse amplitude (mV)
0	Post-conditioning train duration (ms)
0	Post-conditioning train amplitude (mV)
Display data	
1	ADC ch.#15: amplification factor (not 0)
0	display offset: fraction of full screen
1	ADC ch.#14: amplification factor (not 0)
0	display offset: fraction of full screen
1	ADC ch.#13: amplification factor (not 0)
0	display offset: fraction of full screen
1	ADC ch.#12: amplification factor (not 0)
0	display offset: fraction of full screen
0	Segment number to display (0..4) (0 for all)
1	Skip factor: plot every Nth point (1..4)
0	Display averaged data: 0_After each episode, N_After each N runs
0	Autoerase: 0·No, 1·Yes

1 Graph Style: 0·Points, 1·Lines

Units of measure

pA	ADC ch. #15
mV	ADC ch. #14
mV	ADC ch. #13
mV	ADC ch. #12
mV	DAC ch. #0 (command)

Peak detection

0	Search mode: 0·None, 1·A, 2·B, 3·C, 4·D, 5·All, 6·Use sample #
0	Optional sample number to measure, negative for negative peaks
0	Channel number to search
0	Number of samples averaged in search (1-20) (0 for default 5)
0	Baseline: 0·Average first 24 samples, 1·Average interval A
0	Display: 0·Screen, 1·File & screen

Hardware configuration

-50	DAC ch. #0: gain from DAC to cell (mV @ cell/ V @ DAC)
.001	ADC ch. #15: gain from cell to ADC (V @ ADC/ pA @ cell)
10	ADC range, ±V
10	DAC range, ±V
0	Autosample Axopatch1:0·Manual,1·Yes,2·Yes(inverted),3·Disabled
1	Gain multiplier
100000	Filter cutoff frequency

K100MSD

Data Acquisition Parameters

Acquisition

1	Number of trials to perform (-1 for continuous)
1	Number of runs/trial (runs are averaged)
13	Number of episodes/run (if no conditioning pulses)
0	Perform interepisode data write: 0-No, 1-Yes
1	Starting episode number (normally 1)
2	Number of 512-sample segments/episode (1..4)
1	Number of channels to sample (1..4)
0	Trigger mode: 0-External, 2-Space bar, 3-Ext
10	Time between start of episodes (s) (0 for max. rate)
200	First clock interval (samples 1-1024) (³ 0 μ s)
0	Second clock interval (samples 1025-2048)(0 to use 1st clock)
0	Delay between scope trigger and episode start (ms)

Subtraction

0	Number of P/N sub-pulses: 0-None, -N-Add, +N-Subtract
15	ADC channel number
-80	Subpulse holding amplitude (mV)
10	Settling time after change of holding amplitude (ms)
10	Time interval between sub-pulses (ms)

Waveform on analog output channel #0

-80	Holding amplitude (mV)
1	A Epoch type: 1-Step, 2-Ramp
-80	Amplitude initial value (mV)
0	Amplitude increment (mV)
250	Duration initial value (samples)
0	Duration increment (samples)
1	B Epoch type: 1-Step, 2-Ramp
-70	Amplitude initial value (mV)
10	Amplitude increment (mV)
500	Duration initial value (samples)
0	Duration increment (samples)
1	C Epoch type: 1-Step, 2-Ramp
-80	Amplitude initial value (mV)
0	Amplitude increment (mV)

200	Duration initial value (samples)
0	Duration increment (samples)
1	D Epoch type: 1-Step, 2-Ramp
-80	Amplitude initial value (mV)
0	Amplitude increment (mV)
50	Duration initial value (samples)
0	Duration increment (samples)
-80	Inter-episode amplitude: 0-Holding, 1-Last epoch amplitude

Trigger outputs

1000	Duration and polarity of pulse on trigger channel #1 (samples)
1	Sample number at which to start pulse
0	Duration and polarity of pulse on trigger channel #2 (samples)
0	Sample number at which to start pulse
1	First episode at which trigger channels #1 and #2 fire
13	Last episode at which trigger channels #1 and #2 fire

Conditioning train

0	Number of pulses in train (0 for none)
0	Pre-conditioning pulse duration (ms)
0	Pre-conditioning pulse amplitude (mV)
0	Conditioning pulse duration (ms)
0	Conditioning pulse amplitude (mV)
0	Post-conditioning train duration (ms)
0	Post-conditioning train amplitude (mV)

Display data

1	ADC ch.#15: amplification factor (not 0)
0	display offset: fraction of full screen
1	ADC ch.#14: amplification factor (not 0)
0	display offset: fraction of full screen
1	ADC ch.#13: amplification factor (not 0)
0	display offset: fraction of full screen
1	ADC ch.#12: amplification factor (not 0)
0	display offset: fraction of full screen
0	Segment number to display (0..4) (0 for all)
1	Skip factor: plot every Nth point (1..4)
0	Display averaged data: 0-After each episode, N-After each N runs
0	Autoerase: 0-No, 1-Yes

1 Graph Style: 0·Points, 1·Lines

Units of measure

pA	ADC ch. #15
mV	ADC ch. #14
mV	ADC ch. #13
mV	ADC ch. #12
mV	DAC ch. #0 (command)

Peak detection

0	Search mode: 0·None, 1·A, 2·B, 3·C, 4·D, 5·All, 6·Use sample #
0	Optional sample number to measure, negative for negative peaks
0	Channel number to search
0	Number of samples averaged in search (1-20) (0 for default 5)
0	Baseline: 0·Average first 24 samples, 1·Average interval A
0	Display: 0·Screen, 1·File & screen

Hardware configuration

-50	DAC ch. #0: gain from DAC to cell (mV @ cell/ V @ DAC)
.001	ADC ch. #15: gain from cell to ADC (V @ ADC/ pA @ cell)
1	ADC ch. #14: gain from cell to ADC (V @ ADC/ pA @ cell)
1	ADC ch. #13: gain from cell to ADC (V @ ADC/ pA @ cell)
1	ADC ch. #12: gain from cell to ADC (V @ ADC/ pA @ cell)
10	ADC range, ±V
10	DAC range, ±V
0	Autosample Axopatch1: 0·Manual, 1·Yes, 2·Yes(inverted), 3·Disabled
1	Gain multiplier
100000	Filter cutoff frequency

K100MSH

Data Acquisition Parameters

Acquisition

1	Number of trials to perform (-1 for continuous)
1	Number of runs/trial (runs are averaged)
10	Number of episodes/run (if no conditioning pulses)
0	Perform interepisode data write: 0·No, 1·Yes
1	Starting episode number (normally 1)
2	Number of 512-sample segments/episode (1..4)
1	Number of channels to sample (1..4)
0	Trigger mode: 0·External, 2·Space bar, 3·Ext
10	Time between start of episodes (s) (0 for max. rate)
200	First clock interval (samples 1-1024) ($3\ 0\mu\text{s}$)
0	Second clock interval (samples 1025-2048)(0 to use 1st clock)
0	Delay between scope trigger and episode start (ms)

Subtraction

0	Number of P/N sub-pulses: 0·None, -N·Add, +N·Subtract
15	ADC channel number
-80	Subpulse holding amplitude (mV)
10	Settling time after change of holding amplitude (ms)
10	Time interval between sub-pulses (ms)

Waveform on analog output channel #0

-60	Holding amplitude (mV)
1	A Epoch type: 1·Step, 2·Ramp
-60	Amplitude initial value (mV)
0	Amplitude increment (mV)
250	Duration initial value (samples)
0	Duration increment (samples)
1	B Epoch type: 1·Step, 2·Ramp
-70	Amplitude initial value (mV)
-10	Amplitude increment (mV)
500	Duration initial value (samples)
0	Duration increment (samples)
1	C Epoch type: 1·Step, 2·Ramp
-60	Amplitude initial value (mV)

0	Amplitude increment (mV)
200	Duration initial value (samples)
0	Duration increment (samples)
1	D Epoch type: 1-Step, 2-Ramp
-60	Amplitude initial value (mV)
0	Amplitude increment (mV)
50	Duration initial value (samples)
0	Duration increment (samples)
-60	Inter-episode amplitude: 0-Holding, 1-Last epoch amplitude

Trigger outputs

1000	Duration and polarity of pulse on trigger channel #1 (samples)
1	Sample number at which to start pulse
1000	Duration and polarity of pulse on trigger channel #2 (samples)
1	Sample number at which to start pulse
1	First episode at which trigger channels #1 and #2 fire
13	Last episode at which trigger channels #1 and #2 fire

Conditioning train

0	Number of pulses in train (0 for none)
0	Pre-conditioning pulse duration (ms)
0	Pre-conditioning pulse amplitude (mV)
0	Conditioning pulse duration (ms)
0	Conditioning pulse amplitude (mV)
0	Post-conditioning train duration (ms)
0	Post-conditioning train amplitude (mV)

Display data

1	ADC ch.#15: amplification factor (not 0)
0	display offset: fraction of full screen
1	ADC ch.#14: amplification factor (not 0)
0	display offset: fraction of full screen
1	ADC ch.#13: amplification factor (not 0)
0	display offset: fraction of full screen
1	ADC ch.#12: amplification factor (not 0)
0	display offset: fraction of full screen
0	Segment number to display (0..4) (0 for all)
1	Skip factor: plot every Nth point (1..4)
0	Display averaged data: 0-After each episode, N-After each N runs

0 Autoerase: 0-No, 1-Yes
 1 Graph Style: 0-Points, 1-Lines

Units of measure

pA ADC ch. #15
 mV ADC ch. #14
 mV ADC ch. #13
 mV ADC ch. #12
 mV DAC ch. #0 (command)

Peak detection

0 Search mode: 0-None, 1-A, 2-B, 3-C, 4-D, 5-All, 6-Use sample #
 0 Optional sample number to measure, negative for negative peaks
 0 Channel number to search
 0 Number of samples averaged in search (1-20) (0 for default 5)
 0 Baseline: 0-Average first 24 samples, 1-Average interval A
 0 Display: 0-Screen, 1-File & screen

Hardware configuration

50 DAC ch. #0: gain from DAC to cell (mV @ cell/ V @ DAC)
 .001 ADC ch. #15: gain from cell to ADC (V @ ADC/ pA @ cell)
 1 ADC ch. #14: gain from cell to ADC (V @ ADC/ pA @ cell)
 1 ADC ch. #13: gain from cell to ADC (V @ ADC/ pA @ cell)
 1 ADC ch. #12: gain from cell to ADC (V @ ADC/ pA @ cell)
 10 ADC range, $\pm V$
 10 DAC range, $\pm V$
 3 Autosample Axopatch1:0-Manual,1-Yes,2-Yes(inverted),3-Disabled
 1 Gain multiplier
 100000 Filter cutoff frequency

Appendix 2

Data Analysis Parameters

Demohist

Data Analysis Parameters

Analysis Specification

- 2 Mode: 0·Browse, 1·Sums, 2·Events, 3·Latency, 4·Ampl Hist,
5·Pulse Avg
- 0 Begin analysis at this time (ms) or episode (Fetchex or Clampex)
- 0 Digital Gaussian filter cutoff frequency (Hz); 0·No filter
- 1 Initial interaction level: 0·Continuous, 1·Single step
- 0 ADC channel number to analyze (if more than one step)

Subtraction Options

- 0 Factor to multiply sum file before subtraction; 0·No subtraction
- 0 Number of points to use for baseline correction; 0·No correction

List-of-Events and First Latency Analysis

- 0 Ignore Level changes briefer than or equal to this duration (f s)
- 0 Update Levels with running avg: 0·No, 1·Baseline, 2·All
- 0 Percentage contribution of new levels to running averages (1- 100%)

First Latency Analysis

- 0 Period after stimulus to ignor (f s)
- 0 Latency start: 0·A Epoch, 1·B, 2·C, 3·D, 4·Trig1, 5·Trig2

Pulse Averaging Analysis

- 0 Length of pulse average in ms
- 0 Percentage of pulse length to retain before trigger

Display Specification

- 1 Y axis: Amount of data to read for Autoscale (ms); 0·None
- 4.8 Display amplification
- 5.7 Offset (percent of unity-gain full scale); 0·None
- 1 Drawing style: 0·Points, 1·Lines
- 51.2 Length of display trace (ms)
- 4 Number of display windows (1,2,4,8,16)
- 0 Erase whole screen when screen full: 0·No, 1·Yes
- 0 Seconds to pause at end of each screen: 0·No pause

Hardcopy Specification

- 1 **Plot superimposed idealized transitions: 0-No, 1-Yes**
- 1 **Plot markers for time gaps: 0-No, 1-Yes**



